



# TECHNICAL NOTE

D-1155

## CELESTIAL GEODESY

W. M. Kaula

Goddard Space Flight Center  
Greenbelt, Maryland

NATIONAL AERONAUTICS AND SPACE ADMINISTRATION  
WASHINGTON

March 1962



# CELESTIAL GEODESY

by

W. M. Kaula

*Goddard Space Flight Center*

## SUMMARY

The geodetic use of rockets, artificial satellites, and the moon is reviewed. The discussion covers in turn dynamics, geometry, observational techniques, comparison with terrestrial geodesy, and geophysical implications.

# CONTENTS

	Page
Summary . . . . .	i
List of Symbols . . . . .	v
INTRODUCTION. . . . .	1
Section	
<b>I ORBIT ANALYSIS . . . . .</b>	<b>3</b>
1. General Discussion. . . . .	3
2. General Principals and Techniques . . . . .	4
Dynamical Principles . . . . .	4
Characteristics of Methods of Solution. . . . .	14
3. Empirical Orbits . . . . .	18
4. Numerical Integration. . . . .	19
5. General Theories: Close Satellite Problem . . . . .	20
Disturbing Function . . . . .	21
Dynamical Intermediary Theories. . . . .	23
Geometrical Intermediary Theories. . . . .	26
Comparison of Theories . . . . .	28
Special Problems. . . . .	30
6. General Theories: Lunar Problem . . . . .	32
7. Terrestrial Gravitational Effects . . . . .	34
Disturbing Function and Integration. . . . .	35
Secular and Long Period Terms . . . . .	37
Daily and Short Period Terms . . . . .	40
Tidal Effects. . . . .	42
Relativistic Effects. . . . .	44
8. Non-Gravitational Effects . . . . .	45
Mechanical Drag . . . . .	45
Electromagnetic Effects . . . . .	48
Radiation Pressure. . . . .	49
Observed Variations and Theoretical Models of the Atmosphere. .	50
Orbital Accuracy Implications . . . . .	53
<b>II GEOMETRICAL CONSIDERATIONS AND ERROR ANALYSIS . . . . .</b>	<b>55</b>
1. General Discussion. . . . .	55
2. Coordinate Systems . . . . .	55
General Definitions and Notations . . . . .	55
Time and the Precise Definition of Coordinates. . . . .	58

# CONTENTS (Continued)

Section	Page
3. Observation Equations. . . . .	61
4. Configuration Evaluation . . . . .	66
III ROCKET AND ARTIFICIAL SATELLITE TECHNIQUES. . . . .	69
1. General . . . . .	69
Vehicles. . . . .	69
Timing. . . . .	71
Orientation . . . . .	71
2. Optical Techniques. . . . .	72
Attenuation and Illumination. . . . .	72
Refraction and Aberration . . . . .	74
Theodolites. . . . .	76
Cameras. . . . .	76
Satellite Photogrammetry . . . . .	78
3. Radio Techniques. . . . .	79
Environmental Effects on Propagation . . . . .	80
Interferometry. . . . .	84
Doppler . . . . .	85
Ranging . . . . .	85
IV LUNAR TECHNIQUES. . . . .	87
1. Lunar Topography Effects . . . . .	87
2. Eclipses. . . . .	87
3. Occultations . . . . .	88
4. Lunar Camera. . . . .	88
5. Radar Ranging. . . . .	89
V COMBINATION OF CELESTIAL AND TERRESTRIAL GEODESY . . . . .	91
1. Coordinate Forms and Units. . . . .	91
2. Comparison of Observational Results. . . . .	92
VI GEOPHYSICAL IMPLICATIONS . . . . .	97
ACKNOWLEDGMENTS . . . . .	101
References . . . . .	103



## LIST OF SYMBOLS

- A** Earth-moon distance inversely proportionate to mean lunar parallax:  
 $\pi = a_e/A$  (Paragraph 6, Section I; Paragraph 7, Section I)
- A** Cross sectional area of a satellite (Paragraph 8, Section I; Paragraph 4, Section II; Section III)
- a** Semimajor axis of Keplerian orbit (Section I; Section II)
- a** Aperture of a telescope (Section III)
- a<sub>e</sub>** Mean equatorial radius of earth
- (A<sub>nm</sub>, B<sub>nm</sub>)** Coefficients of  $P_{nm}(\sin \phi) (\cos m\lambda, \sin m\lambda)$  in spherical harmonic development of gravity anomalies
- b** Position vector ( $b_1, b_2, b_3$ ) in coordinates referred to the axis of an observing instrument
- b** Coordinates ( $\eta, \xi$ ) measured on a photo plate (Section II)
- b** Radius of a satellite (Section III)
- c** Shape parameter  $a_e J_2^{\frac{1}{2}}$  of ellipsoidal coordinates (Section I; Section III; Section V)
- c** Velocity of light (Paragraph 7, Section I; Section III)
- C<sub>D</sub>** Drag coefficient, a function of the shape of a body
- C** Coefficient matrix of partial derivatives for differential corrections
- C** Moment of inertia of the earth about the polar axis (Section VI)
- E** Eccentric anomaly of Keplerian orbit (Section I; Section II)
- E** Energy density (dimension  $EL^{-2} = MT^{-2}$ ) (Section III)
- E<sub>i</sub>** General notation for any Keplerian orbit element
- e** Vector ( $M, a, e, i, \omega, \Omega$ ) of Keplerian orbit elements

- e Eccentricity of a Keplerian orbit or an earth ellipsoid
- F Hamiltonian in astronomic sign convention (negative potential; dimension  $EM^{-1} = L^2T^{-2}$ )
- F Force (dimension  $MLT^{-2}$ )
- $F_{nmp}(i)$  Inclination function in coefficient of terms containing  $(n - 2p)\omega$  in argument in the disturbing function  $R_{nm}$
- f True anomaly of Keplerian orbit (Section I)
- f Focal length of telescope (Section II; Paragraph 2, Section III)
- f Frequency expressed in cycles, or periods, per unit time:  $\omega/2\pi$  (Paragraph 3, Section III)
- f Flattening of earth ellipsoid (Section V; Section VI)
- f Vector of residuals in matrix expression of observation and condition equations
- G Delaunay canonical variable,  $\left[\mu a(1 - e^2)\right]^{\frac{1}{2}}$
- $G_{npq}(e)$  Eccentricity function in coefficient of term containing  $(n - 2p + q)M$  in argument in disturbing function  $R_{nm}$
- g Delaunay canonical variable  $\omega$ , argument of perigee
- $g_e$  Mean gravity at earth's equator
- H Hamiltonian in physical sign convention, equal to  $-F$  (Equations 22 and 23 only)
- H Delaunay canonical variable  $\left[\mu a(1 - e^2)\right]^{\frac{1}{2}} \cos i$  (Paragraph 2, Section I; Paragraph 5, Section I)
- H Scale height,  $-h\rho/(\partial\rho/\partial h)$  (Paragraph 8, Section I)
- h Delaunay canonical variable  $\Omega$ , longitude of node from equinox (Equations 26 and 28) and page 23
- h Constant of areas  $r^2\dot{f} = \left[\mu a(1 - e^2)\right]^{\frac{1}{2}}$  (Equation 5) and page 27
- h Altitude above earth's surface (Paragraph 8, Section I; Section III)
- i Inclination
- I Unit Matrix

- I** Luminous intensity, energy per steradian per unit time (dimension  $ET^{-1} = L^2 MT^{-3}$ )
- J<sub>n</sub>, J<sub>nm</sub>** Coefficients of  $-(\mu a_e^n / r^{n+1}) [P_n(\sin \phi), P_{nm}(\sin \phi) \cos m\lambda]$  in spherical harmonic development of potential
- K<sub>nm</sub>** Coefficient of  $-(\mu a_e^n / r^{n+1}) P_{nm}(\sin \phi) \sin m\lambda$  in potential
- k** Gaussian constant:  $6.664 \times 10^{-8}$  cgs. (dimension  $L^3 M^{-1} T^{-2}$ ) (Section I; Section V)
- k, h** Love's numbers: ratios of tidal potential to disturbing potential and actual tide height to equilibrium height, respectively (page 43; Section V)
- k** Summation index in  $R_{nm}$ :  $(n-m)/2$ ,  $n-m$  even;  $(n-m-1)/2$ ,  $n-m$  odd (pages 35 through 36)
- L** Delaunay canonical variable  $(\mu a)^{\frac{1}{2}}$
- ℓ** Delaunay canonical variable:  $M$ , mean anomaly
- ℓ** Position vector  $(\ell_1, \ell_2, \ell_3)$  in coordinates referred to a local vertical
- M** Mass of an astronomical body (Equation 1; pages 39 through 40; Section V; Section VI)
- M** Mean anomaly of a Keplerian orbit (Paragraph 2, Section I; Paragraph 3, Section I; Paragraph 5, Section I; pages 35 through 37; Paragraph 8, Section I; Section II)
- M** Coefficient matrix of partial derivatives of observations with respect to parameters for differential corrections
- m** Mass of a small body: artificial satellite, electron, etc. (Paragraph 2, Section I; Paragraph 8, Section I; Section II; Section III)
- m** Ratio of disturbing body mean motion to its differences from satellite mean motion:  $n^*/(n-n^*)$  (Paragraph 6, Section I)
- m** Ratio centrifugal force to gravity at equator  $(\dot{\theta})^2 a_e / g_e$  (Section V; Section VI)
- m** Order index or secondary wave number of spherical harmonic;  $0 \leq m \leq n$  (Paragraph 5, Section I; Paragraph 7, Section I; Section II; Section V; Section VI)
- n** Degree index or primary wave number of spherical harmonic (Paragraph 5, Section I; Paragraph 7, Section I; Section II; Section V; Section VI)

- n Mean motion in Keplerian orbit (Section I; Section II)
- n** Unit vector normal to a surface or a line (in osculating plane)
- N Electron density
- N** Observation matrix of partial derivatives of observed quantities with respect to vector components
- $n_2$  Acceleration in mean motion,  $\dot{n}/n$
- O Order of magnitude
- $P_{nm}$  Associated Legendre function,  $P_{nm}(\sin \phi)$
- P Period,  $2\pi/n$ , or cycle
- p** Vector of momentum, or action, canonical variables; for example, L, G, H (Section I)
- p** Position vector ( $p_1, p_2, p_3$ ) in coordinates referred to observer-satellite line (Section II)
- q** Position vector ( $q_1, q_2$ ) in orbital plane, referred to line of apsides (Section II)
- q** Vector of position, or angle, canonical variables, for example, l, g, h (Section I)
- R Radius of curvature (Section III)
- R Disturbing function (Section I; Section II)
- $R_{nm}$  Disturbing function due to anomalous gravity term
 
$$- \left( \frac{a^n}{r^{n+1}} \right) \mu P_{nm}(\sin \phi) (J_{nm} \cos m\lambda + K_{nm} \sin m\lambda)$$
- $R_i(\theta)$  Rotation matrix for rotation about axis i counterclockwise through angle  $\theta$
- r** Position vector, without specification of coordinate axis directions
- $r, |\mathbf{r}|$  Range, or straight line distance
- s Distance along a curved line
- S, S Energy flux (dimension  $EL^{-2}T^{-1} = MT^{-3}$ ) (Paragraph 8, Section I; Section III)

S	Generating or determining function of a canonical transformation (Paragraph 2, Section I; Paragraph 5, Section I)
$S_{nmpq}(\omega, M, \Omega, \theta)$	Factor in term with coefficients $-\mu a_e^n (J_{nm}, K_{nm})$ and containing argument $[(n-2p)\omega + (n-2p+q)M + m(\Omega-\theta)]$ in the disturbing function $R_{nm}$
T	Kinetic energy
t	Time
$\mathbf{t}$	Unit vector tangential to a line
U	Force function in astronomical sign convention, negative of potential: $-v$ (dimension $L^2 T^{-2}$ )
$\mathbf{u}$	Position vector $(u, v, w)$ or $(u_1, u_2, u_3)$ in earth-fixed geodetic coordinates, referred to polar axis and Greenwich meridian
V	Potential, in physical sign convention (dimension $L^2 T^{-2}$ )
$\mathbf{v}$	Velocity, $ \dot{\mathbf{r}} $ (Paragraph 2, Section I; Section III)
$\nu$	Polar angle measured in orbital plane from a fixed departure point (Paragraph 5, Section I)
W	Covariance matrix
$\mathbf{x}$	Position vector $(x, y, z)$ or $(x_1, x_2, x_3)$ in inertial coordinates, referred to polar axis and vernal equinox
$\mathbf{y}$	Vector of corrections to observations in least squares adjustment
$\mathbf{z}$	Vector of corrections to parameters in least squares adjustment
$z$	Zenith angle (Paragraph 2, Section III)
$z$	Normalized altitude $(h-h_0)/H$ (Paragraph 3, Section III)
$\alpha$	Right ascension
$\beta$	Solar effect on mean lunar distance (Paragraph 6, Section I)
$\beta$	Vertical gradient of scale height, $\partial H / \partial h$ (Paragraph 8, Section I)
$\gamma$	Sine of half the inclination, $\sin(i/2)$
$\delta$	Declination
$\zeta$	Tide height

$\theta$	Greenwich sidereal time
$\kappa$	Reflective efficiency or albedo
$\lambda$	Longitude, counterclockwise from Greenwich meridian (Section I; Section II; Section V)
$\lambda$	Wavelength of light (Paragraph 2, Section III)
$\mu$	Gaussian constant times mass: $\kappa M$ (dimension $L^3 T^{-2}$ ) (Section I; Section II; Section V; Section VI)
$\mu$	Refractive index (Section III)
$\pi$	Perigee subscript
$\rho$	Density (Paragraph 8, Section I; Section III)
$\rho, \sigma, \alpha$ or $\lambda$	Ellipsoidal coordinates (Section I; Section III; Section V)
$\Phi$	Phase angle
$\phi$	Latitude
$\Omega$	Longitude, from vernal equinox, of node of Keplerian orbit
$\omega$	Argument, from node, of perigee of Keplerian orbit (Section I; Section II)
$\omega$	Frequency in radians per unit time: $2\pi f$ (Section III)

### General Notation

- ' " Primes denote parameters or coordinates of an intermediate orbit: for example,  $a'$ ,  $e'$ ,  $F'$ ,  $p'$ ,  $x'$
- \* An asterisk denotes parameters or coordinates of a disturbing body, such as the sun or moon: for example,  $a^*$ ,  $x^*$ ,  $\mu^*$
- o A zero subscript denotes quantities evaluated at a reference time (epoch) or reference coordinate: for example,  $a_0$ ,  $a'_0$ ,  $h_0$ ,  $u_0$
- " Overdots denote total derivatives with respect to time: for example,  $\dot{x}$ ,  $\ddot{x}$
- Overbars denote mean values with respect to a certain duration of time: for example,  $\bar{x}$ ,  $\bar{x}'$
- $\tau, s, D$  These subscripts denote coordinates with origins respectively on the earth's surface, at a satellite, and at the arbitrary origin of a geodetic datum

## INTRODUCTION

We define celestial geodesy to be the use of extraterrestrial objects close enough that their directions are significant functions of position on the earth to accomplish the principal objectives of geodesy: to determine the external gravitational field and form of the earth (including variations in both space and time), and to determine the positions of points with respect to an earth-fixed reference system. In this review extraterrestrial is more precisely defined as being of too great an altitude to be supported by the atmosphere, say, above 40 kilometers; and an outer limit on the zone of interest is set as the distance of the moon, about 400,000 kilometers.

The scope of this review is primarily the exploitation of extraterrestrial objects for the aforesaid geodetic purposes. This approach still entails considerable attention to the effects on the objects, and observations thereof, of the atmosphere, other astronomic bodies, electromagnetic fields, etc., for the same reason that attention to atmospheric refraction is required in conventional geodesy.

This review is divided into six sections. The first section discusses the dynamics of earth satellites proceeding from general principles to the subject of principal geodetic interest, the effects of the earth's gravitational field on their orbits, and thence to the other physical effects most likely to interfere. The second section discusses the geometrical considerations involved, including specification of satellite and orbital parameters and observational configuration for optimum results. The third and fourth sections discuss observational techniques. The fifth section discusses comparison and combination of celestial and terrestrial results. The sixth section discusses the geophysical implications of the geodetic data thus far obtained celestially.

The emphasis of this review is on the dynamical aspects, first because they lead to the scientifically most interesting results and second because the most effective and economic attainment of the geometric as well as the gravitational purposes will require use of the orbits.

The most comprehensive analysis in celestial geodesy is that of Veis (Reference 1). More general discussions are in References 2, 3 and 4. The recent treatise of Berroth and Hofmann (Reference 5) is the most extensive discussion of lunar techniques.

This review was written in February 1961, and brought up to date in July 1961 to incorporate those developments of greatest interest to geodesy.



## SECTION I

### ORBIT ANALYSIS

#### 1. GENERAL DISCUSSION

Celestial mechanics is a branch of classical mechanics, a subject to which some of the most competent mathematical minds have devoted considerable attention in the past and in which even today advances are being made both in understanding of fundamental principles and in techniques of application. Since the problem of greatest interest to celestial geodesy, the close satellite of an oblate planet, is not one which has been of practical interest to astronomers until recent years, and since the geodesist wants to extract as much information as possible about the gravitational field from the orbits of close satellites, close study of a modern text on the fundamental principles of classical mechanics such as References 6, 7 or 8, is well worthwhile. The standard texts on celestial mechanics (References 9, 10, 11, and 12) place less emphasis on mathematical principles and more on astronomical techniques. None of these texts treat the close satellite problem, but it is discussed considerably in the more recent texts (References 13, 14, and 15). Of these texts, Plummer (Reference 9) and Brouwer and Clemence (Reference 15) appear to be the best combinations of clarity and comprehensiveness.

The geometric limits of interest imposed in the introduction define the dynamical problem of celestial geodesy as that of a perturbed Keplerian orbit, that is, the elliptic orbit of a particle of negligible mass in a central force field

$$F_r = -\frac{kMm}{r^2} \quad (1)$$

with departures of an order not greater than  $10^{-2}$  compared to the central force. Near the inner limit of the zone of interest, the most important of the departures arise from the noncentral terms in the earth's gravitational field and from the earth's atmosphere; near the outer limit, from the sun and moon.

Some general principles and techniques are discussed before the particular subjects of interest are investigated. The purposes of these techniques are two-fold: obtaining the most precise and efficient solution and attaining a keener insight into the physical nature of the phenomena. Modern computers have lessened the importance of the former purpose, but not of the latter.

## 2. GENERAL PRINCIPLES AND TECHNIQUES

### Dynamical Principles

The dynamical situation of a satellite in orbit can be expressed at any instant by its position vector  $(x, y, z)$  and velocity vector  $(\dot{x}, \dot{y}, \dot{z})$  referred to inertial space with origin at the earth's center. These six parameters can be transformed to the six parameters of a Kepler ellipse with one focus at the origin:  $(a, e, i, \Omega, \omega, f)$ . The relationship between these parameters and the earth-fixed coordinates  $(u, v, w)$  are shown in Figure 1.

In the angle  $\omega + f$ :  $\omega$  is the argument of perigee, the angle from the ascending node  $\Omega$  to perigee, the point of closest approach of the ellipse to the origin; and  $f$  is the true anomaly, the angle from perigee to the satellite. Alternate ways of expressing the anomaly of the satellite are (Reference 9, pp. 23-24 and Reference 15, pp. 17-25): the eccentric anomaly  $E$  related to  $f$  by

$$\tan \frac{1}{2} E = \left( \frac{1-e}{1+e} \right)^{\frac{1}{2}} \tan \frac{1}{2} f \quad (2)$$

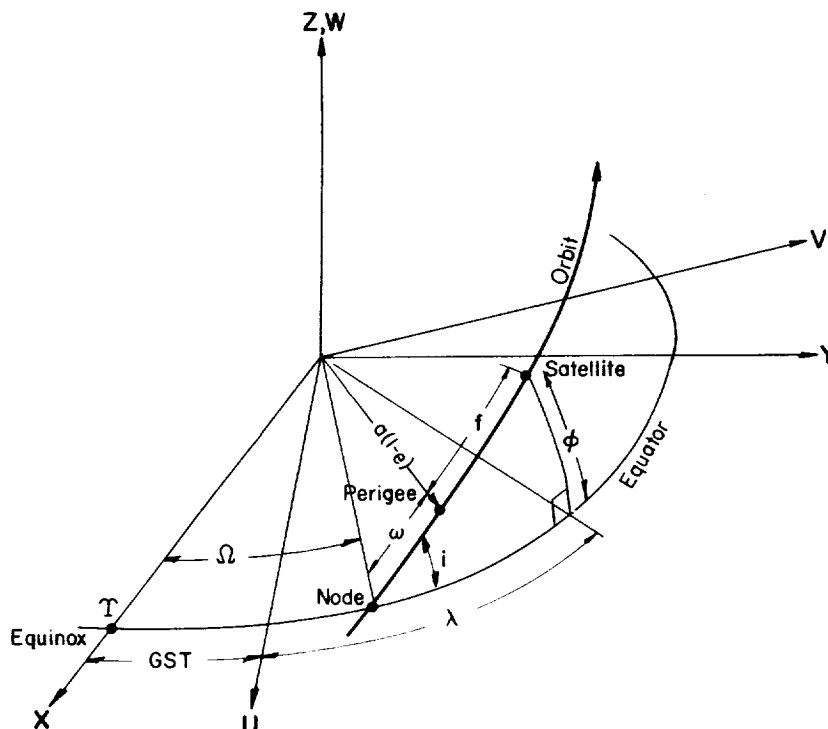


Figure 1 - Orbit and Coordinate Systems

and the mean anomaly  $M$

$$M = E - e \sin E. \quad (3)$$

Equation 3 is known as Kepler's equation.

Further useful relations for elliptic motion (Reference 9, pp. 19-24), using the abbreviation  $\mu$  for  $kM$  in Equation 1, are set forth in Equations 4 through 9.

The equation of energy is

$$\dot{x}^2 + \dot{y}^2 + \dot{z}^2 = v^2 = \mu \left( \frac{2}{r} - \frac{1}{a} \right). \quad (4)$$

The constant of areas (Kepler's second law) is

$$h = r^2 \dot{f} = \left[ \mu a (1 - e^2) \right]^{\frac{1}{2}}. \quad (5)$$

The mean motion (Kepler's third law) is

$$n = \dot{M} = \mu^{\frac{1}{2}} a^{-\frac{3}{2}}. \quad (6)$$

From Equations 3, 5, and 6:

$$dM = \left[ -\frac{r^2}{a^2 \sqrt{1 - e^2}} \right] df = (1 - e \cos E) dE \quad (7)$$

$$r = \frac{a(1 - e^2)}{1 + e \cos f} = a(1 - e \cos E) \quad (8)$$

$$\left. \begin{aligned} df &= \frac{(1 - e^2)^{\frac{1}{2}}}{1 - e \cos E} dE \\ dE &= \frac{(1 - e^2)^{\frac{1}{2}}}{1 + e \cos f} df \end{aligned} \right\} \quad (9)$$

A closed expression relating  $f$  and  $M$  is impossible; series expansions for this and other relationships are given in the standard texts, for example, Reference 9, pp. 33-48 and Reference 15, pp. 71-81. Many formulas particularly applicable to satellites are given in Reference 16.

The elliptic motion described in Equations 2 through 9 results from the motion of a particle of negligible mass in the central field described by Equation 1. This central force can be expressed as the negative of a derivative of a scalar potential. Thus,

$$\left. \begin{aligned} \mathbf{F}_r &= -m \frac{\partial V}{\partial r} \\ V &= -\frac{\mu}{r} \end{aligned} \right\} . \quad (10)$$

Equation 10 follows the sign convention of physics for  $V$ . In astronomy and geodesy this sign convention is reversed and the negative of the potential, sometimes called the force function, is used. Thus,

$$\left. \begin{aligned} \mathbf{F}_r &= m \frac{\partial U}{\partial r} \\ U &= \frac{\mu}{r} \end{aligned} \right\} . \quad (11)$$

Hereafter, we shall always use  $V$  for the potential when following the physical convention of Equation 10 and  $U$  for the force function when following the astronomic convention of Equation 11.

The ellipse results from the solution of the equations of motion, in vectorial form,  $\mathbf{r} = (x, y, z)$  are

$$m \ddot{\mathbf{r}} = \mathbf{F} = -m \nabla V = m \nabla U . \quad (12)$$

All complications and developments of interest arise from the small departure  $R$  of the potential from the form of Equation 10 or Equation 11

$$\left. \begin{aligned} V &= -\frac{\mu}{r} - R \\ U &= \frac{\mu}{r} + R \end{aligned} \right\} . \quad (13)$$

The most significant terms in  $R$  are:

(1) The earth's oblateness

$$R_2 = -\frac{\mu a_e^2}{r^3} J_2 P_2(\sin \phi) \quad (14)$$

where  $a_e$  is the equatorial radius;  $J_2$  is the oblateness, or flattening, parameter (about  $10^{-3}$ ); and  $P_2(\sin \phi)$  is the Legendre Polynomial of second degree.

(2) The sun or moon (Reference 9, p. 254 and Reference 15, p. 308)

$$R_s = \mu^* \left[ \frac{1}{|\mathbf{r} - \mathbf{r}^*|} - \frac{\mathbf{r} \cdot \mathbf{r}^*}{r^{*3}} \right] \quad (15)$$

where the asterisked quantities refer to the disturbing body, sun or moon, in the earth-centered coordinate system.

(3) The atmospheric drag which is derivable from a potential of velocity rather than of position

$$R_d = -\frac{b(r)}{3} |\dot{\mathbf{r}}|^3 \quad (16)$$

from which drag forces  $F_{d,i}$  are obtained by derivatives with respect to velocity; thus,

$$F_{d,i} = m \left( \frac{\partial R_d}{\partial \dot{r}_i} \right) = -mb(r) \dot{r}_i |\dot{\mathbf{r}}|. \quad (17)$$

The development of the effects of  $R_2$ ,  $R_s$ , and  $R_d$  [including definition of the function  $b(r)$ ] are taken up in paragraphs 5, 6, and 8 of this section, respectively. First discussed are some general principles and procedures to treat the equations of motion (Equation 1) with a potential of form of Equation 13, in particular to take advantage of the fact that the motion departs slightly from that of the Kepler ellipse (Equations 2 through 9).

The kinetic energy is

$$T = \frac{m}{2} |\dot{\mathbf{r}}|^2. \quad (18)$$

The momentum is

$$\mathbf{p}_i = \frac{\partial T}{\partial \dot{r}_i} = m \dot{r}_i. \quad (19)$$

Taking  $m = 1$  and  $q_i = r_i$ , Equation 19 becomes

$$p_i = \frac{\partial T}{\partial \dot{p}_i} = \dot{q}_i \quad (20)$$

and from Equation 12 there is obtained

$$\ddot{r}_i = \dot{p}_i = - \frac{\partial V}{\partial q_i} \quad (21)$$

If it is assumed  $R_d = 0$ , the Hamiltonian is defined as

$$H = T + V \quad (22)$$

and the following canonical equations are obtained:

$$\dot{q}_i = \frac{\partial H}{\partial p_i}, \quad \dot{p}_i = - \frac{\partial H}{\partial q_i} \quad (23)$$

The six first order differential equations (Equation 23) replace the three second order differential equations (Equation 12).

In the astronomical sign convention, symbolize the negative of  $H$  by  $F$ . Then,

$$F = U - T \quad (24)$$

and

$$\dot{q}_i = - \frac{\partial F}{\partial p_i}, \quad \dot{p}_i = \frac{\partial F}{\partial q_i} \quad (25)$$

There exist many sets of canonical variables  $p_i, q_i$  which can be used in Equations 23 or 25. The set most closely related to the Keplerian elements is that of Delaunay (Reference 9, p. 152 and Reference 15, p. 290)

$$\left. \begin{aligned} p_1 &= L = (\mu a)^{\frac{1}{2}}, & q_1 &= \ell = M \\ p_2 &= G = [\mu a(1 - e^2)]^{\frac{1}{2}}, & q_2 &= g = \omega \\ p_3 &= H = [\mu a(1 - e^2)]^{\frac{1}{2}} \cos i, & q_3 &= h = \Omega \end{aligned} \right\} \quad (26)$$

49856		10. DUPLICATE <input type="checkbox"/> YES <input type="checkbox"/> NO		VOL. <input type="checkbox"/> 1 <input type="checkbox"/> 2 <input type="checkbox"/> 3		ISSUE <input type="checkbox"/> 1 <input type="checkbox"/> 2 <input type="checkbox"/> 3		17. ACCESSION NO.	
1. NO. OF COPIES AND SOURCE		11. ACTION <input type="checkbox"/> TAB <input type="checkbox"/> PB <input type="checkbox"/> TT <input type="checkbox"/> RECORD CARD <input type="checkbox"/> REJECT		18. NO. OF PAGES ACTUAL		PRICING			
2. TYPE OF DOCUMENT <input type="checkbox"/> MICROFICHE <input type="checkbox"/> HARD COPY		12. HOLD OR <input type="checkbox"/> RELEASE <input type="checkbox"/> POLICY <input type="checkbox"/> REACQ. <input type="checkbox"/> COPYRIGHT		19. PRICE MICRO		HARD COPY			
3. LOAN DOCUMENT <input type="checkbox"/> YES <input type="checkbox"/> NO		13. DOCUMENT <input type="checkbox"/> INCOMPLETE <input type="checkbox"/> NOT REPRODUCIBLE <input type="checkbox"/> REPRODUCIBLE		20. PRESTOCK <input type="checkbox"/> YES <input type="checkbox"/> NO		NO. OF COPIES			
4. DATE RECEIVED YEAR <input type="checkbox"/> MO. <input type="checkbox"/> DAY <input type="checkbox"/>		14. ODD SIZE <input type="checkbox"/> YES <input type="checkbox"/> NO		21. MICROFICHE <input type="checkbox"/> YES <input type="checkbox"/> NO		NO. OF COPIES			
5. TECHNICAL REPORT NO.		15. SPECIAL PRINTING INSTRUCTIONS		22. PUBLICIZE <input type="checkbox"/> YES <input type="checkbox"/> NO					
6. MONITORING AGENCY SERIES NO.		16. EVALUATOR'S INITIALS & DATE		23. ANNOUNCEMENT CATEGORY					
7. CONTRACT NO.		24. REMARKS (GIVE TITLE IF 5, 6, AND 7 ARE BLANK)							
8. SERIAL NO. - DATES OF COVERAGE									
9. DATE OF REPORT YEAR <input type="checkbox"/> MO. <input type="checkbox"/> DAY <input type="checkbox"/>		DOCUMENT TRAVELER FORM		U. S. DEPARTMENT OF COMMERCE NATIONAL BUREAU OF STANDARDS					

FORM NBS-801  
(8/6/64)



49856		17. ACCESSION NO.	
1. NO. OF COPIES AND SOURCE		10. DUPLICATE <input type="checkbox"/> YES <input type="checkbox"/> NO	
2. TYPE OF DOCUMENT <input type="checkbox"/> MICROFICHE <input type="checkbox"/> HARD COPY		11. ACTION <input type="checkbox"/> TAB <input type="checkbox"/> PB <input type="checkbox"/> TT <input type="checkbox"/> RECORD CARD <input type="checkbox"/> REJECT	
3. LOAN DOCUMENT <input type="checkbox"/> YES <input type="checkbox"/> NO		12. HOLD OR <input type="checkbox"/> RELEASE <input type="checkbox"/> POLICY <input type="checkbox"/> REACQ. <input type="checkbox"/> COPYRIGHT	
4. DATE RECEIVED YEAR   MO.   DAY		13. DOCUMENT <input type="checkbox"/> INCOMPLETE <input type="checkbox"/> NOT REPRODUCIBLE <input type="checkbox"/> REPRODUCIBLE	
5. TECHNICAL REPORT NO.		14. ODD SIZE <input type="checkbox"/> YES <input type="checkbox"/> NO	
6. MONITORING AGENCY SERIES NO.		15. SPECIAL PRINTING INSTRUCTIONS	
7. CONTRACT NO.		16. EVALUATOR'S INITIALS & DATE	
8. SERIAL NO. - DATES OF COVERAGE		17. ANNOUNCEMENT CATEGORY	
9. DATE OF REPORT YEAR   MO.   DAY		18. NO. OF PAGES ACTUAL   PRICING	
		19. PRICE MICRO   HARD COPY	
		20. PRESTOCK <input type="checkbox"/> YES <input type="checkbox"/> NO	
		21. MICROFICHE <input type="checkbox"/> YES <input type="checkbox"/> NO	
		22. PUBLICIZE <input type="checkbox"/> YES <input type="checkbox"/> NO	
		23. ANNOUNCEMENT CATEGORY	
24. REMARKS (GIVE TITLE IF 5, 6, AND 7 ARE BLANK)			
FORM NBS-801 (8/6/64)			
U. S. DEPARTMENT OF COMMERCE NATIONAL BUREAU OF STANDARDS		DOCUMENT TRAVELER FORM	

\_\_\_\_\_

From Equations 4, 13, 18, 24, and 26

$$F = \frac{\mu^2}{2L^2} + R. \quad (27)$$

Another set of canonical variables useful when the eccentricity approaches zero ( $g = \omega$  loses definition) or the inclination approaches zero ( $h = \Omega$  loses definition) is (Reference 15, p. 240):

$$\left. \begin{aligned} L, & \quad \ell + g + h \\ G - L, & \quad g + h \\ H - G, & \quad h \end{aligned} \right\}. \quad (28)$$

Using Equations 26 and 27 to transform from canonical to Keplerian variables, and defining  $n$  by Equation 6, the equations of motion in terms of the Keplerian elements are obtained (Reference 9, p. 147 and Reference 15, p. 289):

$$\left. \begin{aligned} \dot{a} &= \frac{2}{na} \cdot \frac{\partial R}{\partial M} \\ \dot{e} &= \frac{1 - e^2}{na^2 e} \cdot \frac{\partial R}{\partial M} - \frac{(1 - e^2)^{\frac{1}{2}}}{na^2 e} \cdot \frac{\partial R}{\partial \omega} \\ \dot{\omega} &= - \frac{\cos i}{na^2 (1 - e^2)^{\frac{1}{2}} \sin i} \frac{\partial R}{\partial i} + \frac{(1 - e^2)^{\frac{1}{2}}}{na^2 e} \frac{\partial R}{\partial e} \\ \frac{di}{dt} &= \frac{\cos i}{na^2 (1 - e^2)^{\frac{1}{2}} \sin i} \frac{\partial R}{\partial \omega} - \frac{1}{na^2 (1 - e^2)^{\frac{1}{2}} \sin i} \frac{\partial R}{\partial \Omega} \\ \dot{\Omega} &= \frac{1}{na^2 (1 - e^2)^{\frac{1}{2}} \sin i} \frac{\partial R}{\partial i} \\ \dot{M} &= n - \frac{1 - e^2}{na^2 e} \frac{\partial R}{\partial e} - \frac{2}{na} \frac{\partial R}{\partial a} \end{aligned} \right\}. \quad (29)$$

Equations 29 are the simplest means of obtaining the first approximation to the effect of a disturbing function  $R$  on the orbital elements. Similar equations can be obtained expressing the disturbing force in radial, transverse, and normal components (Reference 9, p. 151 and Reference 15, p. 301). However, to obtain the second approximation, as is necessary for  $R_2$  in the case of the close satellite and for  $R_s$  in the case of the distant satellite, the algebra in proceeding from Equation 29 becomes exceedingly complex.

Hence, we return to the canonical equations (Equation 25), adhering to the astronomical sign convention.

First, generalize the canonical equations by adding one more dimension each to  $\mathbf{p}, \mathbf{q}$ . Thus,

$$p_4 = t, \quad q_4 = - \int \frac{\partial(F + q_4)}{\partial t} dt \quad (30)$$

which obey Equation 25, using  $F + q_4$  in place of  $F$ .

This generalization is analogous to transforming the expression for a surface from the form  $z = f(x, y)$  to the form  $F(x, y, z) = 0$ ; it is necessary to deal with (negative) Hamiltonians  $F$  containing the time explicitly, and also desirable in that a more symmetrical manner of expression is conducive to improved insight.

If an orbit, called an intermediate orbit, can be found for which the solution of the canonical equations (Equation 25) is known with coordinates  $(\mathbf{p}', \mathbf{q}')$  at any given time close to the coordinates  $(\mathbf{p}, \mathbf{q})$  of the actual orbit, then the solution of the actual orbit can be expressed as that of the intermediate orbit plus a Taylor series development over the small difference  $(\mathbf{p}', \mathbf{q}') \rightarrow (\mathbf{p}, \mathbf{q})$ . An orbit which is solvable is one for which the Hamiltonian  $F'$  is a function of the momenta  $p'_i$  only; then, from Equation 25

$$\left. \begin{aligned} \dot{p}'_i &= \frac{\partial F'}{\partial q'_i} = 0 \\ p'_i &= \text{constant} \\ \dot{q}'_i &= \frac{\partial F'}{\partial p'_i} = \text{constant} \\ q'_i &= q'_{i0} + \text{constant} (t - t_0) \end{aligned} \right\} \quad (31)$$

To keep this intermediate orbit close to the actual orbit, its Hamiltonian  $F'$  must be made equal to the constant part of the actual Hamiltonian  $F$  (or, if drag is being taken into account, to the secularly changing part of  $F$ , which complication is ignored in this section)

$$F'(\mathbf{p}') = F(\mathbf{p}, \mathbf{q}) - \int \frac{\partial U_p}{\partial t} dt = F - \int \frac{\partial R_p}{\partial t} dt \quad (32)$$

where  $U_p = R_p$  is the part of the force function (negative potential) with an explicit periodic dependence on time. The two Hamiltonians are developed in series, with the principal term of  $F$  also a function only of momenta

$$\left[ F'_0(\mathbf{p}') + F'_1(\mathbf{p}') + F'_2(\mathbf{p}') + \dots \right] = \left[ F_0(\mathbf{p}) + F_1(\mathbf{p}, \mathbf{q}) + F_2(\mathbf{p}, \mathbf{q}) + \dots \right] - \int \frac{\partial R}{\partial t} dt \quad (33)$$

where the subscripts 0, 1, 2, . . . indicate the order of magnitude to which the parameters characterizing the disturbing function  $R$  appear as factors in the terms, for example, powers of  $J_2$  for  $R_2$ , or powers of the ratio  $n^*/n$  of solar to satellite mean motion for  $R_s$ . To make the procedure (Equations 31 through 33) possible we must select a coordinate system in which the dominant part  $F_0$  of the Hamiltonian is expressible solely in terms of momenta, such as the Delaunay coordinates (Equations 26 or 28), which yield the form Equation 27 for  $F$ .

The problem now is: given the canonical variables  $(\mathbf{p}', \mathbf{q}')$  at any time, find the variables  $(\mathbf{p}, \mathbf{q})$  of the actual orbit at the same time; that is, make a canonical transformation

$$(\mathbf{p}', \mathbf{q}') \rightarrow (\mathbf{p}, \mathbf{q}) \quad (34)$$

by a method which is as systematic and simple as possible.

The leading method (not the only one) originated by von Zeipel (Reference 17), employs an arbitrary function  $S(\mathbf{p}, \mathbf{q}, \mathbf{p}', \mathbf{q}')$  called a generating function or a determining function. Since by Equations 25, 31 and 33, two of the four sets  $\mathbf{p}, \mathbf{q}, \mathbf{p}', \mathbf{q}'$  are functions of the other two,  $S$  is expressible as a function of only two of the sets. That most commonly used is

$$S = S(\mathbf{p}', \mathbf{q}) \quad (35)$$

The other two sets are then defined as

$$p_i = \frac{\partial S}{\partial q_i}, \quad q'_i = \frac{\partial S}{\partial p'_i} \quad (36)$$

$S$  is developed in a manner similar to  $F$  and  $F'$

$$S = S_0 + S_1 + S_2 + \dots \quad (37)$$

where the subscripts have the same significance as in Equation 33. The term  $S_0$  must have a form such that  $p_i = p'_i$  and  $q_i = q'_i$  in the unperturbed case (that is, when  $S_1 = 0$ ,  $S_2 = 0$ , etc.)

$$S_0 = \sum_i q_i p'_i \quad (38)$$

Substitute Equation 38 in Equation 37, differentiate with respect to  $q_i$  and  $p_i'$ , and substitute in Equation 36

$$p_i = p_i' + \frac{\partial S_1}{\partial q_i} + \frac{\partial S_2}{\partial q_i} + \dots, \quad q_i = q_i' - \frac{\partial S_1}{\partial p_i'} - \frac{\partial S_2}{\partial p_i'} - \dots \quad (39)$$

Making the substitutions from Equation 30 for  $p_4 = p_4'$  and  $q_4 = q_4'$  in Equation 39 and comparing with Equation 32

$$\text{and} \quad \left. \begin{aligned} F' &= F - \frac{\partial S}{\partial t} \\ \frac{\partial S}{\partial t} &= \int \frac{\partial R_p}{\partial t} dt \end{aligned} \right\} \quad (40)$$

Equation 40 is a form of the Hamilton-Jacobi equation; in other forms 0 appears on the left and  $F$  is expressed as

$$U - \frac{1}{2} \sum_i \left( \frac{\partial S}{\partial q_i} \right)^2$$

(from Equations 8, 24, and 36).

Develop  $F$  in Equation 33 in Taylor Series of  $(p_i - p_i')$ ,  $(q_i - q_i')$ , where  $i = 1, 2, 3$  and substitute for  $(p_i - p_i')$ ,  $(q_i - q_i')$  from Equation 39 (summing repeated indices  $i, j$  from 1 to 3 in all products)

$$F - \frac{\partial S}{\partial t} = F_0(p') + \left\{ \begin{aligned} &+ \frac{\partial F_0}{\partial p_i'} \frac{\partial S_1}{\partial q_i} + F_1(p', q') - \frac{\partial S_1}{\partial t} \\ &+ \frac{\partial F_0}{\partial p_i'} \frac{\partial S_2}{\partial q_i} + \frac{1}{2} \frac{\partial^2 F_0}{\partial p_i' \partial p_j'} \left( \frac{\partial S_1}{\partial q_i} \right) \left( \frac{\partial S_1}{\partial q_j} \right) + \frac{\partial F_1}{\partial p_i'} \frac{\partial S_1}{\partial q_i} - \frac{\partial F_1}{\partial q_i'} \frac{\partial S_1}{\partial p_i'} + F_2(p', q') - \frac{\partial S_2}{\partial t} \\ &+ \dots \end{aligned} \right\} = \left\{ \begin{aligned} &F'_0 \\ &+ F'_1 \\ &+ F'_2 \\ &+ \dots \end{aligned} \right\} \quad (41)$$

Equate terms of equal magnitude in  $F$  and  $F'$ . These equations determine the terms in  $S$ ; since  $F'$  can only contain the  $p_i'$ , any  $q_i$  terms in the development of  $F$  (including those terms, if any, with an explicit dependence on time) must be accounted for by the  $S$  terms. For example, split  $F_1$  into two parts

$$F_1 = F_{1s}(p') + F_{1p}(p', q') \quad (42)$$

then,

$$F'_1 = F_{1s}(\mathbf{p}'), \quad (43)$$

and

$$\frac{\partial S_1}{\partial q_i} = - \frac{F_{1p}(\mathbf{p}', \mathbf{q}')}{\partial F_0 / \partial p_i}. \quad (44)$$

For the 1st order term in  $p_i$ ,  $\partial S_1 / \partial q_i$  from Equation 44 is used directly in Equation 39; for the 1st order term in  $q_i$ , Equation 44 is integrated with respect to  $q_i$  and then differentiated with respect to  $p'_i$  for use in Equation 39. These derivatives

$$\frac{\partial S_1}{\partial q_i}, \quad \frac{\partial S_1}{\partial p'_i}$$

are also used in the 2nd order term of Equation 41 to evaluate  $S_2$ ,  $F'_2$  for the second approximations, and so forth. The difficult problem is usually finding

$$\frac{\partial S_1}{\partial q_i}, \quad \frac{\partial S_2}{\partial q_i}$$

which are integrable.

The foregoing development has attempted to bring out those features of orbital theory which help the most to understand the principal methods applied to satellite orbits. However, classical dynamics is impressive for the many different ingenious ways of treating the same problems, and even for the different interpretations of the same mathematics: for example, in the foregoing treatment, we have considered the canonical transformation  $(\mathbf{p}', \mathbf{q}') \rightarrow (\mathbf{p}, \mathbf{q})$  as shifting from one point to another; this transformation may also be considered as holding the point fixed and changing the coordinate systems. The canonical equations (Equation 25) and the generating function  $S$  (Equation 35) are both special cases of more general forms. The independent variable of the canonical equations is not necessarily time; any arbitrary parameter  $w$  may be used for which  $dw/dt$  is known.

The generating function is one of the general category of action integrals

$$A = \int p_i dq_i \quad (45)$$

in which  $p_i, q_i$  defined by Equation 30 are included. Thus, for example, Hamilton's principle states that for integration from given starting coordinates over any time interval a particle will move so that  $A$  is stationary—that is, for any small arbitrary variation of the path of integration  $\delta A = 0$ —from which the equations of motion (Equation 12) can be derived. Also,  $A$  is equal to the integral of the Lagrangian  $L = T + U$  with respect to time over the same interval. For these and other methods, see Reference 6, pp. 1-39, 215-317, Reference 8, pp. 98-197, Reference 9, pp. 129-157, 177-206, Reference 15, pp. 273-306, 530-562, and Reference 18.

## Characteristics of Methods of Solution

Taking into account the considerations discussed above, the following steps must be accomplished, either implicitly or explicitly, in solving any satellite problem (not necessarily in the precise sequence given):

- selection of a coordinate system
- selection of the independent variable
- development of the disturbing function in terms of the selected coordinate system and independent variable
- expression of the equations of motion in terms of the coordinate system and independent variable
- selection of an intermediate orbit, or, alternatively, solution of the principal part of the equations of motion
- definition of the constants of integration
- development and integration of the equations of motion in a manner suitable for their solution for the position and/or velocity at any time.

As an aid to later comparing the different solutions of the satellite problem, the following is an attempt to describe the principal methods of accomplishing each of these steps:

### *Coordinate system*

The logical choice for an origin is the center of mass of the earth; for the lunar problem, the effect of the appreciable mass of the moon on the center of gravity of the system is taken care of by a simple factor applied to the force function referred to the earth's center (Reference 9, pp. 254-257, Reference 15, pp. 310-311, and Reference 19, pp. 2-8).

One coordinate plane is logically determined either by the principal disturbing function (the ecliptic for  $R_1$ , the equator for  $R_2$ ) or by the disturbed body (the plane of the intermediate orbit), with the axis directions in the plane determined by an arbitrary fixed point (the vernal equinox for the ecliptic or the equator, the ascending node or a departure point in the orbital plane) or rotating in a manner determined by the principal disturbing function.

Types of coordinates which have been employed include the rectangular, spherical, and ellipsoidal coordinates as well as the Keplerian and canonical orbit elements.

### *Independent variable*

As pointed out (page 13), time can be replaced by any arbitrary parameter  $w$  for which  $dw/dt$  is known. Some theories substitute the true anomaly  $f$  or the eccentric anomaly  $E$  in order to retain closed expressions for the disturbing function and its effects for each order of approximation; as mentioned (page 5), a closed expression relating  $f$  and  $M$  or  $t$  is impossible while Kepler's equation relating  $M$  and  $E$  is transcendental in the latter. In any theory using one of these parameters in place of time, care must be taken to distinguish the parameter when it appears as the independent variable from when it appears as a coordinate.

### *Development of the disturbing function*

For close satellites, it quickly becomes apparent that an analytical development of the earth's potential in spherical or ellipsoidal harmonics is preferable even for numerical integration, due to the double attenuating effects of extrapolation to altitude and integration of the equations of motion. Transformation to orbital referred coordinates is straightforward, though tedious; see pages 22 and 35. The development of the lunar or solar perturbation is a more complex matter, since two sets of periodicities are involved; see pages 30 and 32.

### *Equations of motion*

The form of the equations is most strongly influenced by the choice of the coordinate system and intermediate orbit. Changes from the familiar inertial rectangular or spherical coordinate form may occur by use of rotating reference axes, in which coriolis

and centrifugal force terms occur; or by separation of effects in the orbital plane from effects on the orbital plane; or by use of an auxiliary function such as a type of action integral (Equation 45); or by transformation to an equation in terms of small departures from the intermediate orbit.

### *Intermediate orbit*

Intermediate orbits can be characterized as of two types: dynamical intermediaries which are defined by the terms in the potential (or force function) taken into account in the exactly solvable orbit, such as Equation 31; and geometrical intermediaries which are specified to have certain parameters and rates of change thereof without an orbit of these properties necessarily being derivable from any possible potential. A method of solution may have more than one intermediary, each characterizing a different stage of the solution: separating short from long period variations, or variations in the orbital plane from variations of the plane.

### *Constants of integration*

The most concise expression of the orbit in any theory are the six independent constants of integration: usually three momentum constants  $p_{i_0}$  and three position constants  $q_{i_0}$  at the epoch  $t_0$  (a particular instant of time). The easiest to visualize are the momentum and position of the actual orbit at epoch, expressed either in rectangular coordinates or osculating Keplerian elements. However, in mathematical practice it is much more convenient to define the constant in terms of the intermediate orbit, since its parameters are either constant or less variable than those of the actual orbit. The obvious choices mathematically are the constant parts of the momentum coordinates  $p_{i_0}$  and the secularly varying part of the position coordinates at the epoch  $q_{i_0}$ . However, in many theories the momentum coordinates are defined so that they are readily deducible from the observations of the position coordinates: the semimajor axis  $a_0$  (or its canonical equivalent  $L$ ) is defined in terms of the mean motion by Equation 6, or a modification of Equation 6; the eccentricity  $e_0$  (or  $G$ ) in terms of the coefficient of the  $\sin E$  or  $\sin f$  periodic variation of the mean longitude ( $\Omega + \omega + M$ ) or mean anomaly, as, for example, in Equation 3; and the inclination  $i_0$  in terms of the coefficient of the  $\sin(\omega + f)$  or similar variation in the sine of the declination or latitude. From the orbit-meridian-equator right spherical triangle in Figure 1 there is obtained:

$$\sin \phi = \sin i \cdot \sin(\omega + f) . \quad (46)$$

In this review the six constants of integration have been defined at an arbitrary time  $t_0$ . However, the epoch could also be specified by an arbitrary value of, or an arbitrary relation between, any of the three variables which have a secular variation:  $M$ ,  $\omega$ , and  $\Omega$  (or  $\ell$ ,  $g$ ,  $h$ ). There are theories in which the epoch is defined by  $M = 0$ ; in others, the

epoch is defined by a particular latitude of the satellite. For the latter definition, we get from Equation 46

$$f_o = \sin^{-1} \frac{\sin \phi_o}{\sin i} - \omega. \quad (47)$$

Thus, in such theories periodicities of  $(k \pm j)\omega$  may appear in place of periodicities  $(jf + k\omega)$  which appear in theories defining the epoch in terms of time. Defining the epoch in terms of the  $M$ ,  $\omega$ , and  $\Omega$ , or relations between them, is often related to the use of  $M$  (or  $E$  or  $f$ ) as the independent variable, and runs similar risks of confusion due to the double use as a position coordinate and independent variable.

Discussions of the constants of integration are given in Reference 15, pp. 411-413, Reference 19, pp. 115-124, and Reference 20.

*Development of the equations of motion and integration*

The usual procedure is a development in a literal series by a process of successive approximations such as is described in Equations 31 through 44. The result is the expression of the coordinates and velocity components in terms of a series expansion of the constants of integration, the parameters of the potential field and the independent variable, or in terms of intermediary functions. Such an expansion can be contracted considerably if in place of the theoretical secular rate of change of a position variable a numerical rate, based on observations, is substituted; this procedure is particularly applicable in the case of the moon for which the departure from perfect Newtonian mechanics is small and can be separated in the analysis of observations. The expansion can be contracted still further if we are willing to accept forms suitable for solution by iteration, for example, if a variable  $p_i$  is expressible as

$$p_i = p'_i [1 + \epsilon(p, q)] \quad (48)$$

where  $\epsilon \ll 1$ .

And finally, of course, the expansion can be contracted completely to the equations of motion themselves if we proceed by numerical integration from the start. However, for each of the steps described above, the different periodicities, interactions, etc., become less apparent, and hence the second purpose of the theory — a keener insight into the physical nature of the phenomena — becomes more difficult to attain.

Before applying the foregoing considerations to the various satellite theories which have been developed, two techniques of very general application are discussed. These techniques are empirical orbits and numerical integration.

### 3. EMPIRICAL ORBITS

As stated in Equation 31, if the dominant part of the (negative) Hamiltonian  $F = U - T$  can be expressed in terms of momenta  $p_i$  only, then each canonical variable can be expressed as a constant plus periodical terms plus, for the position variables, a secular term. The same holds true for the Keplerian elements  $a$ ,  $e$ ,  $i$ ,  $M$ ,  $\omega$ , and  $\Omega$ . Hence, if a purely Newtonian physical situation existed, perfectly observed variations of a Keplerian orbit could be completely accounted for by empirical Fourier series

$$\begin{bmatrix} a \\ e \\ i \\ M \\ \omega \\ \Omega \end{bmatrix} = \begin{bmatrix} a_o \\ e_o \\ i_o \\ M_o \\ \omega_o \\ \Omega_o \end{bmatrix} + \begin{bmatrix} 0 \\ 0 \\ 0 \\ n \\ \dot{\omega} \\ \dot{\Omega} \end{bmatrix} (t - t_o) + \sum_{k=1}^{\infty} \begin{bmatrix} C_{ak} \\ C_{ek} \\ C_{ik} \\ C_{Mk} \\ C_{\omega k} \\ C_{\Omega k} \end{bmatrix} \cos \alpha_k (t - t_o) + \sum_{k=1}^{\infty} \begin{bmatrix} S_{ak} \\ S_{ek} \\ S_{ik} \\ S_{Mk} \\ S_{\omega k} \\ S_{\Omega k} \end{bmatrix} \sin \beta_k (t - t_o). \quad (49)$$

Since, as described in Paragraphs 5 and 7 of this section, the gravitational variations of interest to geodesy appear in the orbit as periodic or secular changes of known frequency, they should be most conveniently deduced from the empirically determined  $C$ 's and  $S$ 's in Equation 49.

Methods of deducing empirical orbits from satellite observations have been most extensively developed in the differential orbit improvement program of Veis and associates at the Smithsonian Astrophysical Observatory (Reference 1, pp. 135-144 and Reference 21). The actual physical situation not being purely Newtonian, polynomial terms, exponential terms, and hyperbolic terms are added to take into account drag and other variations.

The complete expression possible for each orbital element  $E_i$  is thus of the form

$$E_i = \sum_j \left\{ P_{ij} (t - t_o)^j + S_{0ij} \sin [S_{1ij} + S_{2ij} (t - t_o)] \right. \\ \left. + E_{0ij} \exp [E_{1ij} (t - t_o)] + H_{0ij} (H_{1ij} - t)^{H_{2ij}} \right\}. \quad (50)$$

Furthermore, the variations are not perfectly observed. The program is primarily designed for application to directional observations; hence, the semimajor axis is not included in the elements analyzed by Equation 50, but rather taken as deduced from the observed mean motion  $\bar{n}$  using Equation 63. Secondly, the observations are generally made at a frequency that is appreciably less than that of the satellite orbit, so that spurious long period variations could be deduced due to aliasing (Reference 22, pp. 31-33)

by short period variations of frequency  $n$ ,  $2n$ , etc. Hence, the short period variations due to the oblateness  $J_2$  are computed by Kozai's formulae (Reference 23) and removed before applying the analysis (Equation 50).

Empirical orbits are regularly computed by the Smithsonian Institution Astrophysical Observatory and published in their series Research in Space Science, Special Reports.

## 4. NUMERICAL INTEGRATION

Given adequate computing facilities, the easiest solution to the dynamical problem is numerical integration of the equations of motion (Equation 12) in rectangular coordinates by one of the textbook methods for solution of simultaneous higher order ordinary differential equations (Reference 24, pp. 261-306, and Reference 25, pp. 375-411). In astronomy, numerical solution in inertial rectangular coordinates is generally known as Cowell's method; it is described in Reference 9, pp. 218-222, Reference 12, pp. 89-91, and Reference 15, pp. 169-175. Numerical integration in rectangular coordinates is the most widely applied method, and programs for its application exist at all orbit computing centers either as the principal method or as a check on a general theory program.

The numerical integration techniques of probably greatest application in the United States are those developed by Cunningham, essentially described in Reference 26. To retain sufficient precision for geodetic use over several weeks, a double-precision code — one carrying more than 8 significant decimal digits — is required, and the time interval must be 2 minutes or less for a close satellite. In Reference 26, central differences up through the 10th difference are employed. Iterative evaluation of the integrals is used to carry forward the position and velocity components for 9 successive steps, after which a check is made by computing the position components for the 5th step by a central difference formula; if agreement within  $10^{-11}$  is not obtained, the time interval is halved; if agreement within  $10^{-15}$  is obtained, the time interval is doubled. A single precision ( $10^{-8}$ ) code (Reference 27) is ten times as fast, and probably adequate for geodetic use for durations of about a day with a time interval of one minute. See Reference 15, pp. 158-159 and Reference 28 for discussion of error accumulation in numerical integration.

The interval of integration can be greatly increased and hence computing economized if the numerical solution is made for small departures from a known solution, that is, for perturbations to an intermediate orbit. Such methods are known as special perturbations in astronomy, where they have been long applied. The most common method for particles of negligible mass is Encke's (Reference 9, pp. 222-224, Reference 12, pp. 91-105, and Reference 15, pp. 176-182) in which the departures from a Keplerian orbit are computed in rectangular coordinates. These departures ( $\xi = \mathbf{x} - \mathbf{x}'$ ) appear in a differential equation

$$\ddot{\xi} = \frac{\mu}{r'^3} (fq\mathbf{x} - \xi) + \nabla R \quad (51)$$

where  $f_q$  is the negative of the sum of all terms after the first in the binomial expansion of  $(r'/r)^3$ : that is, a quantity of the order  $\xi/r$ . The form of Equation 51 is used because it is convenient for desk calculation since  $f$  can be tabulated as a function of  $q$  (Reference 12, p. 155). For application to earth satellites, Encke's method could be generalized so that  $r'$  referred to an intermediate orbit taking into account the oblateness.

A method analogous to Encke's in polar coordinates is Hansen's (Reference 9, pp. 224-227); however, it is complicated enough that one might as well go directly to numerical integration in terms of the Keplerian elements, using Equation 29 or the similar forms expressing the disturbing forces in orthogonal components. Methods of numerical integration in terms of the Keplerian, or similar, elements are known as variation of arbitrary constants or variation of parameters or variation of elements. Several such methods [Brouwer's (Reference 15, pp. 398-414) or Musen's (Reference 29)] have been developed either in terms of Keplerian elements alone or a combination of some of them with rectangular or polar coordinates. The further theoretical development of numerical methods leads logically to a numerical general theory as discussed on pages 26 through 28.

Another numerical method of considerable potential for problems of interest to geodesy is expression of the perturbations of the elements, or the coordinates, as numerical Fourier series (Reference 30). This method was apparently originated by Airy to apply to the lunar problem (Reference 19, pp. 245-246) and has been recently applied to improving lunar orbit computation by Eckert (Reference 31).

Discussions comparing different numerical methods are found in References 32, 33, and 34; in general, the simpler methods, such as Cowell's, are preferable if it is desired to economize in programming and if large or variable perturbations are to be taken into account, while the more developed methods in the category of variation of constants are preferable if the time duration is long, if the perturbations are small and systematic, and if computer time needs to be economized. The more developed methods also give a better physical sense of what is happening.

## 5. GENERAL THEORIES: CLOSE SATELLITE PROBLEM

We define the close satellite problem as the solution of the equations of motion for a particle of negligible mass in the potential field with the disturbing function  $R_2$  of Equation 14. It may seem historically inappropriate to discuss the close satellite problem before the lunar problem, but the close satellite problem is both the more important

to geodesy and the easier, until recently having ". . . held the distinction of being the simplest of the unsolved problems of celestial mechanics" (Reference 35).

The first order solution of the problem is attained most simply by using  $R_2$  in the Lagrangian equations (Equation 29). As a consequence, perturbations of the elements are obtained all proportionate to  $J_2$ . The coefficient  $J_2$  is about  $10^{-3}$  for the earth; the other coefficients of the earth's gravitational field in which we are interested are  $10^{-6}$  or less, so it is necessary that terms proportionate to  $J_2^2$  also be considered. To keep the number of references to a minimum, we shall discuss only theoretical developments which either carry effects to include  $J_2^2$  (in Paragraph 5 of this section) or develop the first order effects for the general term of coefficient  $J_{nm}, K_{nm}$  (in Paragraph 7 of this section). Of the many derivations of the first order effects of particular terms, only those of Krause (Reference 36) and Spitzer (Reference 37) warrant mention as having priority. This discussion is based on the seven items listed on pages 14 through 17 as characterizing methods of solution. The coordinate systems and the expression of the potential therein are discussed separately. All the solutions discussed also treat the effects of  $J_4$ , and some treat the effects of  $J_3$  and  $J_5$ , but only to the first order, so in this review consideration of  $J_3, J_4$ , and  $J_5$  effects is postponed to Paragraph 7 of this section.

## Disturbing Function

The force function (negative potential) in spherical polar coordinates is

$$U = \frac{\mu}{r} \left[ 1 - J_2 \left( \frac{a_e}{r} \right)^2 \left( \frac{3}{2} \sin^2 \phi - \frac{1}{2} \right) \right] . \quad (52)$$

The force function (negative potential) in rectangular coordinates is

$$U = \frac{\mu}{(x^2 + y^2 + z^2)^{\frac{1}{2}}} \left[ 1 - J_2 \frac{a_e^2}{x^2 + y^2 + z^2} \left( \frac{3z^2}{2(x^2 + y^2 + z^2)} - \frac{1}{2} \right) \right] . \quad (53)$$

In an oblate rotational ellipsoidal coordinate system for which the potential (Equation 52 or 53) coincides with the same ellipsoidal coordinate surface at the equator and the pole (References 38 and 39)

$$U = \frac{\mu}{(c^2 + \rho^2 - c^2 \sigma^2)^{\frac{1}{2}}} \left\{ 1 - \frac{c^2}{2(c^2 + \rho^2 - c^2 \sigma^2)} \left[ \frac{3\rho^2 \sigma^2}{c^2(1 - \sigma^2) + \rho^2} - 1 \right] \right\} \quad (54)$$

where

$$c = a_e J_2^{\frac{1}{2}}$$

$\rho$  specifies an ellipsoidal surface

$\sigma$  specifies a hyperboloidal surface by the sine of the angle between its asymptote and the equator.

The coordinates are not readily separable in Equation 54, so a solution using ellipsoidal coordinates more conveniently uses (References 38 and 39)

$$U_E = \frac{\mu \rho}{\rho^2 + c^2 G^2} = \frac{\mu}{r} \sum_{n=0}^{\infty} (-1)^n J_2^n \left( \frac{a_e}{r} \right)^{2n} P_{2n}(\cos \phi) \quad (55)$$

which differs from  $U$  by a quantity of order  $J_2^2$ .

The potential (Equation 52) in osculating Keplerian elements (References 23, 40, and Reference 15, p. 564, or Reference 41) is

$$U = \frac{\mu}{a} \left\{ \left( \frac{a}{r} \right) - \frac{J_2}{4} \left( \frac{a_e}{a} \right)^2 \left( \frac{a}{r} \right)^3 \left[ (2 - 3 \sin^2 i) + 3 \sin^2 i \cos 2(\omega + f) \right] \right\} \quad (56)$$

and in Delaunay variables (Reference 15, p. 564 and Reference 40) is

$$U = \frac{\mu}{r} + \frac{\mu^4 J_2 a_e^2}{4L^6} \left[ \left( 3 \frac{H^2}{G^2} - 1 \right) \left( \frac{a}{r} \right)^3 + \left( 3 \frac{H^2}{G^2} - 3 \right) \left( \frac{a}{r} \right)^3 \cos 2(g + f) \right]. \quad (57)$$

To eliminate  $r$ ,  $f$  in Equations 56 and 57, elliptic expansions in powers of the eccentricity are required (Reference 9, pp. 44-46, Reference 15, p. 564 and Reference 40).

Methods of solution will be classified here — somewhat arbitrarily — according to whether or not the intermediate orbit is identifiable as an exact solution of a part of one of the potentials (Equations 52 through 57), that is, as dynamical or geometrical intermediaries. The notation has been converted as much as possible from that in the original papers to the notation used in this review. For conversions from other oblateness parameters to  $J_2$ , see Reference 40, 42, or 43.

## Dynamical Intermediary Theories

The theory of Brouwer (Reference 15, pp. 562-573 and Reference 40) is a solution of the Delaunay equations (Equations 25, 26, and 27) using the disturbing function in the form of Equation 57 by the method of canonical transformations as in Equations 37 through 44. To facilitate the integration of the determining function  $S$  and to keep the intermediary close to the actual orbit, two canonical transformations are made; the first to an orbit with Hamiltonian  $F'(L', G', H', g)$ , which thus has the same long period variations as the actual orbit, and the second to an orbit with Hamiltonian  $F''(L'', G'', H'')$ . This two-stage transformation necessitates an additional term  $(\partial F'_1 / \partial g)(\partial S_1 / \partial G')$  on the right of Equation 41. The term  $F'_1$  is completely determined; in performing integrations with respect to the mean anomaly  $\ell$ , the conversions of Equations 7 and 8 are used and the integrations formally made with respect to the true anomaly  $f$ . Only the long period (that is, not functions of  $\ell$ ) variations generated by  $S_2$  are determined, but otherwise the solution is complete to the second order: that is, all variations arising from  $F'_2, F''_2$  are developed. The constants of integration are the mean elements, that is, the constant parts  $a'', e'', i''$ , and the secularly changing parts at epoch  $\ell''_0, g''_0, h''_0$ . The unperturbed mean motion is defined as  $n_0 = \mu^{1/2} a''^{-3/2}$ , which makes the intermediary the Keplerian orbit corresponding to a potential  $U_0 = \mu/r'$ . Brouwer (Reference 40) also develops the first order long period and secular effects of  $J_3, J_4$ , and  $J_5$ . The problems of zero eccentricity and zero inclination can be solved by using the canonical variables (Equation 28). The secular and long period terms arising from  $J_2$ , in Brouwer's theory, where  $\eta = (1 - e''^2)^{1/2}$ ,  $\theta = \cos i''$ , and  $\gamma'_2 = a_e^2 J_2 / (2a''^2 \eta^4)$  are:

$$\left. \begin{aligned} \ell' &= \ell''_0 + n_0 t \left\{ 1 + \frac{3}{2} \gamma'_2 \eta (-1 + 3\theta^2) + \frac{3}{32} \gamma'^2_2 \eta [-15 + 16\eta + 25\eta^2 + (30 - 96\eta - 90\eta^2)\theta^2 \right. \\ &\quad \left. + (105 + 144\eta + 25\eta^2)\theta^4 \right\} + \frac{1}{8} \gamma'_2 \eta^3 \left[ 1 - 11\theta^2 - 40\theta^4(1 - 5\theta^2)^{-1} \right] \sin 2g'' \\ g' &= g''_0 + n_0 t \left\{ \frac{3}{2} \gamma'_2 (-1 + 5\theta^2) + \frac{3}{32} \gamma'^2_2 \left[ -35 + 24\eta + 25\eta^2 + (90 - 192\eta - 126\eta^2)\theta^2 \right. \right. \\ &\quad \left. \left. + (385 + 360\eta + 45\eta^2)\theta^4 \right] \right\} - \frac{1}{16} \gamma'_2 \left[ (2 + e''^2) - 11(2 + 3e''^2)\theta^2 \right. \\ &\quad \left. - 40(2 + 5e''^2)\theta^4(1 - 5\theta^2)^{-1} - 80e''^2\theta^6(1 - 5\theta^2)^{-2} \right] \sin 2g'' \\ h' &= h''_0 + n_0 t \left\{ -3\gamma'_2 \theta + \frac{3}{8} \gamma'^2_2 \left[ (-5 + 12\eta + 9\eta^2)\theta + (-35 - 36\eta - 5\eta^2)\theta^3 \right] \right\} \\ &\quad - \frac{1}{8} \gamma'_2 e''^2 \theta \left[ 11 + 80\theta^2(1 - 5\theta^2)^{-1} + 200\theta^4(1 - 5\theta^2)^{-2} \right] \\ e' &= e'' + \frac{1}{8} \gamma'_2 e'' \eta^2 \left[ 1 - 11\theta^2 - 40\theta^4(1 - 5\theta^2)^{-1} \right] \cos 2g'' \\ i' &= i'' - \frac{1}{8} \gamma'_2 e''^2 \cot i'' \left[ 1 - 11\theta^2 - 40\theta^4(1 - 5\theta^2)^{-1} \right] \cos 2g'' \end{aligned} \right\} \quad (58)$$

There are no long period variations in  $a$ . Note that second order periodic terms derived from  $F_2'$  and  $F_2''$  have become first order in the sense that their coefficients contain  $J_2$  rather than  $J_2^2$ . Also note that  $(-1 + 5\theta^2)$ , contained in the first order secular term for  $g'$ , reoccurs in these second order terms for all variables in the form  $(1 - 5\theta^2)^{-1}$ . Hence, this theory cannot be used near  $\theta = (1/5)^{1/2}$  or  $i = 63^\circ 26'$ . Such orbits must be treated separately; see page 30.

Kovalevsky (Reference 20) has developed a second order theory similar to Brouwer's.

Garfinkel's theory (References 35 and 44) uses as an intermediary the orbit corresponding to the potential  $U_0$ :

$$U_0 = \frac{\mu}{r} \left[ (1 - 3J_2 a_e^2 c_3) - \frac{3J_2 a_e^2 c_1 (\sin^2 \phi - c_2)}{2r} \right] \quad (59)$$

where

$$\begin{aligned} c_1 &= \frac{1}{a(1 - e^2)} \\ c_2 &= \cos^2 i \\ c_3 &= \frac{3 \cos^2 i - 1}{4a^2(1 - e^2)^{3/2}} \end{aligned}$$

The solution of the equations of motion with Equation 59 as the force function is a "pseudo-ellipse" involving two elliptic integrals. The values of the  $c_i$ 's selected cause this intermediary to absorb all first order secular motion. The canonical variables corresponding to the pseudo-ellipse are similar in form to the Delaunay variables (Equation 26) except that  $\mu$  is replaced by  $\mu' = \mu(1 - 3J_2 a_e^2 c_3)$  and  $H$  is multiplied by the factor

$$\left[ 1 + \frac{6J_2 a_e^2 \cos^2 i}{\mu' a^2 (1 - e^2)^2} \right]^{1/2}.$$

All first-order variations and all secular and long-period variations arising from  $F_2'$  in these pseudo-elliptic elements are found by a canonical transformation of the type outlined in Equations 37 through 44.

Sterne (Reference 45) solves for an intermediary orbit corresponding to the potential  $U_0$ :

$$U_0 = \frac{\mu}{r} \left[ 1 - 3J_2 a_e^2 \left\{ \frac{c_1 (\sin^2 \phi - c_2)}{2r} + \frac{c_4}{r^2} \right\} \right] \quad (60)$$

The solution for the intermediary requires four elliptic integrals. First order perturbations only are developed in Reference 45.

Vinti (References 38, 46, and 47) has developed a satellite theory in ellipsoidal coordinates. He obtains the Hamiltonian-Jacobi equations (Equation 40) corresponding to the ellipsoidal potential  $U_E$  of Equation 55 with each of the three coordinates  $\rho, \sigma$ , and right ascension  $\alpha$  separated into different terms, so that they are integrable by numerical integration or power series development in  $J_2$ . The constants of integration can be selected so that they are describable as generalizations of the Keplerian elements. There is no singularity at the critical inclination  $i = 63^\circ 26'$  as in Equation 58; there remains, however, the problem at the critical inclination of the perturbations due to the real  $J_4, J_6$ , etc., differing from the  $J_2^2, -J_2^3$ , etc., of Equation 55 (see page 22). Reference 38 describes the theory fully as far as the separated form of the Hamilton-Jacobi equations; a solution including all secular effects and periodic effects to  $O(J_2^2)$  has recently been published (Reference 46).

Izsak (Reference 39) has accomplished a solution of Vinti's equations which includes all terms to the second order: short period as well as long period. His solution of the Hamilton-Jacobi equations is of the form

$$S(\mathbf{p}, \mathbf{q}) = \int_{\rho_1}^{\rho} \frac{\sqrt{P(\rho)}}{\rho^2 + c^2} d\rho + \int_0^{\sigma} \frac{\sqrt{Q(\sigma)}}{1 - \sigma^2} d\sigma + p_3 \alpha \quad (61)$$

where  $P$  and  $Q$  are quartics of their specified arguments and the three momentum variables. The lower limits of integration are arbitrary and most conveniently set as the minimum of  $\rho$  (analogous to perigee) and the equator. Differentiating Equation 61 with respect to each of the momentum variables in turn to obtain the angle variables results in shifting the square roots to the denominator, making the integrals of elliptic type. Most of the development of Izsak's theory is devoted to transforming these integrals to normal forms and then expanding them in Fourier Series. The elliptic analogue of the true anomaly is made the independent variable, and the canonical momentum variables converted to analogues of  $a$ ,  $e$ , and  $\sin i$ . Closed expressions for  $\rho$  and  $\sigma$  are obtained as elliptic functions of  $a$ ,  $e$ ,  $\sin i$ , and constants which are functions thereof; these constants are developed in series of  $(c/a_e)$  to the fourth power: that is, to  $J_2^2$ . The four integrals obtained on differentiating Equation 61 are developed in Fourier Series of angles analogous to the argument of latitude and the true anomaly in Keplerian motion. Finally, these developments are combined to obtain convenient expressions for the coordinates and for other quantities of interest in terms of the orbital elements  $a$ ,  $e$ ,  $\sin i$ ,  $t_0$ ,  $\Omega$ ,  $\omega$ , and the true anomaly, which in turn is expressible in terms of time, the elements, and the parameters  $c$  and  $\mu$ . No small divisors appear, so the theory is good for all eccentricities and inclinations (including  $63^\circ 26'$ ).

Kozai (Reference 23) proceeds from the Lagrangian equations of motion (Equation 29), from which the first order perturbations are quickly obtained. The second order perturbations are obtained through integrations of the type

$$dE_i = \int \dot{E}_i dt + \sum_j dE_j \int \frac{\partial \dot{E}_i}{\partial E_j} dt - \sum_j \int \dot{E}_j \left( \int \frac{\partial \dot{E}_i}{\partial E_j} dt \right) dt \quad (62)$$

in which  $E_i$  is any element and  $\dot{E}_i$  is obtained from Equation 29. Kozai obtains all the second order long-period and secular terms except those in  $M$ , the mean anomaly. His constants of integration are the same as Brouwer's except for the semimajor axis  $\bar{a}$ :

$$\bar{a} = \left( 1 + \frac{1}{3} p + \frac{23}{27} p^2 \right) \mu^{\frac{1}{3}} (\bar{n})^{-\frac{2}{3}} \quad (63)$$

where

$$p = \frac{3J_2 a_e^2}{4(1-e^2)^{\frac{3}{2}}} (1 - 3 \cos^2 i) \mu^{-\frac{2}{3}} (\bar{n})^{\frac{4}{3}}$$

which is roughly equivalent to modifying  $\mu$  to the  $\mu'$  of Garfinkel.

Brouwer (References 48 and 49) has adapted the Hill-Brown lunar theory (see pages 32 through 34) to the close satellite problem, using rectangular coordinates rotating with the satellite (in the equatorial plane in Reference 48; in the orbital plane in Reference 49 with a circular intermediary). Reference 48 is developed to second order terms, but includes the inclination and eccentricity as power series developments to  $i^3$  and  $e^3$ , and so is precise only for nearly circular, nearly equatorial orbits. Reference 49 solves only the intermediary, and does not include the effect of eccentricity.

## Geometrical Intermediary Theories

The theory of Musen (References 50, 51 and 52) is based on that developed by Hansen for the moon. The treatment of perturbations is separated into two parts, those in the plane of the osculating orbit and those of this plane. This separation is accomplished by using as an intermediary for the in-plane perturbations a uniformly rotating Keplerian orbit referred to  $XY$  rectangular coordinate axes fixed in the orbital plane. The disturbing function  $R$  is developed in numerical Fourier Series (Reference 112, p. 123 and Reference 15, pp. 108-113) of the intermediate eccentric anomaly  $E'$  which is the independent variable. In developing the equations of motion, the polar angle  $v$  from the fixed  $X$  axis, or departure point, to the actual satellite is set equal to that for the fictitious satellite in the intermediate orbit; the perturbations computed are thus of the time the satellite passes

a specified polar angle:  $\delta z = z - t$ . The radial perturbations  $r(t)$  are expressed by a small ratio  $\nu$ :

$$r(t) = (1 + \nu) r'(z). \quad (64)$$

Both perturbations  $\delta z$  and  $\nu$  in the Hansen plane are determined by a single Hansen function  $\bar{W}$  most succinctly expressed as

$$\bar{W} = -1 - \left(\frac{h}{h'}\right) + 2 \left(\frac{h}{h'}\right) \left(\frac{1}{1 + \nu}\right), \quad (65)$$

where  $h$  is defined by Equation 5. (The  $h$  in Hansen's and Musen's notation is the reciprocal of  $h$  as used in this report.) The dimensionless quantity  $\bar{W}$ , like  $\delta z$  and  $\nu$ , vanishes in the unperturbed case: a principle applied throughout for convenience in computation. The function initially determined from the disturbing function  $R$  is  $dW/dE'$  where  $E'$  is used as the independent variable rather than a position parameter. In the integration with respect to  $E'$  to obtain  $W$  there are no constant terms or terms of argument  $E'$ , these parts of the motion being completely absorbed by the intermediary. This procedure effectively defines the constant of integration  $e'$  as the coefficient of the  $\sin E'$  variation in the osculating mean anomaly, in accordance with Kepler's equation (Equation 3). The constant of integration  $a'$  is defined by the "mean" mean motion  $\bar{n} = n'$  and Kepler's third law (Equation 6). The orientation of the osculating plane is expressed by four parameters, two differing slightly from  $\sin(i/2)$  and  $\cos(i/2)$  respectively and two differing slightly from zero; this redundancy of expression gains the advantages of symmetry. Fourier series expansions in  $E'$  are made for the orientation parameters and the intermediary inclination  $i'$  is defined so that  $\sin i'$  is the coefficient of all  $\sin(f + \omega)$  variation of  $\sin \phi$  as in Equation 46. The intermediary also absorbs all secular motion of the node. Given a set of constants of integration ( $a'$ ,  $e'$ ,  $i'$ ,  $\omega'_0$ ,  $\Omega'_0$ ,  $M'_0$ ) and parameters of the gravitational field ( $\mu$ ,  $J_2$ , etc.) Fourier series and auxiliary constants are developed by iteration using the principle expressed by Equation 48. Then, for any specified time the position vector  $r$  can be determined by iterating Kepler's equation (Equation 3) with the mean anomaly expressed as  $[M'_0 + \bar{n}(t - t_0) + \bar{n}\delta z]$  to obtain the eccentric anomaly  $E'$  which is then used in the Fourier Series. The use of iteration enables the precision of the computation to be set numerically as a limit beyond which the computer no longer iterates. Musen's theory fails for very small eccentricities because the use of  $E'$  as the independent variable requires a well defined perigee. It also fails at the critical inclination  $63^\circ 26'$ . The theory has been extensively applied by Herget and collaborators as the basis for the orbital programs at the NASA computing center (References 53, 54, and 55).

Musen has recently published a new theory (Reference 56) with several improvements. The polar angle  $\nu$  from a departure point is used as the independent variable; consequently, the radius vector and orientation of the orbit plane can be expressed by closed

trigonometric polynomials in place of truncated infinite series, yielding more rapid convergence in the iteration process.

In the theory of King-Hele (Reference 57), the satellite is taken to be always in a reference plane of fixed inclination. The intermediary in this plane is a Keplerian orbit with a fixed perigee argument equal to that of the actual satellite at epoch. This epoch perigee is treated as a departure point from which the angular position of the satellite is expressed in terms of the polar angle. A first approximation of the equations of motion is solved by assuming that the equation for  $1/r$  (from Equation 8) is modified on the right by terms of order  $J_2$  and that the longitude of the node of the reference plane  $\Omega$  has a secular motion proportionate to  $J_2$ . These first approximations are then used in successive solutions for terms of order  $J_2 e$  and  $J_2^2$ . No terms of higher order are derived, so presumably the theory will give results of precision comparable to those previously described only for small eccentricities.

The theory of Brenner and Latta (Reference 58) is similar to that of King-Hele's, the principal modifications being that the reference plane has a variable inclination, and that the secular motion of perigee in the plane is allowed for in expressing the angular position of the satellite. Terms of order  $J_2 e^2$  or higher are not derived.

Zhongolovich (Reference 59) has developed a second-order theory from the equations of motion similar to Equation 29 but expressing the disturbing forces in orthogonal components: radial, transverse, and normal. The constants of integration are defined as the osculating elements at the ascending node.

Merson (Reference 60) has also developed a theory to secular effects of  $J_2^2$  using the equations of motion with orthogonal components of perturbations and nodal elements. He then determines an intermediate orbit such that  $a$  and  $e$  are constant to  $O(J_2^2)$ .<sup>†</sup>

## Comparison of Theories

For the first of the purposes mentioned in the beginning of this section, precision and efficiency of solution, the theory of Musen (References 50 and 56) is probably the best attained for most satellites, since the method of solution by iteration is equivalent to taking into account terms of order higher than  $J_2^2$ . Among the literal theories, those of Vinti (Reference 46) and Izsak (Reference 39) is the most complete solution of the two-parameter ( $\mu, J_2$ ) problem, as well as being applicable to the greatest variety of orbital specifications. However, the theories in References 35, 40, 59, and 60, should all be

<sup>†</sup>Since writing this review, there have come to our attention further second- or higher-order theories of close satellites by Barrar (Reference 61), Struble (Reference 62), Petty and Breakwell (Reference 63), and Michielsen (Reference 64).

adequate for the principal geodetic uses, as well as those in Reference 23 when the mean motion is obtained empirically, and those in References 57 and 58 when the eccentricity is small. The second purpose, attainment of a keener physical insight, is largely an individual matter; it is only hoped the foregoing descriptions will help as a guide to the theory most suitable.

Two other criteria by which the theories might be judged are the ease of incorporation of additional effects and the ease of comparison of results obtained from a theory with those from another or from numerical integration. For analysis of phenomena significant only for first order effects such as the higher degree gravitational harmonics, all theories are equal since residuals from any numerical or literal theory are essentially the same. Incorporation of phenomena having significant second order effects, such as drag, has been investigated thus far only for Brouwer's theory (References 15, pp. 514-582, and Reference 65). The irregular variations of drag are so large, however, as to make any considerable theoretical development of dubious value. The extent of incorporation of drag into the numerical application of the Musen theory has been to include a term expressing secular change of the mean motion  $n$  (Reference 54):

$$n = n_0(1 + n_2 t) . \quad (66)$$

The principal test of any theory is that it gives the same position and velocity vector at any instant as are obtained by numerical integration, or the same osculating elements as a theory already known to be reliable. Bailie and Bryant (Reference 66) give formulas to enable the latter sort of comparison with the Musen theory. It is also useful and more conducive to understanding to be able to transform directly from the constants of integration of one theory to another. Such transformations are easiest between those theories using mean elements as constants and spherical coordinate systems, such as those of Brouwer (Reference 40), Garfinkel (Reference 35), and Kozai (Reference 23); Garfinkel (Reference 35) gives the transformations between Brouwer's constants and his, while Equation 63 has obtained agreement between Kozai's and Brouwer's theory to better than  $10^{-5}$  in the secular motions of node and perigee. It is appreciably more difficult to obtain transformations between the theories in spherical coordinates and those in ellipsoidal coordinates, or between theories using dynamical intermediaries and those using geometric intermediaries. The only such transformation published, by Message (Reference 67), is limited to a circular orbit between Brouwer's (Reference 40) and King-Hele's (Reference 57) theories. The difficulty seems to be algebraic complexity, rather than error or imprecision of definition, as suggested by Kovalevsky (Reference 20). The use of osculating elements at perigee or the ascending node as constants of integration in References 57, 58, 59, and 60, causes these theories to have different powers of eccentricity in coefficients, as well as giving rise to different periods, as indicated by Equation 47. For example, Zhongolovich's theory (Reference 59) has terms proportionate to  $J_2^2 \cos \omega$  in  $\dot{\Omega}$  and  $\dot{\omega}$ .

The use of general theories of oblateness perturbations to determine better values of  $J_2$  is discussed on pages 37 through 39.

## Special Problems

The problem of the critical inclination,  $5 \cos^2 i - 1 = 0$  or  $i = 63^\circ 26'$ , is solved by Hori (Reference 68), Garfinkel (Reference 69), Hagihara (Reference 70), Kozai (Reference 71), and Struble (Reference 62), using development in powers of  $J_2^{1/2}$  as occurs in the ellipsoidal theories (References 38 and 39). The value of  $J_4$  becomes significant by determining the width of a zone of inclination  $i$  in which the perigee oscillates rather than moving secularly.

For orbits of small eccentricity or small inclination, the canonical elements (Equation 28) may be used. The imprecision which will exist in the  $h$  or  $g+h$  does not have a commensurate effect on the precision of satellite position or velocity because functions of  $h$  and  $g+h$  are always multiplied by coefficients of  $O(\sin^2 i)$  and  $O(e)$ , respectively. An alternative set of elements which, in effect, incorporates these coefficients is given by Kozai (Reference 23). The problem of small eccentricities is also considered in References 72, 73, and 74.

Kozai (Reference 75) investigates the effect of the precession and nutation of the earth's axis, which make the  $J_2$  term of  $R$  a function slowly varying with time if the inertial coordinates are used. The largest effect is a secular change amounting to something more than  $20''$  in a year. In addition, these are periodic variations of amplitude up to  $8''$ . Smaller periodic terms appear if coordinates are referred to the moving equator of date. (See page 60.)

Kozai (Reference 76) and Musen, Bailie, and Upton (References 77 and 78) develop the effect of lunar and solar perturbations on a close satellite. The disturbing function  $R_s$  given in Equation 15 is expandable as a sum of Legendre polynomials:

$$R_s = \frac{\mu^*}{r^*} \sum_{n=2}^{\infty} \left( \frac{r}{r^*} \right)^n P_n(S) \quad (67)$$

where

$$S = \cos(\mathbf{r}, \mathbf{r}^*) = \sum_i F_i(\gamma, \gamma^*) \cos \left[ f + \omega + \begin{pmatrix} 1 \\ 0 \\ -1 \end{pmatrix} \Delta\Omega \pm (f^* + \omega^*) \right] : \quad (68)$$

a sum of six terms in which  $\gamma = \sin(i/2)$  and  $\Delta\Omega = \Omega - \Omega^*$ . The  $(r/r^*)^n$  factor makes only the two leading terms ( $n = 2, 3$ ) of possible significance in  $R_s$ . Substituting

for  $S$  from Equation 68 and carrying out all the multiplications expands  $P_2(S)$  to 23 terms, including a constant, of the form

$$P_2(S) = \sum_i F_i(\gamma, \gamma^*) \cos [a_i(f + \omega) + b_i(f^* + \omega^*) + c_i \Delta\Omega] \quad (69)$$

where  $a_i = 0$  or  $2$ ;  $b_i = -2, 0$ , or  $+2$ ; and  $c_i = -2, -1, 0, +1$ , or  $+2$ .

The expansion for  $P_3(S)$  contains 56 terms. Next, the disturbing function is converted from true anomalies  $f$  and  $f^*$  to the mean anomalies  $M$  and  $M^*$  by applying a standard elliptic expansion for the form  $(r/a)^p \cos(qf + a)$ , for example, Reference 9, pp. 44-46. Since the satellite anomaly changes much faster than any other angle appearing in the disturbing function, the significant effects upon integration with respect to time will be those from which the satellite mean anomaly  $M$  is absent

$$\begin{aligned} \text{Long Period } \mu^* \left( \frac{r^2}{r^*3} \right) P_2(S) &= \mu^* \frac{a^2}{a^{*3}} \sum_i F_i(\gamma, \gamma^*) G_i(e) \\ &\cdot \sum_j G_j(e^*) \cos [a_i \omega + b_i \omega^* + (b_i + j) M^* + c_i \Delta\Omega] \end{aligned} \quad (70)$$

where  $j$  ranges from  $-\infty$  to  $+\infty$ ;  $G_i(e)$  is  $O(e^{a_i})$ , and  $G_j(e^*)$  is  $O(e^{*|j|})$ ;  $e^* = 0.017$  for the sun and  $0.055$  for the moon.

It is evident that the important terms, for which  $F_i G_i$  is large and

$$\{a_i \dot{\omega} + b_i(\dot{\omega}^* + \dot{M}^*) + c_i \Delta\dot{\Omega}\}$$

is small, depend strongly on the eccentricity and inclination of the orbit acting directly in  $F_i$  and  $G_i$  and indirectly through the  $J_2$  effect in  $\dot{\omega}$  and  $\dot{\Omega}$  and must be sought out separately for each satellite. For example (Reference 77, p. 39), for satellite 1958  $\beta 2$  ( $i = 34.2^\circ$ ,  $e = 0.19$ ) the term  $a_i = 2$ ,  $b_i = -2$ ,  $c_i = 2$  is the most important, despite the  $e^2$  coefficient; applying this term in Equation 29 yields an oscillation of amplitude 1.458 km in perigee height. (Some accounts of lunar and solar effects overlook these  $e^2$  terms.)

The complete development of the  $P_2(S)$  and  $P_3(S)$  long period terms is given in Reference 77, plus the  $P_2(S)$  short period terms in terms of the eccentric anomaly for use in the Hansen-type theory of Musen (Reference 50).

## 6. GENERAL THEORIES: LUNAR PROBLEM

In the motion of the moon,  $a = 3.84 \times 10^5$  km, the second order effects of  $J_2$  in Equation 58 are negligibly small; conversely,  $r/r^*$  in  $R_s$  (Equation 67), is appreciably larger, so that the solar disturbance  $R_s$  is dominant. Hence, Equations 68 through 70 can be simplified by making the ecliptic the reference plane so that  $\gamma^* = 0$ . However, the lunar mean motion  $n$  is now appreciable compared to the solar mean motion,  $n^*/n \approx 1/13$ , so short period terms must be considered; higher order terms up to  $R_{s,4}$  containing  $P_4(S)$  must be taken into account; and finally,  $a$ ,  $\gamma$ , and  $e$  in Equation 70 cannot be assumed constant, nor  $\omega$  and  $\Omega$  secularly changing, so that higher order approximations must be developed.

The lunar problem has had a long history, culminating in the researches of Hansen (References 79 and 80), Delaunay (Reference 81), and Hill (References 82 and 83). The theories of Hansen and Delaunay are of great historical interest as the most extensive applications of certain dynamical principles and techniques, and as the precursors of the close satellite theories of Musen (Reference 50) and Brouwer (Reference 40), respectively; detailed descriptions of the Hansen and Delaunay theories are given in References 19 and 84. The theory actually used today is that of Hill as extended by Brown (Reference 85) and Eckert (References 31 and 86).

The Hill-Brown lunar theory is described in the standard texts (Reference 9, pp. 254-291, and Reference 15, pp. 335-374). It employs a rectangular coordinate system  $XYZ$  rotating uniformly in the ecliptic plane so that the  $X$ -axis points to the mean sun and the  $Z$ -axis is normal to the ecliptic. Coriolis and centrifugal force terms thus modify the equations of motion (Equation 12):

$$\ddot{\mathbf{r}} - 2\dot{\mathbf{r}} \times \mathbf{n}^* - (\mathbf{r} \times \mathbf{n}^*) \times \mathbf{n}^* = \nabla U \quad (71)$$

where  $\mathbf{n}^* = (0, 0, n^*)$ .

Hill substituted  $u = x + y\sqrt{-1}$ ,  $s = x - y\sqrt{-1}$ ,  $\nu = n - n^*$ ,  $m = n^*/(n - n^*)$ ,  $\kappa = (\mu_E + \mu_M)/(n - n^*)^2$ , made the independent variable  $\zeta = \exp[\nu(t - t_0)\sqrt{-1}]$ , and defined the operators  $D = \zeta(d/d\zeta)$ ,  $D_t = \zeta(\partial/\partial\zeta)$ . These substitutions in Equation 71 and some further manipulations transform the equations of motion to

$$\left. \begin{aligned} D^2(us + z^2) - Du \cdot Ds - (Dz)^2 + 2m(sDu - uDs) + \frac{9}{4}m^2(u + s)^2 - 3m^2z^2 &= C - \sum_{n=2}^{\infty} (n+1)R'_{s,n} + D^{-1}(D_t R'_s) \\ D(uDs - sDu - 2mus) + \frac{3}{2}m^2(u^2 - s^2) &= S \frac{\partial R'_s}{\partial s} - u \frac{\partial R'_s}{\partial u} \\ D^2z - m^2z &= -\frac{\kappa z}{r^3} = -\frac{1}{2} \frac{\partial R'_s}{\partial z} \end{aligned} \right\} \quad (72)$$

where  $C$  is a constant of integration and  $R'_{s,n}$  is the term of  $R'_s$  containing  $P_n(S)$ . The term  $R'_s$  differs from  $R_s$  in Equation 67 in three respects: (1)  $(a/a^*)$  is replaced by

$$\left(\frac{a}{a^*}\right) \left(\frac{\mu_E - \mu_M}{\mu_E + \mu_M}\right)$$

throughout, to allow for the moon's mass (significant only in  $R'_{s,3}$ ); (2) the solar coordinates  $\mathbf{r}^*$  are with respect to the center of gravity of the earth-moon system; and (3) a term

$$-\frac{3m^2(u+s)^2}{4} - m^2(us+z^2)$$

has been subtracted from  $R'_{s,2}$  and the corresponding derivatives subtracted on the left of Equation 72 (Reference 9, pp. 256-259).

The intermediate orbit is the periodic solution of Equation 72 with  $e^*$ ,  $a/a^*$ ,  $z$ , and  $e$  all set zero. This causes all terms on the right in Equation 72 to vanish except  $C$ , as well as all left-side terms containing  $z$ . The result is that the disturbing force is constant and always in the direction of the  $x$ -axis. The intermediary is called the variational curve; it is an oval rotating so that its shorter axis is in the direction of the  $x$ -axis. The assumption of periodicity requires that the coordinates  $u, s$  be developable in the form

$$\left. \begin{aligned} u &= A \sum_{-\infty}^{\infty} a_{2i} \zeta^{2i+1} \\ s &= A \sum_{-\infty}^{\infty} a_{-2i-2} \zeta^{2i+1} \end{aligned} \right\} \quad (73)$$

where  $A$  is a constant scale factor,  $a_0$  is set as unity, and the other constants  $a_{2i}$ ,  $a_{-2i-2}$ , together with  $c$ , are determined as functions of  $m$  by a process of successive approximation, taking the derivatives  $D$ ,  $D^2$ , etc., of  $u$  and  $s$  and substituting Equation 72 (with the  $R'_s$  and  $z$  terms set zero, as mentioned) and requiring the coefficient of each power of  $\zeta$  to vanish separately. The great advantage of Hill's method is that this process converges rapidly in  $m$  whose numerical value is substituted at this point in the theory. The scale factor  $A$  is also determined by a modification of Equation 72 in which  $\kappa$  appears. The quotient  $a_e/A$  is the mean parallax as modified from that which would exist in the absence of the sun according to Kepler's law (Equation 6). This relationship is best expressed for geodetic purposes as (Reference 87)

$$(1+\epsilon)A = \left[ n^{-2} \mu_E \left( 1 + \frac{\mu_M}{\mu_E} \right) \right]^{\frac{1}{3}} \quad (74)$$

The solution for the intermediate orbit involves only two arbitrary constants:  $t_0$ , the epoch, and  $n$  defined as the mean motion in longitude. The next stage is the complete solution of Equation 72 with the  $R'_s$  and  $z$  terms set zero, which is equivalent to including  $e$ , but keeping  $e^*$ ,  $a/a^*$ , and  $z$  zero. The principal part of this stage is the determination of a quantity  $c_0$ , where  $(1 - c_0)n$  is that part of the mean motion of perigee that depends solely on  $m$ , by solution of an infinite symmetric determinant.

The following stages of solution compute the changes in the solution of Equation 72 by including successively higher powers of the small parameters  $e^*$ ,  $e$ ,  $A/a^*$ , and  $\sin(i/2)$ . The arbitrary constants  $e$  and  $\sin(i/2)$  are defined as coefficients of the principal periodic variations in the longitude and in  $z$ , respectively (Reference 85, v. 53, p. 69). Brown (Reference 85) carried the solution to terms of the 6th order, where order is defined as the sum of the powers of  $e^*$ ,  $e$ ,  $A/a^*$ , and  $\sin(i/2)$  in a product thereof, called a characteristic. The aim of the development was a precision of 0".01. The final form is about 900 periodic terms with numerical coefficients. Brown (Reference 85, v. 59) also calculates the planetary effects and the effects of the figures of the earth and moon.

Brown compiled tables based on his solution which were used for lunar ephemerides 1919-1951. Due to small errors in the tables, insufficient terms, and round-off accumulation in the published positions, these ephemerides were insufficient for geodetic uses, and special numerical solutions were made by Sundman (Reference 88) and Hirvonen (Reference 89 and Reference 5, pp. 128-146) for the motion over the brief periods of the eclipses of 1945 and 1947. With the advent of computers, Brown's equations were programmed directly on the computer and additional terms were developed numerically by Eckert (References 31 and 86). A special lunar ephemeris (Reference 86) covers the years 1952-1959, and the improved lunar ephemeris is incorporated in the regular ephemeris starting in 1960, giving positions to 0".001 in right ascension, 0".01 in declination, and 0".001 in parallax.

## 7. TERRESTRIAL GRAVITATIONAL EFFECTS

Paragraphs 5 and 6 examine those gravitational effects which have appreciable second order effects. This section examines those effects which are of greatest geodetic interest, the departures of the earth's gravitational field from that of an oblate ellipsoid. We shall also examine the numerical solutions for improved values of  $\mu = kM$  and  $J_2$ , since the best solution for these parameters must generally be concurrent with solution for the smaller parameters.

## Disturbing Function and Integration

The earth's gravitational potential may be expressed as a sum of spherical harmonics:

$$U = \frac{\mu}{r} + \sum_{n=2}^{\infty} \sum_{m=0}^n R_{nm} \quad (75)$$

$$= \frac{\mu}{r} \left\{ 1 - \sum_{n=2}^{\infty} \left( \frac{a_e}{r} \right)^n \left[ J_n P_n(\sin \phi) + \sum_{m=1}^n (J_{nm} \cos m\lambda + K_{nm} \sin m\lambda) P_{nm}(\sin \phi) \right] \right\}.$$

In Equation 75,  $\phi$  is geocentric latitude, of negligible difference from geodetic latitude for terms other than  $J_2$  and  $P_n = P_{n0}$ ,  $P_{nm}$  are conventional associated Legendre functions:

$$P_{nm}(\sin \phi) = \frac{\cos^m \phi}{2^n \cdot n!} \sum_{t=0}^k \frac{(2n-2t)!}{(n-m-2t)!} \binom{n}{t} (-1)^t \sin^{n-m-2t} \phi \quad (76)$$

where  $k = (n-m)/2$ ,  $(n-m)$  even, and  $k = (n-m-1)/2$ ,  $(n-m)$  odd.

Equation 75 extends the most generally used notation for zonal harmonic coefficients  $J_n$ , introduced in Reference 90, and adopted in References 35, 38, 39, 40, 42, 60, and 68. The expression for  $R_{nm}$  transformed to osculating Keplerian elements (Reference 41) is

$$R_{nm} = \frac{a_e^n \mu}{a^{n+1}} \sum_{p=0}^n F_{nmp}(i) \sum_{q=-\infty}^{\infty} G_{npq}(e) S_{nmpq}(\omega, M, \Omega, \theta). \quad (77)$$

The functions in Equation 77 are defined by equations 78 thru 81:

$$F_{nmp}(i) = \sum_t \frac{(2n-2t)!}{t!(n-t)! 2^{2n-2t}} \sin^{n-m-2t} i \sum_s \binom{m}{s} \cos^s i$$

$$\cdot \sum_c \binom{n-m-2t+s}{c} \binom{m-s}{p-t-c} \frac{(-1)^{c-k}}{(n-m-2t)!} \quad (78)$$

where  $t$  is summed from 0 to  $p$  or  $k$ , whichever is less;  $s$  is summed from 0 to  $m$ ; and  $c$  is summed over all values making the two binomial coefficients non-zero.

For  $q = 2p - n$ ,

$$G_{np(2p-n)}(e) = (1-e^2)^{\frac{1}{2}-n} \sum_{d=0}^{p'-1} \binom{n-1}{2d+n-2p'} \binom{2d+n-2p'}{d} \left(\frac{e}{2}\right)^{2d+n-2p'} \quad (79)$$

where  $p' = p$  if  $p \leq n/2$ , and  $p' = n-p$  if  $p \geq n/2$ .

For  $q \neq 2p - n$ ,

$$G_{npq}(e) = X_{(n-2p+q)}^{-(n+1);(n-2p)} \quad (80)$$

Hansen's coefficients, expanded in Bessel and hypergeometric functions (Reference 9, pp. 44-46).  $G_{npq}(e)$  is always  $O(e^{1/2})$ .

$$\begin{aligned} S_{nmpq}(\omega, M, \Omega, \theta) &= \begin{bmatrix} -J_{nm} \\ K_{nm} \end{bmatrix}_{(n-m) \text{ odd}}^{(n-m) \text{ even}} \cos \left[ (n-2p)\omega + (n-2p+q)M + m(\Omega - \theta) \right] \\ &\quad - \begin{bmatrix} K_{nm} \\ J_{nm} \end{bmatrix}_{(n-m) \text{ odd}}^{(n-m) \text{ even}} \sin \left[ (n-2p)\omega + (n-2p+q)M + m(\Omega - \theta) \right] \end{aligned} \quad (81)$$

where  $\theta$  is Greenwich sidereal time.

Denote the derivative of  $S_{nmpq}$  with respect to its *argument* by  $S'_{nmpq}$ , and denote the integrals of  $S_{nmpq}$  and  $S'_{nmpq}$  with respect to *time*, assuming  $\omega$ ,  $M$ ,  $\Omega$ , and  $\theta$  to change secularly, by  $\overline{S_{nmpq}}$  and  $\overline{S'_{nmpq}}$ , respectively; so that, for example,

$$\overline{S'_{nmpq}} = \frac{S_{nmpq}}{(n-2p)\dot{\omega} + (n-2p+q)\dot{n} + m(\dot{\Omega} - \dot{\theta})} \quad (82)$$

except in the case  $n$  even,  $p = k$ ,  $q = 0$ ,  $m = 0$ .

Differentiating Equation 77 with respect to the orbital elements, putting the derivatives in Equation 29, and integrating with respect to time gives the total first order effect of any term  $R_{nm}$ ; for example, on the node:

$$\Delta \Omega_{nm} = a_e^n \mu \sum_{p,q} \frac{G_{npq} \overline{S_{nmpq}}}{na^{n+3} (1-e^2)^{\frac{1}{2}} \sin i} \left( \frac{dF_{nmp}}{di} \right). \quad (83)$$

In defining  $\overline{S_{nmpq}}$ , it has been assumed that  $\omega$ ,  $\Omega$ ,  $M$  change secularly. It is an observed fact that for satellites high enough to be useful for gravitational purposes, changes other than secular in these elements are of negligible second-order effect so far as the gravitational harmonics are concerned. In working with observations,  $\dot{\omega}$  and  $\dot{\Omega}$  are obtained empirically, as described on pages 18 through 19. In constructing a mathematical theory good to  $O(J_2^2)$ ,  $\dot{\omega}$  and  $\dot{\Omega}$  are expressed as first order effects of  $J_2$ .

A development similar to Equations 77 through 83 is given by Groves (Reference 91), differing principally in that there is more than one inclination function, like arguments  $S_{nmpq}$  are not combined in one term, and the simplified form (Equation 79) is not used for long-period  $G_{npq}$ . Musen (Reference 52) develops the terms  $R_{nm}$  in a form suitable for their numerical Fourier analysis to be incorporated in his Hansen-type theory of satellite motion (Reference 50).

Examining the denominator of  $\overline{S'_{nmpq}}$  in Equation 82, we see that: (1) the largest perturbations will occur for  $m = 0$ ,  $n - 2p + q = 0$ , that is, the secular and long period effects of zonal harmonics; and (2) a term with  $m \neq 0$  will not give rise to any effect of frequency lower than  $m(\dot{\Omega} - \dot{\theta})$ . The perturbations (1) will be investigated further on pages 37 through 40, and the perturbations (2) will be investigated further on pages 40 through 42.

## Secular and Long Period Terms

For the principal secular or long period effect of a zonal harmonic, or  $m = 0$ , the disturbing function in Equation 77 can be simplified to

$$\text{Long Period } R_{no} = -\mu J_n \frac{a_e^n}{a^{n+1}} F_{nok}(i) G_{nk}(2k-n)(e) \begin{cases} 1, & n \text{ even} \\ 2 \sin \omega, & n \text{ odd} \end{cases} \quad (84)$$

The 2 appears because Equation 84 is actually the sum of two equal terms for  $n$  odd:  $p = k$  and  $p = k + 1$ . In addition to the principal term  $p = k$ , there will be other long period effects for  $n \geq 4$  of appreciably smaller magnitude, since  $G_{np}(2p-n)$  is  $O(e^{1/2 p-n})$ .

Taking partial derivatives of Equation 84 and placing them in the equations of motion (Equation 29), it is apparent that  $J_n$ ,  $n$  even, will give rise to secular changes in  $M$ ,  $\omega$ , and  $\Omega$ , but have no effect on  $a$ ,  $e$ , and  $i$ , while  $J_n$ ,  $n$  odd, will cause periodic variations of frequency  $\omega$  in  $e$ ,  $i$ ,  $M$ ,  $\omega$ , and  $\Omega$ . For  $J_2$ , the second order effects must be taken into account by, for example, Equation 58. Further, as pointed out by Kozai (Reference 92), the second order interactions between  $J_2$  and  $J_n$ ,  $n$  odd, must be taken into account by Equation 62 or other means.

The earliest application of satellite motion to determine the earth's gravitational field was probably in 1884 by Helmert (Reference 93, p. 470) who obtained  $J_2 = (1084 \pm 12) \times 10^{-6}$  from the moon's motion using Hansen's theory (Reference 77). Tisserand (Reference 84, pp. 155-158) analyzed the effect of  $J_3$  on lunar motion, and concluded it was negligible.

Since 1957, the exploitation of the long-period and secular effects on close satellite orbits arising from the disturbing function defined in Equation 84 to obtain improved numerical estimates of the  $J_n$  has been the subject of about forty papers. Table 1 gives the most recent published results of the principal workers in the subject: King-Hele (Reference 94); O'Keefe and collaborators (Reference 87); Kozai (Reference 95); and Michielsen (Reference 96). Other recent summaries of results are given in References 42, 43, 94, and 97.

Table 1  
Estimates of Zonal Harmonics from Satellite Motions

Source	$J_2 \times 10^6$	$J_3 \times 10^6$	$J_4 \times 10^6$	$J_5 \times 10^6$	$J_6 \times 10^6$	Motions Used	Type Observations	Duration Days	Orbits		
									$h_{77}$ Km	e	i
King-Hele (Reference 94)	$1082.79 \pm 0.15$		$-1.4 \pm 0.2$		$0.9 \pm 0.8$	$\dot{\Omega}$	RI R, O KT	207	650	0.19	$34^\circ$
								120	550	0.03	$50^\circ$
								130	230	0.07	$65^\circ$
O'Keefe, Eckels, and Squires (Reference 87)	$1082.49 \pm 0.06$	$-2.39 \pm 0.26$	$-1.70 \pm 0.06$	$-0.30^\dagger \pm 0.53$		$\dot{\Omega}, \dot{\omega}, \Delta e, \Delta \omega, \Delta \Omega$	RI	300	650	0.19	$34^\circ$
Kozai (Reference 95)	$1082.19 \pm 0.02$	$-2.29 \pm 0.02$	$-2.13 \pm 0.04$	$-0.23 \pm 0.02$		$\dot{\Omega}, \dot{\omega}, \Delta e, \Delta \omega, \Delta \Omega, \Delta i$	BN, RI	90	650	0.19	$34^\circ$
							BN, RI	90	510	0.19	$33^\circ$
							BN, RI	50	550	0.03	$50^\circ$
Michielsen (Reference 96)	$1082.66$	$-2.5$	$-1.72$	$+0.25$	$0.73$	$\dot{\Omega}, \dot{\omega}, \Delta e$	RI	$\approx 900$	650	0.19	$34^\circ$
							O	$75^\dagger$	290	0.03	$51^\circ$
							O	$75^\dagger$	280	0.03	$65^\circ$

Notes: RI = Radio Interferometric (Minitrack), R = Radar, O = Optical, KT = Kinetheodolite  
BN = Baker-Nunn Telescope

$^\dagger$ Arithmetic error in Reference 87 corrected.

$^\ddagger$ For each satellite, two sets of observations, each set of two weeks duration or less, two or three months apart were used.

In addition to the quantities listed in Table 1, Michielsen (Reference 96) has made estimates of  $J_7$  ( $-0.6 \times 10^{-6}$ ),  $J_8$ , and  $J_9$  which are of dubious value.

As is usually the case in such comparisons, the results disagree by more than their respective internal standard deviations. The discrepancies are probably not due to any failing in the gravitational theory: lunar-solar and second-order  $J_2$  terms were included

in all the investigations, while the contribution of zonal harmonics higher than  $J_6$  should be slight. All the investigations also removed secular drag effects before analyzing for the  $J_n$ 's. The most pertinent data on length of record, orbit, and means of observation are listed in the table; additional data which would be of interest, but which is not readily deducible from the sources, are the range in latitude from which observations were made, the total motion of the perigee with respect to the sun over the duration of the observations, and, for observations using reflected light, the total motion of the node with respect to the sun. Of the causes for error discussed in more detail on pages 41 through 42, the results of King-Hele (Reference 94) may possibly be affected by a high noise level from 1957  $\beta$  ( $h_p = 230$  km) due to both drag and the theodolite observations; the results of O'Keefe et al by the lack of variety in orbital specifications and by systematic errors of the radio interferometric observations; the results of Kozai by the shortness of the record used, which may induce some geometrical "aliasing" with the reflected sunlight observations; and the results of Michielsen by the shortness of the record used and the high noise level from both observations and drag for the optically-observed, low perigee satellites.

An estimation of  $J_3$  in addition to those in Table 1 is that by Cohen and Anderle (Reference 98) based on Doppler observations of satellite 1960  $\gamma$  1 (Transit 1b):  $J_3 = -2.3 \times 10^{-6}$ . In addition to the differences of satellite specifications, orbit, and means of observation, Cohen and Anderle computed the orbit by numerical integration in rectangular coordinates, as described on page 19. This method of computation effectively ruled out any possibility of overlooked  $J_2^2$  terms of argument  $\omega$ , as suggested by Reference 99 on the mistaken belief that the anomaly of the intermediary is defined as in Equation 47.

Newton (Reference 100) has recently obtained from the orbits of 1958  $\beta$  2, 1960  $\gamma$  1, and 1960  $\eta$  1,  $J_3 = (-2.42 \pm 0.10) \times 10^{-6}$ ,  $J_5 = (-0.22 \pm 0.07) \times 10^{-6}$ , and  $J_7 = (-0.27 \pm 0.07) \times 10^{-6}$ .

Since the differences in results are probably due as much to differences in treatment as to inaccuracies in the data, it is difficult to make a prudent compromise among the values in Table 1. Conservative estimates might be:

$$J_2 = (1082.3 \pm 0.2) \times 10^{-6}$$

$$J_3 = (-2.3 \pm 0.1) \times 10^{-6}$$

$$J_4 = (-1.8 \pm 0.2) \times 10^{-6}$$

$$J_5 = (-0.3 \pm 0.2) \times 10^{-6}.$$

In addition to the zonal harmonics, it is appropriate to mention here determination of the leading term in the potential  $kM = \mu$  essentially from the mean motion and Kepler's third law (Equation 6). The necessary modification of Equation 6 for close satellites is Equation 58, plus terms for drag and higher even degree zonal harmonics; for the moon, it is Equation 74. Measuring the length of record in satellite periods, observations of satellite 1958  $\beta$  2 already well exceed modern observations of the moon. However, aside

from the difficulty of removing drag effects from the mean motion of close satellites, the necessary length scale is obtained from the relative position of tracking stations, the accuracy of which depends on the connecting geodetic triangulation: also the principal limitation on the accuracy of  $kM$  from terrestrial data. An independent determination thus depends on the scale being obtained from range measurements of the satellite, which makes the moon the most suitable object. In Equation 74, the values  $\beta = 0.00090768$  and  $n = 2.6616997 \times 10^{-6}$  radians/second (Reference 85, v. 57, p. 109) can be considered as of negligible uncertainty. The ratio  $\mu_M/\mu_E$ , or rather the equal quantity which is the proportionate displacement of the earth's center of mass from the center of mass of the earth-moon system, is essentially determined by the variations in parallax of observations of the minor planet Eros upon its close approach. The most recent determinations of  $\mu_M/\mu_E$  are: by Jeffreys (Reference 101) (using Spencer Jones' data)  $1/81.291 \pm 0.027$ ; by Rabe (Reference 102)  $1/81.375 \pm 0.026$ ; and by Delano (Reference 103)  $1/81.219 \pm 0.030$ . Rabe's solution is the most comprehensive, using 19 year's data to obtain corrections to the orbits of Eros and the earth, the masses of the four inner planets, and the equinox and equator of epoch; while Delano's solution is confined to obtaining corrections to the orbit of Eros and the earth's mean motion in the eight months around the close approach of 1930-31. The mean distance  $A$  is the most uncertain quantity in Equation 74. Until recently, the primary method of estimating  $A$  was essentially by triangulating, through occultations observed from points in the same geodetic control system; the most recent discussions are by O'Keefe and Anderson (Reference 104) and Fischer (Reference 105). Now the more accurate method is by radar measurement of the lunar distance; such a program has been carried out by Yaplee and collaborators (References 106, 107, and 108). Their latest result,  $A = 384402 \pm 1.2$  km (Reference 108), obtains  $kM = (3.986141 \pm 0.000040) \times 10^{14} \text{ m}^3/\text{sec}^2$  with Rabe's  $\mu_M/\mu_E$  and  $3.986048 \times 10^{14} \text{ m}^3/\text{sec}^2$  with Delano's value.

## Daily and Short Period Terms

The first estimate of the effect of a tesseral or sectional harmonic effect on a satellite orbit was by O'Keefe and Batchlor (Reference 109), who showed that the sectorial harmonic  $J_{22}$  estimated by Jeffreys (Reference 110, p. 187) should give rise to a readily observable semidaily oscillation in a circular orbit. A more general study (Reference 41), using amplitudes estimated from autocovariance analysis of terrestrial gravimetry (Reference 111), shows that even degree terms such as  $n_m = 22, 41, 42, 61$  should give rise to daily and semidaily oscillations on the order of  $\pm 100$  meters in orbits of semimajor axis less than  $10^4$  kilometers, while odd degree terms such as  $n_m = 31, 32$  should cause comparable effects for orbits of eccentricity 0.2. It is further indicated that the total of all gravitational harmonic effects of frequency  $n$  or higher (other than those of  $J_2$ ) should be on the order of  $\pm 50$  meters or less. Hence for estimation of tesseral and sectorial harmonics the disturbing function (Equation 77) can be expressed as

$$\text{Long Period } R_{nm} = \frac{\mu a^n}{a^{n+1}} \sum_{p=1}^{n-1} F_{nmp}(i) G_{np}(2p-n)(e) \cdot \left\{ \begin{aligned} & \begin{bmatrix} -J_{nm} \\ K_{nm} \end{bmatrix}_{(n-m) \text{ odd}}^{(n-m) \text{ even}} \cos [(n-2p)\omega + m(\Omega - \theta)] \\ & - \begin{bmatrix} K_{nm} \\ J_{nm} \end{bmatrix}_{(n-m) \text{ odd}}^{(n-m) \text{ even}} \sin [(n-2p)\omega + m(\Omega - \theta)] \end{aligned} \right\}, \quad (85)$$

in which  $F_{nmp}$  and  $G_{np}(2p-n)$  are defined by Equations 78 and 79, respectively.

Solutions thus far obtained for tesseral and sectorial harmonics from Baker-Nunn camera observations (References 112 and 113) are probably distorted by the neglect of the interaction with datum error for non-uniformly distributed observations, and those from Minitrack radio interferometers (References 114 and 115) by errors in orientation of the antennas. As of this writing, the only results which might be reasonably close to the correct values are for  $R_{22}$  and  $R_{41}$ , for which Kozai (Reference 113) obtains from 66 day's Baker-Nunn camera observations of three satellites:

$$\begin{aligned} J_{22} &= (-0.60 \pm 0.19) \times 10^{-6}, & K_{22} &= (+2.24 \pm 0.19) \times 10^{-6}, \\ J_{41} &= (+0.25 \pm 0.04) \times 10^{-6}, & K_{41} &= (-0.08 \pm 0.03) \times 10^{-6}; \end{aligned}$$

and for which Kaula (Reference 115) obtains from 385 day's Minitrack observations of one satellite:

$$\begin{aligned} J_{22} &= (-0.38 \pm 0.59) \times 10^{-6}, & K_{22} &= (+1.64 \pm 0.58) \times 10^{-6}, \\ J_{41} &= (-1.12 \pm 0.14) \times 10^{-6}, & K_{41} &= (+0.26 \pm 0.15) \times 10^{-6}. \end{aligned}$$

The orbital variations of satellites may properly be considered as stochastic time series in which there is a mixture of discrete spectra for the gravitational effects and a continuous spectrum for drag. However, the texts on the analysis of time series, for example, References 22, 116, and 117 are not of much help because the dominant statistical consideration for close satellites is the non-uniform distribution of observations. This non-uniformity arises mainly from a geometrical limitation: observations at any given station will always be at times when the satellite is within a few degrees of the values of the angles  $(\Omega - \theta)$  and  $(\omega + f)$  corresponding to the station zenith. In the case of optical observations, there is also the limitation of dependence on solar illumination of the satellite. Since  $m(\Omega - \theta)$  is the principal argument in Equation 85 for even  $n$ , and

$m(\Omega - \theta) \pm \omega$  for odd  $n$ , the effects of even-degree gravitational terms for any duration, or odd-degree terms for short durations, as observed from one or a few stations are difficult to separate from each other or from the effects of station position, orientation, and timing errors. Non-uniform distribution also greatly increases the contamination of estimated  $R_{nm}$ 's by longer period effects such as drag and lunar-solar attraction, and increases the absorption of the effects of the  $R_{nm}$ 's by the parameters of the reference orbit.

The various interactions affecting determination of the tesseral and sectorial harmonics from satellite orbits are further explored in Reference 115 which suggests: (1) using observations over several rotations of node and perigee; (2) weighting observations inversely proportionate to their density with respect to  $(\Omega - \theta)$ ; (3) using initial weighted estimates of the datum parameters and gravitational coefficients, as described by Equations 137 and 138 below; (4) using reference orbits covering at least fifty observations; and (5) absorbing secular and long period accelerations by at least 0.15 W parameters, where W is the duration in days covered by the reference orbit.

Physical considerations affecting these suggestions are further discussed in Paragraph 8 of this Section, and geometrical considerations in Paragraph 4 of Section II.

An interesting possibility which should be mentioned in connection with the tesseral and sectorial harmonics is resonance, that is, in the disturbing function (Equations 77 and 81) the following condition occurs:

$$(n - 2p)\dot{\omega} + (n - 2p + q)n + m(\dot{\Omega} - \dot{\theta}) = 0. \quad (86)$$

Such resonance is discussed by Groves (Reference 91) and Cook (Reference 118). From Kepler's third law (Equation 6) we obtain

$$a = \mu^{\frac{1}{3}} n^{-\frac{2}{3}} \approx \mu^{\frac{1}{3}} \left[ \frac{m}{n - 2p + q} (\dot{\theta} - \dot{\Omega}) \right]^{-\frac{2}{3}} > \left[ \frac{\mu}{m^2 \dot{\theta}^2} \right]^{\frac{1}{3}} \quad (87)$$

which yields for  $m = 1$ , 42,200 km; for  $m = 2$ , 26,000 km; for  $m = 3$ , 20,300 km, etc. These conditions are most likely to be realized in connection with communication systems which require an orbit of  $\dot{\Omega} + \dot{\omega} + n = \dot{\theta}$  and near circularity, for which the lunar-solar effects would be small even at  $a = 42,200$  km.

## Tidal Effects

Historically the most renowned geophysical application of celestial data is that of the secular acceleration of the moon's motion, the deceleration of the earth's rotation, and the energy dissipation in the earth inferred therefrom. The secular acceleration was

first discovered in the 17th century, and its geophysical explanation by tidal friction suggested in the 18th century, but its mathematical determination was a subject of much controversy in the 19th century (Reference 84, pp. 240-256) and its geophysical explanation is still unsettled in the 20th century (Reference 110, pp. 230-263 and Reference 119, pp. 198-249).

The close satellites cannot contribute to the tidal friction problem, but the response of satellite orbits to the lunar and solar perturbations (Equation 67) suggest that they may be perceptibly perturbed by the tides on the earth, which are poorly determined for much of the surface. We follow the usual division of the subject into earth tides and ocean tides.

The potential due to earth tides may be expressed as (Reference 120):

$$R_T = K(r)R_S. \quad (88)$$

At the earth's surface  $K$  is Love's number  $k$  which we assume constant. We also assume that only the  $P_2(S)$  term in Equation 67 is significant. These assumptions make  $R_T$  a second degree harmonic at the earth's surface, which must therefore extrapolate proportionate to  $(a_e/r)^3$ . Setting  $r = a_e$  in Equation 67 and using Equation 69 yields:

$$R_T = \frac{k\mu^* a_e^2}{r^3} \left(\frac{a_e}{r}\right)^3 \sum_i F_i(\gamma, \gamma^*) \cos [a_i(f + \omega) + b_i(f^* + \omega^*) + c_i\Delta\Omega] \quad (89)$$

Apply Equation 7 and Equation 8 to integrate with respect to the mean anomaly to obtain the long period terms:

$$\text{Long Period } R_T = \frac{k\mu^* a_e^2}{r^3} \left(\frac{a_e}{r}\right)^3 \sum_{i \neq \ell} F_i(\gamma, \gamma^*) \sum_j G_j(e^*) \cos [b_i\omega^* + (b_i + j)M^* + c_i\Delta\Omega] \quad (90)$$

where  $a_\ell = 2$ . Since  $R_T$  is proportionate to  $r^{-3}$  (instead of to  $r^2$  as is  $R_S$ ) there are no long period terms containing  $2\omega$ , such as are most significant in  $R_S$ . For the terms  $a_i = 0$ ,  $R_T \approx k(a_e/a)^5 R_S$ ; taking typical values  $k = 0.3$ ,  $a = 8.0 \times 10^6$  m,  $a_e = 6.37 \times 10^6$  m, we obtain  $R_T \approx 0.1 R_S$ .

For oceanic tides, the dimensions of the ocean basins become significant; approaches to resonance may cause tides to be more than ten times the equilibrium tide (which is less than a meter in amplitude). The patterns of ocean tides are the amphidromic systems (Reference 121): lines of equal phase radiating from nodes on the order of  $60^\circ$  arc apart. We can represent the tide  $\zeta$  at any point by

$$\begin{aligned} \zeta(\phi, \lambda, t) &= \sum_i \zeta_i(\phi, \lambda) \cos [b_i(f^* + \omega^*) + c_i\Omega^* \pm \theta + d_i(\phi, \lambda)] \\ &= \sum_{i,n,m} \zeta_{inm} P_{nm}(\sin \phi) \cos [b_i(f^* + \omega^*) + c_i\Omega^* \pm \theta + m\lambda + d_{inm}]. \end{aligned} \quad (91)$$

From the formula for a surface layer, the corresponding potential coefficient is

$$J_{inm} = - \frac{4\pi k a_e^2}{(2n+1)\mu} \rho_w \zeta_{inm} \quad (92)$$

where  $k$  is, once again, the gravitational constant and  $\rho_w$  is the density of water. The complexity of the ocean tidal pattern makes it unlikely that any  $\zeta_{inm}$  exceeds one meter for normalized harmonics, even though the total tide may be quite large. Assuming a  $\zeta_{i22}$  (normalized) of one meter yields  $J_{i22}$  (conventional) of  $-10^{-8}$ , or two orders of magnitude smaller than the  $J_{22}$  mentioned on page 41. Hence, for any ocean tide term  $\zeta_{inm}$  to have a perceptible effect, its argument must yield frequencies on the order of 0.01 cycles/day when Equation 91 is transformed to orbital elements, analogous to Equation 77.

## Relativistic Effects

The largest relativistic effect is the secular motion of perigee (Reference 122, p. 217):

$$\dot{\omega} = \frac{3\mu}{c^2 a (1-e^2)} n = \frac{3\mu^{\frac{3}{2}}}{c^2 a^{\frac{5}{2}} (1-e^2)} \quad (93)$$

where  $c$  is the velocity of light. Table 2 compares the relativistic effect on satellites of eccentricity 0.20, inclination  $0^\circ$ , with the effects anticipated from the even degree zonal harmonics, which are maximized for equatorial orbits. The zonal harmonic effects were computed using amplitudes from autocovariance analysis (Reference 111) in Equations 84 and 29.

Table 2  
Comparison of Relativistic and Estimated  
Zonal Harmonic Effects on Perigee Motion

Inclination 0		Eccentricity 0.2				
Semimajor Axis Km	Relativistic $\dot{\omega}$ Sec <sup>-1</sup>	$J_2$ $\dot{\omega}$ Sec <sup>-1</sup>	$J_4$ $\dot{\omega}$ Sec <sup>-1</sup>	$\sigma(J_6)$ $\dot{\omega}$ Sec <sup>-1</sup>	$\sigma(J_8)$ $\dot{\omega}$ Sec <sup>-1</sup>	$\sigma(J_{10})$ $\dot{\omega}$ Sec <sup>-1</sup>
$10^4$	$8.66 \times 10^{-13}$	$9.10 \times 10^{-7}$	$1.76 \times 10^{-9}$	$\pm 8.1 \times 10^{-10}$	$\pm 4.3 \times 10^{-10}$	$\pm 2.0 \times 10^{-10}$
$2 \times 10^4$	$1.54 \times 10^{-13}$	$8.02 \times 10^{-8}$	$3.89 \times 10^{-11}$	$4.5 \times 10^{-12}$	$5.9 \times 10^{-13}$	$6.9 \times 10^{-14}$
$3 \times 10^4$	$5.50 \times 10^{-14}$	$1.94 \times 10^{-8}$	$4.18 \times 10^{-12}$	$2.1 \times 10^{-13}$	$1.3 \times 10^{-14}$	$6.5 \times 10^{-16}$
$4 \times 10^4$	$2.69 \times 10^{-14}$	$7.04 \times 10^{-9}$	$8.6 \times 10^{-13}$	$\pm 2.5 \times 10^{-14}$	$\pm 8.2 \times 10^{-16}$	$\pm 2.4 \times 10^{-17}$

Table 2 indicates that the relativistic effect need not be taken into account in attempting to determine  $J_{10}$  or lower zonal harmonics from close satellites; and, conversely, that the anomalous variations in the gravitational field will be a serious hindrance to observation of the relativistic perigee motion for satellites less than  $10^4$  km in altitude. Furthermore, Equation 93 is not the relativistic effect of principal interest, since it has already been confirmed by the orbit of Mercury. Those effects which are of interest to investigators of relativity (References 123, 124, 125, and 126) are on the order of  $10^{-2}$  smaller: the effects of the earth's rotation, the earth's velocity in its orbit, the relativistic correction to the  $J_2$  effect, the difference between atomic and gravitational time, secular change in the gravitational constant, etc. The difficulties in extracting these effects from a satellite orbit will be between drag and terrestrial gravitational effects for orbits which are too low and complicated higher order effects of the lunar-solar perturbations (Equation 67) for orbits which are too high.

## 8. NON-GRAVITATIONAL EFFECTS

Regarding non-gravitational effects as things to be eliminated or avoided as much as possible to attain the geodetic objectives, the physical effects on a close satellite orbit of mechanical drag by the atmosphere, of electromagnetic effects, and of radiation pressure are examined; the extent to which the phenomena causing these effects have been described in observed or theoretical models and the extent to which observed orbital variations remain unexplained are investigated; and finally the implications of these results for the accurate description of an orbit necessary for its geodetic use are discussed.

### Mechanical Drag

At the altitudes of geodetically useful satellites, the mean free path of air particles is large in comparison to the diameter of the satellite. Consideration of the momentum transfer between the air molecules and the satellite leads to an equation for the vector of the force on the satellite (References 127, 128, and 129):

$$\mathbf{F}_d = -m \frac{C_D}{2} \left( \frac{A}{m} \right) \rho(r) \dot{\mathbf{r}} |\dot{\mathbf{r}}| \quad (94)$$

where  $A$  is the cross sectional area of the satellite,  $\rho$  is the air density, and  $C_D$  is a coefficient dependent upon the shape of the satellite and the manner of reflection of the air particles. For specular elastic reflection from a sphere,  $C_D = 2.0$ ; for diffuse reflection,  $C_D = 2.67$ ; usually some intermediate value is used. Thus the  $b(r)$  in Equations 16

and 17 is  $(C_D/2)(A/m) \rho(r)$ . As in Paragraphs 2 through 7 of this section, we set the first  $m$  in Equation 94 as unity. Using  $F_d$  in the Lagrangian equations for orthogonal force components (References 9, p. 151, and 15, p. 301) leads to (References 129 and 130)

$$\frac{dP}{dt} = -3C_D \left(\frac{A}{m}\right) a \int_0^\pi \frac{(1 + e \cos E)^{\frac{3}{2}}}{(1 - e \cos E)^{\frac{1}{2}}} \rho(r) dE \quad (95)$$

where the period  $P = 2\pi/n$ .

Equation 95 is exact; to proceed further, it is necessary to assume a law for  $\rho(r)$ . The simplest assumption is constant temperature and hydrostatic equilibrium, leading to

$$\rho = \rho_\pi \exp \left[ - \frac{(r - r_\pi)}{H} \right] \quad (96)$$

where the subscript  $\pi$  refers to perigee and  $H$  is the scale height (on the order of 100 km). Before solving Equation 95 for  $P$  and the other elements, King-Hele (References 130 and 131) and Sterne (References 129 and 132) introduce the rotation of the atmosphere, most simply expressed by multiplying the force (Equation 94) by a factor

$$\left( \frac{1 - r_\pi \dot{\theta} \cos i}{|\dot{\mathbf{r}}_\pi|} \right)$$

which lies between 0.9 and 1.1. The integral is then evaluated as a power series expansion in  $e$ , most conveniently in Bessel functions of the first kind with imaginary argument  $I_n(a_e/H)$ .

The rates of decay of  $\rho$  in Equation 96 are such that the drag is concentrated around perigee for all orbits except those which are virtually circular. The leading terms in the resulting equations for eccentricity, perigee radius, and period (Reference 131) are

$$\left. \begin{aligned} \frac{e}{e_o} &= \sqrt{1 - \frac{t}{t_L}} \left[ 1 - \frac{e_o}{6} \left( 1 - \frac{19}{3} e_o \right) \left( 1 - \sqrt{1 - \frac{t}{t_L}} \right) - \dots \right] \\ r_{\pi_o} - r_\pi &= \frac{H}{2} \left[ \sqrt{1 - \frac{t}{t_L}} - 1 - \dots \right] \\ \frac{P}{P_o} &= 1 - \frac{3e_o}{2} \left( 1 - \sqrt{1 - \frac{t}{t_L}} \right) \left[ 1 + \frac{e_o}{12} \left( 17 \sqrt{1 - \frac{t}{t_L}} - 3 \right) + \dots \right] \end{aligned} \right\} \quad (97)$$

where the lifetime  $t_L$  is defined by

$$t_L = - \frac{3e_o P_o}{4P_o} \left[ 1 + \frac{7e_o}{6} + \frac{H}{2a_o e_o} + \dots \right] \quad (98)$$

Also applicable is

$$\rho_{\pi} = - \frac{\dot{P}_m}{3AC_D} \sqrt{\frac{2e}{\pi a H}} \left[ 1 - 2e - \frac{H}{8ae} + \dots \right] . \quad (99)$$

Equation 97 indicates that the perigee radius decreases much more slowly than either the eccentricity or period. This suggests that for gravitational analyses the drag effect could be deduced empirically from the change in the mean motion and the small second order effects on the other elements computed therefrom, assuming the perigee radius to remain constant. This method is used by O'Keefe and collaborators (Reference 87), who obtain:

$$\left. \begin{aligned} \Delta e &\approx - \frac{2}{3} (1 - e) \frac{\Delta n}{n_o} \\ \Delta \omega &= \frac{4 - 5 \sin^2 i}{4(1 - e^2)^2} \left( \frac{7 - e}{1 + e} \right) J_2 \left( \frac{a_e}{a} \right)^2 \Delta M \\ \Delta \Omega &= - \frac{\cos i}{2(1 - e^2)} \left( \frac{7 - e}{1 + e} \right) J_2 \left( \frac{a_e}{a} \right)^2 \Delta M \end{aligned} \right\} \quad (100)$$

where  $\Delta n$  could be obtained from Equation 66 or a sum of such terms for different segments, whence

$$\Delta M = \int n n_2 t \, dt \approx \sum_i n_i n_{2i} \frac{(\Delta t_i)^2}{2} = n_o \sum_{i=1}^k n_{2i} \Delta t_i \left( \frac{\Delta t_i}{2} + \sum_{j=i+1}^k \Delta t_j \right) \quad (101)$$

where  $n_2$  is the negative of  $\dot{P}/P$ .

Brouwer and Hori (Reference 65 and Reference 15, pp. 574-582) have developed a canonical theory of drag which assumes an exponential atmospheric density of the form of Equation 96 and which takes into account the interaction of drag with the oblateness  $J_2$ .

Izsak (Reference 133) developed expressions for the short period drag perturbations due to an exponential atmosphere from which he obtained oscillations about a secular change of about 0.6 km in semimajor axis,  $+0.02^\circ$  in mean anomaly, and  $-0.008^\circ$  in perigee argument for  $e = 0.10$  and  $\rho_{\pi} = 1.9 \times 10^{-12}$  gm/cm<sup>3</sup>, nearly all of it occurring within  $30^\circ$  of perigee.

Jacchia (Reference 134) and Groves (Reference 135) consider the effect of an additional term in the scale height  $H$ :

$$H = H_{\pi} + \beta(r - r_{\pi}) . \quad (102)$$

Existing atmospheric models indicate  $\beta$  may be as much as 0.2. The relative error resulting in the  $\dot{P}$  of Equation 95 from assuming  $H$  constant is at most  $\beta/2$ , and varies but slightly with eccentricity (Reference 134).

The effect of the rotation of the atmosphere (References 132 and 136) is to cause slight diminutions in the rates of decrease of period, mean distance and eccentricity, and a gradual decrease in the inclination of a direct orbit (with reversal of signs in a retro-grade orbit), plus a variation in the node of frequency  $2\dot{\omega}$ . For 1958  $\beta 2$  ( $h_{\pi} = 650$  km) the computed rate of inclination change is  $-0''.004/\text{day}$  (Reference 132).

The effect of the oblateness of the atmosphere (References 132 and 137) is to cause oscillations of frequency  $2\dot{\omega}$ .

## Electromagnetic Effects

The satellite moves in a partly ionized medium and in a magnetic field, and, most of the time, in the energy field of the sun. The resulting electromagnetic effects anticipated include (References 128 and 138):

- (1) The satellite is bombarded by electrons moving at a much higher velocity and thus acquires a negative charge.
- (2) When the satellite is in sunlight the charge may be increased due to increase in the high energy population of electrons.
- (3) When the satellite is in sunlight the charge may be decreased due to photoejection of electrons.
- (4) The negative charge of the satellite causes an electrostatic deflection of the more slowly moving positive ions with a resulting momentum transfer and thus an increased drag.
- (5) The attraction of the negatively charged satellites for positive ions results in an increased number of collisions and hence an increase in mechanical drag.
- (6) The overtaking of positive ions by the satellite results in a non-symmetric charge distribution which modifies effects (4) and (5).
- (7) The motion of the satellite across the geomagnetic field induces a voltage in the satellite, affecting the distribution of incident electrons (1) and hence of the negative charge.
- (8) The charge of the satellite will be increased if it carries a powerful radio transmitter.

- (9) The non-uniform charge from effects (6) through (8) causes an electrical current in the satellite which interacts with the geomagnetic field, resulting in an additional mechanical drag.

It is estimated by Jastrow and Pearse (Reference 128) and Beard and Johnson (Reference 138) that the increased mechanical drag (5) is much more important than purely electrostatic drag (4) or magnetic field interaction (9) [except possibly for satellites more than 50 meters in diameter at altitudes above 1200 km (Reference 138)]. Whether the total electromagnetic effects are appreciable compared to the neutral mechanical drag depends on the magnitude of the satellite potential (1) as modified by (2), (3), (6), (7), and (8). Jastrow and Pearse (Reference 128) assumed a mean electron energy of 1.5 ev, and estimated therefrom that a potential of -30 volts could be acquired by the satellite, in which case the charged drag could be appreciable. Benefiting from more recent knowledge of the atmosphere, Beard and Johnson (Reference 138) assume a mean electron energy of 0.1 ev, leading, in conjunction with the magnetically induced effect (7), to a satellite charge of a few tenths of a volt, which has been borne out by measurements on rockets. This small a charge makes the estimated electromagnetic effects small compared to the fluctuations in the neutral mechanical drag.

The electromagnetic effects all act to increase the drag force vector in Equation 94, and hence to increase the magnitudes of the effects in Equation 97. Hence, if the description of energy dissipating effects is obtained empirically, the electromagnetic effects are lumped in with the neutral drag. The present situation is that no orbital effect has been observed ascribable to electromagnetic effects; if they do account for part of the discrepancy between observation and theory, it is for a minor part compared to atmospheric variations in response to solar effects. However, the theory of electromagnetic effects is still incomplete, and it is not to be ruled out that they may be of significance for geodetically interesting satellites with perigees in excess of 1200 km altitude. An extensive recent review by Chopra (Reference 139) expresses doubt about many conclusions in References 128 and 138 and estimates electromagnetic effects to be more important than mechanical drag above about 300 km altitude, negating most of the deductions as to air density described on pages 50 through 53.

## Radiation Pressure

An energy flux  $S$  incident on a surface at angle  $\theta$  to the normal will give rise to a pressure normal to the surface (Reference 140, p. 616):

$$p_n = (1 + \kappa) \frac{S \cdot \mathbf{n}}{c} \cos \theta \quad (103)$$

where  $c$  is the velocity of light and the coefficient  $(1 + \kappa)$  varies between 1 (perfect absorption) and 2 (perfect specular reflection). The force on a body is then obtained by integrating Equation 103 vectorially over the illuminated surface.

The radiation pressure due to the sun is a known force:  $S$  is  $1.4 \times 10^6$  ergs/cm<sup>2</sup>/sec near the earth (Reference 141), except for uncertainty as to the reflection coefficient  $\kappa$  for some satellites. Solar radiation pressure was first successfully invoked to explain long period residuals on the order of 2 km in the orbit of 1958  $\beta 2$  (References 142 and 143), and has since been amply confirmed by the large Echo satellite (References 144, 145, and 146) to include specular reflection.

Musen (Reference 147) has analyzed the long period effects of solar radiation pressure and neglecting the effect of the earth's shadow. These long period effects have six terms for the variation of each orbital element, the arguments of the six terms comprising all possible combinations of the form

$$\text{Arg} = \omega + \begin{Bmatrix} 1 \\ 0 \\ -1 \end{Bmatrix} \Omega + \begin{Bmatrix} 1 \\ -1 \end{Bmatrix} (f^* + \omega^*). \quad (104)$$

The combination  $\omega + \Omega - (f^* + \omega^*)$  gives rise to an 890-day period for 1958  $\beta 2$ , accounting for most of the 2 km perturbation. Musen also analyzes the resonant case of a satellite whose perigee follows the sun.

An adequate theory of radiation pressure effect must incorporate short-period terms because there are long-period variations of the orientation of the orbit with respect to the shadow (Reference 148). These variations are significant because they cause long-period variations of the semimajor axis, or energy, of the orbit. The resulting accelerations will exceed those due to drag for perigees above 1000 km, and have been the subject of much investigation in the orbit of 1960  $\alpha 1$  (References 149 and 150).

Terrestrial radiation pressure also exists. Of the total insolation, an average of 36 percent is reflected or back-scattered, and 64 percent is absorbed and, after redistribution in latitude, reradiated (Reference 141). The 36 percent reflected would be mainly directed counter to the direct solar radiation, while the 64 percent reradiated would be mainly directed counter to the principal gravitational term, so it is doubtful that terrestrial radiation pressure will ever be identifiable in a satellite orbit.

## Observed Variations and Theoretical Models of the Atmosphere

As mentioned, no electromagnetic effects on orbits have yet been distinguished from mechanical, while radiation pressure is a known force, so discussion toward improved knowledge of orbital variations is confined to mechanical drag, dependent on the density  $\rho(r)$  in Equation 94.

In the three years of satellite observations 1957-1960, a description of the atmosphere has been constructed therefrom up to 700 km, a limit set by the perigee height of 1958  $\beta 2$  (650 km). The results of the many investigations published are summarized in the recent papers (References 151, 152, 153, 154, 155, 156, 157, and 158). The principal characteristics for the zone 300 to 700 km inferred from orbits in these papers are:

- (1) A density at midnight for latitudes below  $50^\circ$  averaging  $4 \times 10^{-14}$  gms/cm<sup>3</sup> at 300 km decreasing to about  $5 \times 10^{-17}$  gms/cm<sup>3</sup> at 700 km
- (2) A slight decrease from this midnight density until dawn, after which there is a rapid rise reaching a peak at 2 p.m. of about  $6 \times 10^{-14}$  gms/cm<sup>3</sup> at 300 km, decreasing to about  $6 \times 10^{-16}$  gms/cm<sup>3</sup> at 700 km
- (3) A variation of the density closely correlated with the fluctuations of the solar flux at wavelengths of the order of 10 to 20 cm, in which the 27-day solar rotation period is often prominent: these variations are much more pronounced at higher altitudes and on the day side of the atmosphere, with a maximum to minimum density ratio of about 2:1
- (4) Brief increases in density during magnetic storms
- (5) A decrease in the average atmospheric density from 1958 to 1960, more pronounced at higher altitudes and on the day side of the atmosphere, and coinciding with a decrease in the 11-year cycle of solar activity (References 151 and 153)
- (6) Little variation of density with latitude (Reference 153)
- (7) A semiannual variation of density with a minimum in June-July-August about 0.6 times the maximum at 300 km (Reference 155), and a less pronounced minimum in January correlated with the  $k_p$  index of magnetic activity (Reference 158)
- (8) Erratic fluctuations of  $\dot{P}$  about a model describing (1), (2), (3), and (4) above with an rms magnitude between  $0.5$  and  $1.0 \times 10^{-7}$  and including components of several day's period for satellites of perigee between 500 and 700 km (Reference 151).

Jacchia (Reference 151) has formed empirical models to describe the variations (1), (2), (3), and (5) of the form

$$\rho H^{\frac{1}{2}} = f_0(h) F_{20} \left[ 1 + f_1(h) \cos^n \frac{\psi'}{2} \right] \quad (105)$$

where  $f_0(h)$  and  $f_1(h)$  are exponential functions of altitude,  $F_{20}$  is proportionate to the 20-cm flux intensity, and  $\psi'$  is the angular distance from the high point of the daily bulge — which, as stated in (2), lags  $30^\circ = 2$  hours behind the subsolar point. A similar formulae has been developed by Priester (Reference 158).

The recent Echo satellite 1960  $\nu$  adds a new datum to the above results of about  $10^{-18}$  gm/cm<sup>3</sup> density at 1500 km altitude. The analysis of 1960  $\nu$  1 orbit is complicated by its small eccentricity, the radiation pressure effects, decreasing mass due to gas loss, and probably significant electromagnetic effects, so the interpretation of this density is unsure (References 146, 149, 150, and 158).

Most of the foregoing conclusions apply to variations in the atmosphere of frequency less than 0.25 cycle/day since the observations on which they are based are smoothed by using  $\dot{P}$  averaged over periods on the order of two days. An autocovariance analysis (Reference 115) of Jacchia's data for satellite 1958  $\beta$ 2 over 462 days (Reference 151) obtains as a quite consistent estimate of spectral density of the acceleration  $D = 0.6$  and  $q = 19.2$  in

$$\sigma_f^2(P) = D(\bar{\dot{P}})^2 \exp(-qf)/(\text{cycle/day}) \quad (106)$$

for  $0.022 < f < 0.216$  cycle/day, where  $\bar{\dot{P}}$  is the mean acceleration, which for 92 days blocks varied from  $2.0 \times 10^{-7}$  to  $5.4 \times 10^{-7}$ . For frequencies higher than 0.216 cycle/day,  $0.0035 (\dot{P}^2/f)$  cycle/day can be taken as a safe maximum. Another statistical analysis of drag by Moe (Reference 159) assumed randomness of density fluctuations from one satellite period to the next (except for a 27-day sinusoidal oscillation) which greatly exaggerates the high-frequency spectral density compared to Equation 106.

For an extension of the reference model above 700 km, for an estimation of variations with latitude and longitude, and for a physically deduced estimate of the short period fluctuations in atmospheric density, appeal must be made to theory: (References 152, 156 and 157). The range of interest is divided into two parts: (1) the thermosphere, from about 100 km to 600 km, characterized by strong heating due to the absorption of solar soft x-rays and ultraviolet radiation (plus possibly other solar emissions), which dissociate oxygen molecules and ionize nitrogen and oxygen; and (2) the exosphere, above 600 km, characterized by atoms and molecules which are ejected from the thermosphere and either escape or return to the thermosphere without collision in most cases. Besides the mentioned photodissociation and photoionization, significant processes in the thermosphere are diffusion and thermal conduction. The diffusion results in the settling out of the heavier constituents so that above 250 km the principal component is atomic oxygen and above about 1600 km, atomic hydrogen or helium. The thermal conduction provides the heat transport from the region of intense energy absorption below 200 km, necessary for the "boiling up" of the atmosphere which results in the strong correlation of density and solar activity at altitudes 500-700 km. Assuming solar heating below 140 km, diffusive separation, hydrostatic equilibrium, and thermal conduction Jastrow and Kyle (Reference 152) extrapolate an atmospheric model above 700 km. For the day maximum, a hydrogen atmosphere of about  $5 \times 10^{-21}$  gm/cm<sup>3</sup> density is reached at about 2100 km; for the night minimum, a hydrogen atmosphere of  $7 \times 10^{-21}$  gm/cm<sup>3</sup> is reached at 1400 km. The greatest theoretical difficulty is that such models continue to decrease rapidly

in density from midnight to dawn, instead of decreasing slowly, as deduced from satellites [(1) and (2) above]; the heating mechanism may be hydromagnetic waves, or the explanation may be electromagnetic effects on the satellite.

The large population of charged particles makes the geomagnetic field significant in determining latitudinal, and possibly longitudinal, variations in atmospheric density, particularly by channeling charged solar particles into the auroral zones around the magnetic poles. That little density variation with latitude (6) has been noticed is mainly the consequence of there being no satellite combining an inclination above  $51^\circ$  and a perigee height above 300 km.

In view of the difficulties obtaining a satisfactory theoretical explanation of the main features of atmospheric density, little work has been done on the characteristics of the short term irregularities to be expected. The spectral density (Equation 106) and the lag of only two hours of the diurnal bulge behind the sun (2) indicate that the spectrum of variations extends from periods of several days down to less than an hour. A similar spectral variety is found in ionospheric sounding (Reference 160); however, at the rarefied altitudes of interest for geodetic satellites, it is not at all necessary that the neutral atmosphere move with the plasma of charged particles causing the fluctuations in radio response.

## Orbital Accuracy Implications

There are two ways in which the atmosphere could distort or interfere with geodetic deductions from satellite orbits: (1) the presence of variations which rotate with the solid earth and hence give rise to a spectrum of orbital oscillations similar to that of geodetic effects; (2) a "noise level" that distorts or even drowns out the geodetic effects depending on the number and distribution of observations used.

The principal distortion of type (1), the influence of the geomagnetic field, is believed to exist mainly on theoretical grounds. The long term observational evidence of geomagnetic effect would be an oscillation of argument  $2\omega$  due to density variation with latitude. An analysis of such variation by Parkyn (Reference 137) finds an effect of opposite sign from what is expected from a geomagnetic cause.

If the evidence of long period effect is so unsure, it can be safely assumed the effect at the daily or semidaily frequency level is negligible.

Of the drag noise, frequencies below about  $h/2W$  will be absorbed by the drag parameters of the reference orbit, where  $h$  is the number of drag parameters and  $W$  is the duration covered by the reference orbit. For frequencies above this cutoff level of  $h/2W$

if it is assumed that the spectrum (Equation 106) applies to all frequencies, the root-mean-square effect on the mean anomaly will be

$$\sigma(M, d) = \pm \frac{1}{2\pi P^2} \left[ \int_{h/2W}^{\infty} \frac{\sigma_f^2(\dot{P})}{f^4} df \right]^{\frac{1}{2}} \approx \frac{0.015 \dot{P} \exp\left(\frac{4.8h}{W}\right)}{P^2 \left(\frac{h}{2W}\right)^2} \quad (107)$$

where  $M$  is in radians and  $P$  in days. The "contamination index" (Reference 115) from drag in determining the coefficient of a variation of expected rms amplitude  $\sigma(c_x)$  and argument  $A_x t$  (for example, a gravitational term) for a set of observations with index  $i$  will be

$$C(c_x, D) = \pm \frac{\left[ \int_{h/2W}^{\infty} \sigma_f^2(\dot{P}) \left( \sum_i \cos 2\pi f t_i \cos A_x t_i \right)^2 \frac{df}{f^4} \right]^{\frac{1}{2}}}{2\pi P^2 \left[ \frac{\partial(M + \omega + \Omega)}{\partial(c_x \cos A_x t)} \right] \sigma(c_x) \sum_i \cos^2 A_x t_i} \quad (108)$$

For an undistorted determination of the coefficient  $c_x$  this contamination index should be small compared to unity. Of the ways to make it small with a given orbit and observing system, the only reliable one is to increase the length of record: that is, increase the number of observations used. Increasing  $h$  or decreasing  $W$  increases the absorption of some of the effect of  $c_x$  by the reference orbit parameters.<sup>†</sup>

<sup>†</sup> Since writing this review, there has come to our attention a study by Kochi and Staley (Reference 161) which covers much of the subject matter of Paragraphs 7 and 8 of this section.

## SECTION II

### GEOMETRICAL CONSIDERATIONS AND ERROR ANALYSIS

#### 1. GENERAL DISCUSSION

Thus far, the satellite orbit and the influences upon it have been discussed with only slight mention of the manner of observation and of the reference frames in which both orbit and observations are described. In this section the principal coordinate systems (inertial, geodetic, and instrumental), the relations between them, and their precise definition and variations in time are described. These systems and their interrelations are then used in the mathematical description of observations. Finally, the geometry is combined with statistics of orbital variations and instrumental errors to estimate their effect on the sought for results.

#### 2. COORDINATE SYSTEMS

##### General Definitions and Notations

General notational schemes are given by References 1, 41 and 162. The notation of this report follows Reference 41 with slight modifications.

As in Section I,  $\mathbf{r}$  is a position vector for an origin at the earth's center of mass but without specification as to the coordinate axes used. For origins other than geocentric, we use a subscript:  $\mathbf{r}_T$  topocentric with origin at a point on the earth's surface;  $\mathbf{r}_s$  origin at the satellite;  $\mathbf{r}_D$  origin that of a geodetic datum with a known bias with respect to the earth's center of mass (as distinguished from an uncertainty with respect thereto). For  $\mathbf{r}$  referred to specific coordinate axis directions different symbols are used. Some of these coordinate systems (all right-handed) are:

$\mathbf{x}$  (inertial):  $x = x_1$  toward vernal equinox,  $z = x_3$  toward north pole

$\mathbf{q}$  (orbital):  $q_1$  toward perigee,  $q_3$  normal to orbit plane

$\mathbf{u}$  (geodetic):  $u = u_1$  toward Greenwich meridian-equator intersection,  $w = u_3$  toward north pole

$\ell$  (station or local):  $\ell_2$  horizontal northward in station meridian,  $\ell_3$  toward local zenith

$\mathbf{a}$ :  $a_3$  station-satellite line,  $a_1$  normal thereto in plane containing local vertical

$\mathbf{p}$ :  $p_3$  station-satellite line,  $p_1$  normal thereto in satellite meridian

$\mathbf{b}$ :  $b_3$  instrument axis,  $b_1$  normal thereto in station meridian.

Refinements of these systems discussed on pages 58 through 60 are shown by an overbar to indicate removal of periodic variations and an argument to indicate an epoch: for example,  $\bar{\mathbf{x}}(t_o)$ .

For rotation matrices use the symbol  $\mathbf{R}_i(\theta)$  where  $i$  is the axis about which rotated and  $\theta$  is the angle rotated, a positive rotation being counterclockwise as viewed from the positive end of the rotation axis toward the origin. The elements  $r_{\ell m}$  of  $\mathbf{R}_i(\theta)$  are:

$$\left. \begin{aligned} j &= i \text{ (modulo 3) } + 1, \quad k = j \text{ (modulo 3) } + 1 \\ r_{ii} &= 1 \\ r_{ij} &= r_{ji} = r_{ik} = r_{ki} = 0 \\ r_{jj} &= r_{kk} = + \cos \theta \\ r_{jk} &= + \sin \theta, \quad r_{kj} = - \sin \theta \end{aligned} \right\} \quad (109)$$

Using these rules we have, for example, for the topocentric local coordinates of a satellite referred to a station of geodetic coordinates  $\mathbf{u}_o$  and local vertical directed toward  $(\phi, \lambda)$ :

$$\begin{aligned} \ell_T &= \mathbf{R}_3\left(\frac{\pi}{2}\right) \mathbf{R}_2\left(\frac{\pi}{2} - \phi\right) \mathbf{R}_3(\lambda) \left[ \mathbf{R}_3(\theta) \mathbf{R}_3(-\Omega) \mathbf{R}_1(-i) \mathbf{R}_3(-\omega) \mathbf{q} - \mathbf{u}_o \right] \\ &= \mathbf{R}_{\ell_a} \left[ \mathbf{R}_{u_q} \mathbf{q} - \mathbf{u}_o \right] \end{aligned} \quad (110)$$

For the topocentric instrumental coordinates of a satellite with the camera axis directed toward  $(\alpha_b, \delta_b)$  we have

$$\begin{aligned} \mathbf{b}_T &= \mathbf{R}_2\left(\delta_b - \frac{\pi}{2}\right) \mathbf{R}_3(\alpha_b - \pi) \left[ \mathbf{R}_3(-\Omega) \mathbf{R}_1(-i) \mathbf{R}_3(-\omega) \mathbf{q} - \mathbf{R}_3(-\theta) \mathbf{u}_o \right] \\ &= \mathbf{R}_{b_x} \left[ \mathbf{R}_{x_q} \mathbf{q} - \mathbf{R}_3(-\theta) \mathbf{u}_o \right] \end{aligned} \quad (111)$$

where

$$\mathbf{q} = \begin{bmatrix} r \cos f \\ r \sin f \\ 0 \end{bmatrix} = \begin{bmatrix} a (\cos E - e) \\ a \sqrt{1 - e^2} \sin E \\ 0 \end{bmatrix}. \quad (112)$$

The second lines of Equations 110 and 111 give alternative abbreviated notation for rotation matrices. In astronomy, the rotation matrix  $\mathbf{R}_{\mathbf{xq}}$  is usually expressed differently: often as coefficients which are functions of  $\gamma = \sin(i/2)$  times trigonometric functions of  $\Omega$  and  $\omega$  such as the orbital plane orientation functions of Musen (Reference 50), mentioned on page 27.

In Equation 110 it is to be emphasized that  $(\phi, \lambda)$  define a direction, and have no necessary connection with position, defined by  $\mathbf{u}_0$ . Of course,  $\mathbf{u}_0$  may be expressed in geodetic coordinates  $(\phi, \lambda, h)$ , but throughout Sections II through IV  $(\phi, \lambda)$  are to be understood as direction angles such as the astronomical vertical of an altazimuth instrument or the "electrical" vertical of a radio interferometric system (even if, as is sometimes the case, arbitrary corrections are applied to refer observations to an axis  $(\phi, \lambda)$  numerically the same as the geodetic coordinates of the station on some datum).

In a vector equation such as Equation 110 and Equation 111 the orientation parameters  $(\phi, \lambda)$  or  $(\alpha, \delta)$  and the time  $\theta$  will generally be known by means separate of observations of a satellite to a much higher degree of accuracy than the orbital parameters. Hence, for practical purposes, the differential of a local vector can be expressed as

$$d\mathbf{L}_T = \mathbf{R}_{\mathbf{L}_T} [\mathbf{R}_3(\theta)d\mathbf{x} - d\mathbf{u}_0]. \quad (113)$$

Then, for  $d\mathbf{x}$  we have

$$d\mathbf{x} = \left[ \frac{\partial \mathbf{R}_{\mathbf{xq}}}{\partial \Omega} \mathbf{q} \quad \frac{\partial \mathbf{R}_{\mathbf{xq}}}{\partial i} \mathbf{q} \quad \frac{\partial \mathbf{R}_{\mathbf{xq}}}{\partial \omega} \mathbf{q} \quad \mathbf{R}_{\mathbf{xq}} \right] \begin{bmatrix} d\Omega \\ di \\ d\omega \\ d\mathbf{q} \end{bmatrix} = \mathbf{C}_{\mathbf{xq}} \begin{bmatrix} d\Omega \\ di \\ d\omega \\ d\mathbf{q} \end{bmatrix} \quad (114)$$

where, for example,

$$\frac{\partial \mathbf{R}_{\mathbf{xq}}}{\partial \Omega} = \frac{\partial \mathbf{R}_3(-\Omega)}{\partial \Omega} \mathbf{R}_1(-i) \mathbf{R}_3(-\omega) = \begin{bmatrix} -\sin \Omega & -\cos \Omega & 0 \\ \cos \Omega & -\sin \Omega & 0 \\ 0 & 0 & 0 \end{bmatrix} \mathbf{R}_1(-i) \mathbf{R}_3(-\omega) \quad (115)$$

and

$$d\mathbf{q} = d \begin{bmatrix} a(\cos E - e) \\ a\sqrt{1-e^2} \sin E \\ 0 \end{bmatrix}$$

$$= \begin{bmatrix} \cos E - e, & -\frac{a \sin E}{1-e \cos E}, & -a \left(1 + \frac{\sin^2 E}{1-e \cos E}\right) \\ \sqrt{1-e^2} \sin E, & \frac{a\sqrt{1-e^2} \cos E}{1-e \cos E}, & a\sqrt{1-e^2} \sin E \left(\frac{\cos E}{1-e \cos E} - \frac{e}{1-e^2}\right) \\ 0 & 0 & 0 \end{bmatrix} \begin{bmatrix} da \\ dM \\ de \end{bmatrix}$$

$$= \mathbf{C}_{qe} de. \quad (116)$$

A simpler form of Equation 114 due to Eckert and Brouwer (Reference 163 and Reference 12, pp. 82-83) is obtained by using differential rotations  $(\psi_1, \psi_2, \psi_3)$  around the X, Y, and Z-axes respectively instead of  $d\Omega, di, d\omega$ . Then,

$$d\mathbf{x} = \begin{bmatrix} 0 & z & -y \\ -z & 0 & x \\ y & -x & 0 \end{bmatrix} \mathbf{R}_{\mathbf{xq}} \begin{bmatrix} \psi \\ \vdots \\ d\mathbf{q} \end{bmatrix}. \quad (117)$$

## Time and the Precise Definition of Coordinates

Explanations of the various types of time and their relationships are given by Clemence (References 164 and 165), Danjon (Reference 166, pp. 113-128), Veis (Reference 1), Rice (Reference 167), Gabbard (Reference 168), and each issue of the American Ephemeris and Nautical Almanac. The applications of the various types of times in celestial geodesy are:

ET — Ephemeris time, defined by the mean frequency of revolution of the earth around the sun for the year 1900.0, is used for the computation of all orbits, as described in Section I.

UT — Universal time, defined by the frequency of rotation of the earth.

UTO — Instantaneous frequency about the instantaneous axis. UTO is obtained by observation of the frequency of rotation of the fixed stars with respect to the local vertical at an observatory.

UT1 — Instantaneous frequency about the mean axis with respect to the earth's crust [defined by averaging over about six years (Reference 169)]. UT1 is required to relate correctly observed directions to the equinox.

UT2 — Mean frequency (defined by subtracting known seasonal variations of 0.<sup>s</sup>03 amplitude from UT1) about the mean axis, still contains secular and irregular variations with respect to ET.

AT — Atomic time, defined by the frequency of vibration of an atom, such as cesium, is the most accurate frequency standard over durations up to some years; A.1, provided by time series such as that of the U. S. Naval Observatory (Reference 170), is essentially the same as ET with its reference longitude shifted so as to differ as little as possible from UT.

The essential requirement is the relationships between times and coordinate systems for the different data used: the satellite orbit, computed in ephemeris time, and referred to axes either fixed at an epoch within the duration covered by the ephemeris, or uniformly rotating; and the observations, timed by signals referred to A.1 (or, practically, ET), and referring directions either to axes fixed with the earth or to a star catalogue defined in terms of mean axes at a standard epoch such as 1950.0. Veis (Reference 1, pp. 97-100) adopts the following coordinate systems (all geocentric) to express the necessary relationships; his notations are in capitals, and ours in the appropriate modifications of the notation of page 55:

$\mathbf{X} = \bar{\mathbf{u}}(\bar{t})$ :  $u_3$  toward mean north pole,  $u_1$  toward intersection of mean equator and mean Greenwich meridian (re-emphasize: a direction, not a coordinate), corresponding to UT2

$\mathbf{Y} = \bar{\mathbf{u}}(t)$ :  $u_3$  toward mean north pole,  $u_1$  toward intersection of mean equator and instantaneous Greenwich meridian, corresponding to UT1

$\mathbf{Z} = \mathbf{x}(t)$ :  $x_3$  toward the instantaneous direction with respect to the celestial sphere of the mean (with respect to earth) polar axis,  $x_1$  toward the instantaneous vernal equinox

$\tilde{\mathbf{Z}} = \bar{\mathbf{x}}(t)$ : at the same instant,  $x_3$  toward the mean (secularly changing) direction of the mean polar axis,  $x_1$  toward the mean (secularly changing) vernal equinox

$\mathbf{W} = \bar{\mathbf{x}}(t_0)$ : at a specified epoch,  $x_3$  toward the mean direction of the mean polar axis,  $x_1$  toward the mean vernal equinox.

For the rotations between these systems, we have

$$\left. \begin{aligned} \bar{\mathbf{u}}(t) &= \mathbf{R}_2(x) \mathbf{R}_1(y) \bar{\mathbf{u}}(\bar{t}) \\ \mathbf{x}(t) &= \mathbf{R}_3(-\theta) \bar{\mathbf{u}}(t) \\ \mathbf{x}(t) &= \mathbf{R}_3(-\Delta\mu) \mathbf{R}_2(\Delta\nu) \mathbf{R}_1(-\Delta\epsilon) \bar{\mathbf{x}}(t) \\ \bar{\mathbf{x}}(t) &= \mathbf{R}_3(-\omega) \mathbf{R}_2(\nu) \mathbf{R}_3(-\kappa) \bar{\mathbf{x}}(t_0) \end{aligned} \right\} \quad (118)$$

where  $x, y$  are the displacements (with respect to the earth's crust) of the instantaneous from the mean north pole in the directions of Greenwich and  $90^\circ\text{W}$ , respectively (Reference 169, p. 349);  $\theta$  is the instantaneous, or apparent, Greenwich Sidereal Time;  $\Delta\mu, \Delta\nu, \Delta\epsilon$  are the nutations in right ascension, declination, and obliquity, respectively;  $(\kappa + \omega)$  is the precession in right ascension, to the first order —  $\kappa$  is defined as the half in the plane of the mean equator at  $t_0$  and  $\omega$  is defined as the half in the plane of mean equator at  $t$ ;  $\nu$  is the precession in declination. The values of  $x, y, \Delta\mu, \Delta\nu$ , and  $\Delta\epsilon$  are all small enough that 1 may be substituted for cosines, arguments for sines, and 0 for products of sines thereof in Equation 118. See also Reference 166, pp. 79-128.

Veis (Reference 1, pp. 102-105) also derives transformations between geodetic systems  $\bar{\mathbf{u}}$  and  $\bar{\mathbf{u}}_0$  for not only translation but also small orientation and scale differences. The latter two seem unnecessary considerations since for celestial geodetic observations terrestrial geodetic control only enters to give the translatory differences between tracking stations: orientation is obtained from the stars, the only conceivable difficulty therein being obtaining an adequate aircraft for orientation of a radio interferometric system.

In 1903 ET and UT were equal, but now ET is 34 seconds fast with respect to UT. Also, ET may gain as much as 1.5 seconds per year (or  $5 \times 10^{-8}$ ) on UT so the difference is easily perceptible in lunar mean motion but will not become geodetically significant until length measurements in celestial geodesy approach a comparable accuracy.

The principal difficulty arising purely from definition of coordinate systems is that of the precession and nutation changing the  $J_2$  secular effect, analyzed by Kozai (Reference 75), as discussed on page 30. The solution adopted by the Smithsonian Astrophysical Observatory is to refer the inclination and the argument of perigee to the true equator of date and to measure the longitude of the node from a departure point shifted from the mean equinox of the date by an amount equal to the precession in right ascension since 1950.0 (Reference 171). Other possible coordinate systems are discussed by Herrick (Reference 172). Difficulties of an observational nature are discussed in Paragraph 1 of Section III.

### 3. OBSERVATION EQUATIONS

Any observation can be expressed as a function of one of the vectors on pages 55-56. For example, for photographic plate measurements  $\eta, \xi$  (Reference 173, p. 281) with a camera of focal length  $f$  (Reference 41)

$$\begin{bmatrix} \eta \\ \xi \end{bmatrix}_{\text{comp}} = \mathbf{b}_{\text{comp}} = \begin{bmatrix} \frac{f}{b_3} & 0 & 0 \\ 0 & \frac{f}{b_3} & 0 \end{bmatrix} \mathbf{b}_T = \mathbf{N}_{bb} \mathbf{b}_T \quad (119)$$

and for the observation equation using Equation 111

$$\begin{aligned} \mathbf{b}_{obs} + d\mathbf{b}_{obs} &= \mathbf{b}_{\text{comp}} + d\mathbf{b}_{\text{comp}} \\ &= \mathbf{b}_{\text{comp}} + \mathbf{N}'_{bb} \mathbf{R}_{bx} \left[ d\mathbf{x} - \mathbf{R}_3(-\theta) d\mathbf{u}_o \right] \end{aligned} \quad (120)$$

where

$$\mathbf{N}'_{bb} = \begin{bmatrix} \frac{f}{b_3} & 0 & -\frac{fb_1}{b_3^2} \\ 0 & \frac{f}{b_3} & -\frac{fb_2}{b_3^2} \end{bmatrix} \approx \mathbf{N}_{bb} \quad (121)$$

Equation 120 is essentially the observation equation for simultaneous observations of a celestial object from two or more points, the treatment of which has been developed in detail by Väisälä (References 174 and 175), Kukkamäki (Reference 176), Brown (References 177, 178, and 179), and Veis (Reference 1, pp. 115-135). Equation 120 differs from those familiar in either astrometry (Reference 173, pp. 288-291, 404-411) or photogrammetry in that no plate constants, or dependencies, or orientation and scale parameters, appear, since the  $\mathbf{b}_{obs}$  in Equation 120 is a consequence of the solution of this problem. Any error in orientation (or in timing) will be absorbed by the  $d\mathbf{b}_{obs}$  in Equation 120. The greater part of  $d\mathbf{b}_{obs}$  should be due to imperfections of the object and to shimmer.

Since the object will normally be very close to the camera axis, Equations 119 through 122 can be written as referring to the vector  $\mathbf{p}$  in place of  $\mathbf{b}$ .

If observations are non-simultaneous, then Equation 120 refers to a satellite in orbit and  $d\mathbf{x}$  must be expressed in terms of differentials of all parameters of significant uncertainty affecting the orbit: the six constants of integration, the parameters of the

gravitational field, the atmospheric density, and the shape factor and area-to-mass ratio of the satellite. From Equations 114 and 116 define  $C_{xe}$  as

$$C_{xe} = C_{xq} \begin{bmatrix} I \\ \dots \\ C_{qe} \end{bmatrix}; \quad (122)$$

then

$$dx = C_{xe} de \quad (123)$$

where  $de$  is a vector comprising differential corrections to the six osculating elements. We next have to express  $de$  in terms of the constants of integration — usually elements of an intermediary at epoch — and the other parameters affecting the orbits in an equation such as

$$de = J de'_o + C_{eg} \begin{bmatrix} \vdots \\ dJ_{nm} \\ dK_{nm} \\ \vdots \end{bmatrix} + C_{ep} \begin{bmatrix} \vdots \\ dn_{2i} \\ \vdots \end{bmatrix}. \quad (124)$$

In Equation 124,  $J$  will be a unit matrix plus one element

$$\frac{\partial M}{\partial a'_o} = \frac{-3n(t - t_o)}{2a'_o}$$

(from Equation 6) for  $(t - t_o)$  on the order of one day; if  $(t - t_o)$  is several days, then there must be added nine additional elements

$$\frac{\partial(\Omega, \omega, M)}{\partial(i'_o, a'_o, e'_o)}$$

to take into account the secular changes due to  $J_2$  expressed by Equation 58 (Reference 41). The term  $C_{eg}$  is a matrix of the changes of the osculating elements due to changes of the gravitational harmonic coefficients, obtained by using the disturbing function  $R_{nm}$  of Equation 77 in Equation 29 and integrating as in Equation 83. The term  $C_{ep}$  is a  $6 \times k$  matrix of changes of the osculating elements at the time of observation with respect to the accelerations  $n_{2i}$  for  $i = 1, \dots, k$  segments of the orbit from  $t_o$  to the time of observation (an alternative to the  $n_{2i}$  would be the coefficients of a power series expansion

of  $n$ ). The term  $\partial M / \partial n_{2i}$  would be obtained from Equation 101, thence  $\partial e / \partial n_{2i}$ ,  $\partial \omega / \partial n_{2i}$ , and  $\partial \Omega / \partial n_{2i}$  from Equation 100 and  $\partial a / \partial n_{2i}$  from Equations 66 and 6. Any provision for change of inclination due to drag would entail additional parameters for atmospheric rotation or crosswind. Substituting Equation 124 in Equation 123 and substituting Equation 123 in Equation 120 gives the complete observation equation.

A process similar to Equations 123 and 124 could be carried out for an orbit numerically integrated in rectangular coordinates, developing  $6 \times 6$  matrices

$$\frac{\partial \begin{bmatrix} x_i & \dot{x}_i \end{bmatrix}}{\partial \begin{bmatrix} x_{i-1} & \dot{x}_{i-1} \end{bmatrix}}$$

in Taylor series. To limit the Taylor series to terms of order  $\ddot{x}$ , the interval  $(t_i - t_{i-1})$  must be on the order of five minutes.

If the observed object is the moon, then  $db_{obs}$  on the left of Equation 120 includes the correction of the center of the moon with respect to the edge of the moon which is actually measured. The mathematics of the geodetic use of lunar photography has been developed by Markowitz (References 180, 181), Potter (Reference 182), and Veis (Reference 1), the former two of whom use  $(\alpha, \delta)$  rather than  $(\eta, \xi)$  as the observations to be adjusted. The alternative lunar method of occultations and eclipses, where the sunlight or starlight is interrupted by the moon, could be treated similarly, with the light ray as the  $b_{3,T}$  axis or the line through the moon's center as the  $p_{3,T}$  axis. The actual development by Bonsdorff (Reference 183), Lambert (Reference 184), O'Keefe and Anderson (Reference 104), and Henriksen (Reference 185), has been in terms of the Besselian fundamental plane (Reference 5, pp. 14-22 and Reference 148, pp. 368-403), equivalent to a geocentric  $p$  coordinate system with the  $p_3$  axis fixed on the star, not on the moon. The treatment by O'Keefe and Anderson (Reference 104) and Henriksen (Reference 185) includes the refinement of the equal limb, or controlled, occultations: a pair observed a short time apart from stations located so that the correction to the lunar radius is considered to be equal for the two stations. This situation results in a geometrically weak solution in the  $p_3$  direction, in addition to the weakness in the  $x_3$  direction due to the low inclination of the moon's orbit, so  $du = 0$  is assumed for one station and  $d\ell_3 = 0$  for the second to obtain, in effect, an equation for difference in latitude and longitude.

A final possibility of the photographic method is to place the camera in the satellite and photograph geodetically controlled points on the ground. The strongest solution will be to have photos overlapping in coverage, so the problem is essentially one of stereotriangulation, which has been most extensively developed by Schmid (Reference 186) and Brown (Reference 177). The output of the stereotriangulation adjustment would be a set of satellite positions on a geodetic datum  $u_0$  with an associated covariance matrix, which would be used as observations in equations analogous to Equation 120. Reference 41 also has equations for theodolite observations.

The ranging observation equation is relatively simple since it can be written in terms of inertial coordinates (References 41 and 162):

$$|\mathbf{x}_T|_{\text{obs}} + d|\mathbf{x}_T|_{\text{obs}} = |\mathbf{x}_T|_{\text{comp}} + \frac{1}{|\mathbf{x}_T|} \mathbf{x}_T \cdot [\mathbf{dx} - \mathbf{R}_3(-\theta) d\mathbf{u}_o] . \quad (125)$$

For range rate observations, the observation equation becomes more complicated because of the contribution of the earth's rotation:

$$\begin{aligned} \dot{|\mathbf{x}_T|}_{\text{obs}} + d\dot{|\mathbf{x}_T|}_{\text{obs}} = \dot{|\mathbf{x}_T|}_{\text{comp}} + \frac{1}{|\mathbf{x}_T|} \mathbf{x}_T \cdot \left[ \mathbf{d}\dot{\mathbf{x}} - \frac{\partial \mathbf{R}_3(-\theta)}{\partial \theta} d\mathbf{u}_o \dot{\theta} \right] \\ + \left\{ \frac{d\mathbf{x} - d\mathbf{u}_o}{|\mathbf{x}_T|} - \mathbf{x}_T \frac{\mathbf{x}_T \cdot (d\mathbf{x} - d\mathbf{u}_o)}{|\mathbf{x}_T|^3} \right\} \cdot \dot{\mathbf{x}}_T \end{aligned} \quad (126)$$

where  $\dot{\theta}$  is the frequency of the earth's rotation. The terms within braces are small, of second order. Hence, range rate observations are insensitive to  $du_3$ , and it is necessary to assume  $du_3 = 0$  near the equator and  $d\ell_3 = 0$  elsewhere.

For  $d\dot{\mathbf{x}}$  in terms of corrections to orbital elements  $d\mathbf{e}$

$$d\dot{\mathbf{x}} = \left[ \frac{\partial \mathbf{R}_{\mathbf{xq}}}{\partial \Omega} \dot{\mathbf{q}} \quad \frac{\partial \mathbf{R}_{\mathbf{xq}}}{\partial i} \dot{\mathbf{q}} \quad \frac{\partial \mathbf{R}_{\mathbf{xq}}}{\partial \omega} \dot{\mathbf{q}} \quad \mathbf{R}_{\mathbf{xq}} \mathbf{C}_{\dot{\mathbf{q}}\mathbf{e}} \right] d\mathbf{e} \quad (127)$$

where

$$\dot{\mathbf{q}} = \begin{bmatrix} -\sin f \\ e + \cos f \\ 0 \end{bmatrix} \frac{na}{\sqrt{1-e^2}} = \begin{bmatrix} -\sin E \\ \sqrt{1-e^2} \cos E \\ 0 \end{bmatrix} \frac{na}{1-e \cos E} \quad (128)$$

and

$$\begin{aligned} \mathbf{C}_{\dot{\mathbf{q}}\mathbf{e}} = \begin{bmatrix} \frac{\sin E}{2a} (1-e \cos E), & e - \cos E, & -\frac{1}{2} \sin 2E \\ -\frac{\sqrt{1-e^2}}{2a} \cos E (1-e \cos E), & \sqrt{1-e^2} \sin E (2e \cos E - 1), & \frac{\cos E}{\sqrt{1-e^2}} (\cos E - e) \\ 0 & 0 & 0 \end{bmatrix} \\ \times \begin{bmatrix} \frac{na}{(1-e \cos E)^2}, & 0 & 0 \\ 0 & \frac{na}{(1-e \cos E)^3}, & \frac{na \sin E}{(1-e \cos E)^3} \\ 0 & 0 & \frac{na}{(1-e \cos E)^2} \end{bmatrix}, \end{aligned} \quad (129)$$

and  $\mathbf{R}_{\mathbf{x}_q}$  and its derivatives are defined in Equations 111 and 115. Range rate theory has been developed most extensively in connection with Doppler tracking by Guier and Weiffenbach (References 187, 188, and 189) who work in terms of the central angle between the station and the satellite rather than  $\hat{\mathbf{x}}_T$ . See also References 190, 191 and Reference 5, pp. 315-320.

For radio interferometric observations measuring direction cosines with respect to a baseline of azimuth  $A$ , clockwise from north (Reference 41)

$$\begin{aligned} \ell_{\text{obs}} + d\ell_{\text{obs}} = & \mathbf{N}_{\ell\ell} \mathbf{R}_3\left(\frac{\pi}{2}\right) \mathbf{R}_2\left(\frac{\pi}{2} - \phi\right) \mathbf{R}_3(\lambda) \mathbf{u}_T \\ & + \mathbf{N}'_{\ell\ell} \mathbf{R}_3\left(\frac{\pi}{2}\right) \mathbf{R}_2\left(\frac{\pi}{2} - \phi\right) \mathbf{R}_3(\lambda) \left[ \mathbf{R}_3(\theta) d\mathbf{x} - d\mathbf{u}_o \right] \end{aligned} \quad (130)$$

where

$$\mathbf{N}'_{\ell\ell} = \left[ \frac{\sin A}{p_3} - \frac{\ell_1^2 \sin A + \ell_1 \ell_2 \cos A}{p_3^3}, \frac{\cos A}{p_3} - \frac{\ell_1 \ell_2 \sin A + \ell_2^2 \cos A}{p_3^3}, -\frac{\ell_3(\ell_1 \sin A + \ell_2 \cos A)}{p_3^3} \right] \quad (131)$$

and

$$\mathbf{N}_{\ell\ell} = \left[ \frac{\sin A}{p_3}, \frac{\cos A}{p_3}, 0 \right]. \quad (132)$$

Kahn (Reference 192) analyzes interferometric observations by considering the cone which is the locus of points with the observed direction cosine  $\ell_{\text{obs}}$ .

The general treatment of observations is also developed by Groves and Davis (Reference 193).

Range, Doppler, and interferometric observations are generally made by electronic means and hence continuous, so that the fullest use entails considerable data. Ideally, an estimate of all six orbital elements should be obtainable from each pass (Reference 189); however, for some elements this determination would be so weak that the linear correction assumption of least squares would be wrong. Reference 41 suggests integrating over segments of passes. For the results of each pass to be given proper weight, however, careful attention to statistical aspects is necessary. This subject is discussed in Paragraph 4 of this section.

#### 4. CONFIGURATION EVALUATION

All the differential corrections in Paragraph 3 of this section — for example,  $db_{obs}$ ,  $du_o$ , and  $dx$  (or  $de_o'$ ),  $dJ_{nm}$ ,  $dK_{nm}$ ,  $dn_{2,i}$  — in a particular set of observation and condition equations can be collected together in two large vectors:  $y$ , called corrections to observations, and  $z$ , called corrections to parameters. The essential difference between the observations and parameters is that for the observations estimates of variance and covariance can be made from data outside that expressed by the observation equations, while for the parameters they cannot. The set of observation and condition equations can then be expressed in matrix form

$$Cy + Mz = f \quad (133)$$

in which the elements of  $C$  and  $M$  are coefficients of the differential corrections in the equations, and the elements of  $f$  are the differences between the observed and computed quantities. Put the estimates of variance and covariance in a covariance matrix  $W$  and solve by the generalized least squares criterion

$$y^T W^{-1} y = \text{Minimum.} \quad (134)$$

Solutions of the general case (Equations 133 and 134) for both  $y$  and  $z$  and their covariance matrices are given in References 194, 195, and 179. In most problems involving observations of satellites, a simpler special case can be applied, in which  $C$  is an identity matrix  $I$ . The solution in this case is

$$z = [M^T W^{-1} M]^{-1} M^T W^{-1} f. \quad (135)$$

The covariance matrix of the adjusted parameters is

$$V_o = \frac{1}{n-m} [M^T W^{-1} M]^{-1} \cdot [f^T W^{-1} f - z^T M^T W^{-1} f] \quad (136)$$

where  $n$  is the number of equations and  $m$  is the number of parameters.

If it is desired to give weight to initial estimates of some of the  $z_i$ 's based on observations outside those in the adjustment, as expressed by a covariance matrix  $V_i$ , then the solution becomes (Reference 115)

$$z = [M^T W^{-1} M + V_i^{-1}]^{-1} M^T W^{-1} f. \quad (137)$$

For  $z_i$ 's which do not have weighted initial estimates, the corresponding rows and columns of  $V_i^{-1}$  are all zeroes. The covariance matrix of the adjusted parameters is

$$V_o = \frac{1}{n-m+r} \left[ M^T W^{-1} M + V_i^{-1} \right]^{-1} \left[ f^T W^{-1} f - z^T M^T W^{-1} f \right] \quad (138)$$

where  $r$  is the number of  $z_i$ 's with weighted initial estimates.

To evaluate a particular configuration of station locations, orbital specifications, frequency of observations, duration of observations, type of observation, and uncertainty of observations, we would want to estimate certain quantities in  $V_o$ , and find the configuration which minimized these quantities within limits imposed by technological capability, economic factors, etc. The  $V_o$  from Equation 136 and Equation 138 employs actual residuals  $f$  to correct the magnitude of  $W$ ; other defects in  $W$ , such as neglect of covariance, remain uncorrected. In a beforehand estimate we are forced to assume that  $W$  is correct in which case  $V_o$  becomes

$$\left[ M^T W^{-1} M + V_i^{-1} \right]^{-1}.$$

The term  $W$  should express variance and covariance due to all phenomena affecting the observations which are not accounted for by the reference model or by the corrections to parameters  $z$ . The difficult part of  $W$ , neglect of which causes most least squares estimates of uncertainty to be too low, is the off-diagonal elements which express covariance. Covariance can be appreciable in a large number of observations due to systematic error, such as timing. Covariance can also be appreciable due to neglected gravitational effects and to drag. Following Equation 107 the drag-caused covariance in mean anomaly between two times an interval  $\Delta t$  apart will be

$$\text{Cov (Drag, } \Delta t) = \frac{1}{16\pi^2 P^4} \int_{h/2W}^{\infty} \frac{\sigma_f^2(\dot{P})}{f^4} \cos 2\pi f \Delta t df. \quad (139)$$

It is thus understandable that the only solutions for covariance matrices which have been made have either taken into account only instrumental error (Reference 196) or have been for particular configurations of simultaneous observations (References 178 and 197). Brown (Reference 178) assumed: (1)  $\pm 2$  micron plate measurement errors; (2) 600 mm focal length; (3) five stations on North American Datum from the Aleutians to southern California; (4) one station each on Hawaii and Midway; (5) satellite altitude about 1800 km; (6) three groups of nine flashes each over an arc about  $48^\circ$  long; (7a) zero uncertainty in NAD positions; (7b)  $\pm 6$  m standard deviation in each coordinate, but zero covariance in NAD positions. He obtained uncertainties less than  $\pm 6$  m in each coordinate of Midway and Hawaii, under assumption (7a), less than  $\pm 8$  m under assumption (7b).

Qualitative and partially numerical analyses (References 1, 191, 198, 199, and 200), however, generally favor use of orbital interpolation methods for transoceanic connections between geodetic datums of an order of accuracy  $\pm 10$  meters. The principal reason is the desirability of observing the satellite at as close a range as possible, to limit the degradation of accuracy which takes place with increased range. The minimum perigee height to limit drag effects to negligible levels (assuming  $A/m$  about  $0.05 \text{ cm}^2/\text{gm}$ ) is generally concurred to be 700 to 1000 km. Other specifications generally concurred: inclinations  $55^\circ$  to  $70^\circ$  to be accessible to most areas of interest; eccentricity less than 0.05 to keep the satellite always within accurate observing range; timing within  $\pm 0.001^s$ . Newton (Reference 201), considering geodetic use of Doppler observations, proposes a perigee height on the order of 1500 km.

Specification of satellite orbits for analysis of the gravitational field has received little discussion. A perigee height on the order of 700 to 1000 km is also desirable from drag considerations, but a larger eccentricity is preferable: on the order of 0.2, enough to give a well-defined perigee direction, but not so much as to require a semimajor axis severely attenuating the effects of higher harmonics. The optimum inclination for a particular term could be deduced from the effect of its inclination factor  $F(i)$  (Equations 77 and 78) in the perturbing equations (Equation 29), but for general analysis all that can be suggested is variety.

## SECTION III

### ROCKET AND ARTIFICIAL SATELLITE TECHNIQUES

#### 1. GENERAL

##### Vehicles

Some characteristics reasonably attainable in satellites less than 100 cm in diameter and less than 100 kg in weight, such as are most likely to be available for geodetic purposes (References 3, 198, 202, and 203) are:

- (1) Power accumulation at a rate of 25 watts while in sunlight. The principal uncertainty in this rate is that of the deterioration of solar cells due to radiation, micrometeorities, etc., though experience with 1958  $\beta 2$  indicates it is slow.
- (2) Usable energy storage capacity of  $10^6$  watt-seconds. "Usable" means that only a small percentage of the battery capacity is discharged, to insure long life, and that there is about a 0.15 loss in charging, etc.
- (3) Capacitors of 0.35 efficiency able to discharge 1500 watt-seconds within 0.001 second.
- (4) A frequency standard of stability  $10^{-8}$  per day or  $2 \times 10^{-10}$  per minute.
- (5) Attitude sensing within one degree by horizon sensor or magnetic field sensor.
- (6) Spin damping to less than one revolution per 40 minutes.
- (7) Automatic, solar sensor, or command operation of switches.
- (8) Area-to-mass ratio less than  $0.08 \text{ cm}^2/\text{gm}$ .

These values are intended to be order-of-magnitude ideas only, since actual specifications are subject to sudden obsolescence.

Limitations on orbital specifications may exist for the inclination due to political or safety considerations around the launch site. Use of a retrograde in place of a direct orbit may reduce weight capacity by as much as 10 percent.

Pertinent specifications of satellites which have been used geodetically, or which are of possible interest to geodesy (indirectly, in the case of the Echo satellite), are given in Table 3.

Table 3  
Specifications of Earth Satellites

Name	Designation	Launch Date	Tracking Radio		Maximum Ratio Area-Mass $A/m$ $\text{cm}^2/\text{gm}$	Perigee $h_p$ $\text{km}$	Eccentricity $e$	Inclination $i$
			Frequency $10^6$ cps	Termination Date				
Sputnik II (Down 1958 April 14)	1957 $\beta$	1957 Nov. 3	20,40	1957 Nov. 10	0.07	230	0.07	$65^\circ$
Vanguard I	1958 $\beta 2$	1958 Mar. 17	108		0.14	650	0.19	$34^\circ$
Vanguard II	1959 $\alpha 1$	1959 Feb. 17	108	1959 Mar. 16	0.21	560	0.16	$33^\circ$
Vanguard III	1959 $\eta$	Sept. 18	108	1959 Dec. 12	0.27	510	0.19	$33^\circ$
Explorer VII	1959 $\epsilon 1$	Oct. 19	108	1959 Dec. 5	0.11	550	0.03	$50^\circ$
Tiros I	1960 $\beta 2$	1960 April 1	108		0.07	690	0.00	$48^\circ$
Transit IB	1960 $\gamma 1$	April 13	0		0.14	290	0.03	$51^\circ$
	1960 $\gamma 2$	April 13	54,324; 162,216	1960 June 19 1960 July 12	0.06	370	0.03	$51^\circ$
Sputnik IV	1960 $\epsilon 1$	May 15	20	1960 July 2	0.02	280	0.03	$65^\circ$
Transit IIA	1960 $\eta 1$	June 22	54,324; 162,216		0.07	630	0.03	$67^\circ$
NRL Radiation	1960 $\eta 2$	June 22	108	1961 April 18	0.12	610	0.03	$67^\circ$
Echo I	1960 $\epsilon 1$	Aug. 12	108	1960 Dec.	100.0	1450	0.02	$47^\circ$
	1960 $\epsilon 2$	Aug. 12	0		0.05	1530	0.01	$47^\circ$
Courier IB	1960 $\nu 1$	Oct. 4	108		0.06	810	0.02	$28^\circ$
Tiros II	1960 $\pi$	Nov. 23	108		0.07	620	0.01	$48^\circ$
Explorer XI	1961 $\nu$	1961 April 27	108		0.20	490	0.10	$29^\circ$
Transit IV-A	1961 $\epsilon 1$	June 20	54,324; 162,216		0.12	880	0.01	$67^\circ$
Tiros III	1961 $\rho 1$	July 12	108		0.07	730	0.01	$48^\circ$

Comparatively inexpensive vehicles of potential value for geometrical geodetic purposes are sounding rockets fired from balloons at 20-30 km altitude. One such rocket is the U. S. Loki-II Rockoon which is able to carry a 4 kg payload to about 120 km altitude (Reference 204, pp. 149-153); another is the Japanese Sigma rocket, designed to carry a 2.5 kg payload to about 100 km (Reference 204, pp. 283-286). Tests carried out thus far of rocket flash photography (Reference 205) have, however, used ground-launched rockets, for which there is better control of timing and trajectory.

## Timing

Accuracy of  $\pm 10$  meters positionally for satellites in orbit implies timing accuracy of  $\pm 0.001^s$  or better. Attainment of such accuracy requires use of recently developed techniques in time service determinations and broadcasts and in station instrumentation, (References 170, 203, and 206).

Starting in 1960, the essential control of time signals is by a system of about ten cesium oscillators operated by the U. S. Naval Observatory and other national time services. These oscillators monitor VLF time signals broadcast by Station NBA, Canal Zone (18 kc/sec) and Station GBR, England (16 kc/sec) and HF signals broadcast by Station MSF, England, Station WWV, United States, and Station WWVH, Hawaii. The probable errors of the VLF stations as monitored in Washington are  $\pm 0.4$  milliseconds or less; of the HF stations, less than  $\pm 1.0$  milliseconds. These stations are also all coordinated to transmit the same basic frequency within  $10^{-10}$ . It is expected that other national time services will soon join this system (Reference 170).

This atomic time (A.1) is compared to ET through observations of the moon's orbit by the Markowitz moon camera (Reference 181). The variations of UT with respect to A.1 are observed as frequently as weather permits by the photographic zenith telescopes (PZT's) and Danjon astrolabes, each of which have probable errors of about  $\pm 0''.06$  in latitude and  $\pm 0.005$  in time (internal; not including effect of star catalogue error: see the following paragraph) for a single night's observations (Reference 169, pp. 334-340). Corrections resulting from these observations are published within a few months by the national times services and a year or more later in the Bulletin Horaire.

The time should be obtainable from VLF signals at distances up to about 8,000 km with an uncertainty of about 0.5 millisecond (Reference 170). To preserve this accuracy for a day, a frequency standard which is stable to better than  $10^{-8}$  is necessary; the quartz crystal control clocks currently used in the tracking of artificial satellites are stable to better than  $10^{-9}$  (Reference 206). There are other technical difficulties in the timing system such as accuracy of the frequency divider and time delay in the receiver, but probably the limitation on timing accuracy of any optical observation is in the optical and mechanical parts — in the operation of the shutter on a camera or of a gas discharge lamp.

## Orientation

Any type of non-simultaneous observations incorporating directions (that is, all types except range and range-rate) depends upon accurate referral to the inertial coordinate system. This referral is through the stars: directly in the case of photographic observations by stellar images on the same plate as the satellite image; or indirectly by

conventional astronomic positions in the case of theodolites and by tracking an aircraft equipped with a flashing light in the case of radio interferometry. Hence, these methods are, in turn, dependent upon the accuracy of the star catalogue. The density of stellar images needed for photographs (or for accurate astronomic latitude) is about one per  $2^\circ \times 2^\circ$  square, or about 10,000 stars for uniform world coverage. Fundamental catalogues therefore do not have sufficient density and resort must be had to general catalogues.

The best general catalogues now available are the Yale Zone Catalogue and Zweiter Katalog der Astronomischen Gesellschaft (AGK2) for latitudes north of  $30^\circ\text{S}$ , and compilations by the Royal Observatory, Capetown, South Africa, south of  $30^\circ\text{S}$ . The Yale Catalogue and AGK2 are based on observations made mainly in the 1920's and 1930's with proper motions dependent upon observations back to the mid-19th century. For epoch 1960, their errors are on the order of  $\pm 0''.2$  to  $\pm 0''.4$  in each coordinate (Reference 207, p. 225). South of  $30^\circ\text{S}$  the errors are larger because of the lack of 19th century observations, and include appreciable systematic variations due to poor positions of reference stars as well as the random error due to proper motion.

Currently in preparation is AGK3R, a fundamental catalogue of more than 20,000 stars of latitude north of  $2^\circ\text{S}$ , observed on meridian circles (forming the reference system for AGK3). The anticipated mean error of AGK3R is  $\pm 0''.13$  in each coordinate, and  $\pm 0''.008/\text{year}$  proper motion. Similar work is now underway for the southern hemisphere, as also are new photographic catalogues. So by the late 1960's star positions of  $\pm 0''.15$  error and a density on the order of one per  $1^\circ \times 1^\circ$  square should be available; see Reference 207 for discussions of the problems involved, and Reference 197 for discussion of the accuracy required for geodesy.

## 2. OPTICAL TECHNIQUES

### Attenuation and Illumination

Light of wave length  $\lambda$  will be scattered by gas molecules in the atmosphere proportionate to  $\lambda^{-4}$  and by water droplets independent of wave length. For the proportionate transmission  $T$  of light from a source at altitude  $h^*$  and zenith angle  $z$  with respect to the observer at altitude  $h_o$

$$T = \exp \left\{ - \sec z \int_{h_o}^{h^*} [\beta_m \rho_m(h) + \beta_w \rho_w(h)] dh \right\} = e^{-\tau \sec z}. \quad (140)$$

The molecular effect  $\beta_m \rho_m(h)$  is given quite accurately by  $0.00114\lambda^{-4}$ ,  $\exp(-0.126h)$  for  $h$  in kilometers and  $\lambda$  in microns (Reference 208), while data in Reference 208 suggest

for the water effect  $\beta_w \rho_w(h)$  of clear air the much cruder estimate of  $0.145 \cdot \exp(-0.65h)$ . For a source outside the atmosphere and an observer at sea level,  $\tau$  becomes  $(0.0090\lambda^{-4} + 0.223)$ .

Sunlight is the only means of illumination thus far applied extensively to satellites. Applying Equation 140 to equations given by Reference 209, there is obtained for the received flux  $S_R$ :

from a diffusely reflecting sphere of radius  $b$  and albedo  $\kappa$  due to an incident flux  $S_I$

$$\frac{S_R}{S_I} = \frac{2\kappa b^2}{3\pi r^2} [\sin \sigma + (\pi - \sigma) \cos \sigma] e^{-\tau(\lambda) \sec z}; \quad (141)$$

from a specularly reflecting sphere

$$\frac{S_R}{S_I} = \frac{\kappa b^2}{4r^2} e^{-\tau(\lambda) \sec z}. \quad (142)$$

For sunlight in the vicinity of the earth,  $S_I$  is about  $1.2 \times 10^5$  lumens/meters<sup>2</sup> and  $\lambda$  about 0.52 microns, giving a  $\tau(0.52, \infty, 0)$  of 0.348. For a flux  $S$  in lumens/meters<sup>2</sup>, the corresponding stellar magnitude is  $-2.5 (\log_{10} S + 5.65)$ . Many results of value have been obtained from solar-illuminated satellites (see Table 1), but satellites of high enough perigee and small enough area-to-mass ratio to be of further geodetic value have only been tracked consistently by the Baker-Nunn telescopes of the Smithsonian Astrophysical Observatory. Under a favorable combination of perigee latitude and right ascension and nodal longitude, they obtain as much as 200 observations in a 20-day period of Vanguard satellites ( $h_p = 600$  km,  $i = 33^\circ$ ,  $e = 0.18$ ) (Reference 112), concentrated, however, in less than half of the orbit. Reference 1 discusses geometrical conditions of observability.

Methods of faceting or sectoring the surface of a satellite to give periodically brighter reflections have been suggested by References 210 and 211.

Searchlight tracking was originally proposed by O'Keefe, and has been most carefully examined by Hoffman (Reference 210). The essential requirement is "corner-cube" retro-directive reflectors on the satellite, which are now made with only 2" dispersion. An array of eight such reflectors with a filler of refractive index 1.7 on a satellite, four each along two parallels, at  $55^\circ$  to the axis, will assure a reflection at least 0.72 maximum within  $45^\circ$  of satellite rotation with respect to the observer. For a light source of luminous intensity  $I$ , the received flux  $S_R$  from a retrodirective reflector of efficiency  $\kappa$ , dispersion  $\psi$ , and area  $A$  is

$$\frac{S_R}{I} = \frac{4\kappa A}{\pi r^2 \psi^2} e^{-2\tau \sec z}. \quad (143)$$

Allowing for diffraction, rotation of the satellite, imperfect pointing, light loss in the glass filler of the reflector, aberrational shift, etc.,  $\kappa$  is about 0.4. The aberration due to satellite motion coupled with the sharp decline in intensity from the central axis of the searchlight [about  $\exp(-4 \times 10^{-4} \theta^2)$  at angle  $\theta$ ] make atmospheric back-scatter negligible. For  $I = 1.2 \times 10^9$  cp (two standard searchlights),  $z = 45^\circ$ ,  $r = 2000$  km,  $\lambda = 0.52$  microns and a camera of 500 mm aperture, equation 143 yields a required area per reflector on the satellite of  $100 \text{ cm}^2$ . The method appears entirely feasible, the principal difficulty probably being accurate prediction and aiming.

For a light source on the satellite of luminous intensity  $I$ , the received flux  $S_R$  is

$$\frac{S_R}{I} = \frac{1}{r^2} e^{-\tau \sec z} \quad (144)$$

Xenon discharge lamps have been developed to a high degree of reliability by Edgerton. Specifications which appear feasible are an efficiency of about 35 lumens per watt, a flash duration of about one millisecond, and a lifetime on the order of a million flashes (Reference 212). As specified on page 69, about 1500 watt-seconds per flash is reasonably available. Assuming  $\lambda$  is 0.52 microns and coverage over a hemisphere, the received energy density will be about  $(8300/r^2) \exp(-0.348 \sec z)$  lumen-seconds/meters<sup>2</sup>. Reference 198 has essentially the same figures for flash efficiency, a lower value of attenuation  $\tau$ , and assumes full spherical coverage.

Assuming 0.6 of the orbit in sunlight and 0.6 of the orbit visible to stations in the dark, the accumulation rate on page 69 would permit one 1500 watt-second flash per three minutes and the energy storage capacity could save up 200 such flashes.

Equation 144 also applies to pyrotechnic flares, which can attain a peak luminous intensity of about 20 million candle power, mostly in the near infrared (1.0 micron), and an effective (half peak) duration of 3 to 5 milliseconds (References 178 and 197).

## Refraction and Aberration

To cover as much as possible of a satellite orbit, and to attain the strongest geometry for simultaneous techniques, observations from any station should be made at all zenith distances to the maximum at which accurate results are obtainable. The sole limitation on accuracy is refraction, analyses of which with special reference to satellites, rockets, etc., have been made by Veis (Reference 1), Väisälä (References 174 and 175) and Brown (References 179 and 213). The change  $\delta z$  to be added to the observed zenith distance  $z_o$  is most succinctly expressed as an integral along the ray path from the observed object  $s$  to the observer  $0$ :

$$\delta z = - \int_s^o \frac{ds}{R} = \int_s^o \frac{\mathbf{n} \cdot \nabla \mu}{\mu} ds \quad (145)$$

where  $R$  is the radius of curvature of the ray path,  $\mu$  is the refractive index, and  $\mathbf{n}$  is the unit vector normal to the ray path.

Equation 145 may be deduced from Snell's law, or by treating  $\int \mu ds$  as an action integral (Equation 45) and applying Hamilton's principle (called Fermat's in optics). For zenith distances less than  $45^\circ$ , assumption of a flat earth model and exponential decrease with altitude of  $(\mu - 1)$  are adequate, but for greater zenith distances, formulas for solving the integral become complicated because of the necessity of using a spherical earth model, and the necessity of expressing the manner of variation of  $\mu$  and  $\nabla \mu$  with  $s$ . Solutions which have been applied to the latter problem, besides the exponential decrease with altitude, are numerical integration using  $\mu$  based on meteorological measurements, and expression of the integral in the form

$$\sum_i a_i \tan^{(2i+1)} z_o$$

where the  $a_i$ 's are obtained by observation.

The case of greatest interest to celestial geodesy is the difference in refraction of an object and its stellar background; Veis (Reference 1) obtains

$$\Delta \delta z = - 435''.0 \frac{\tan z_o}{\cos z_o} \left( 1 - e^{-0.1385 \cos z_o} \right) \quad (146)$$

which is adequate for  $z < 45^\circ$ ; References 1 and 179 give additional terms for  $z > 45^\circ$ .

A form of refraction more troublesome than Equation 146 is irregular shimmer in the immediate vicinity of the telescope, which will not be averaged out for brief flashes as it is normally for long stellar exposures. Shimmer has been investigated by Nettleblad (Reference 214) and further examined by Brown (Reference 197) who find that the magnitude of shimmer is approximately proportionate to  $\sec^{\frac{1}{2}} z$ , that it may vary an order of magnitude from night to night, and that it has a characteristic wave length on the order of 2 to 4 cm. Hence, shimmer should decrease in effect with increase in aperture. Experimentally determined angular shimmer effects for apertures greater than 100 mm fit the formula

$$\sigma(\alpha) = \pm \frac{k}{a} \sec^{\frac{1}{2}} z \quad 0.05 < k < 0.30 \quad (147)$$

for  $\alpha$  in radians and  $a$  in microns. This effect creates a point of diminishing returns of

roughly  $f \approx 100 \sqrt{a}$  in the accuracy gained by increasing the focal length for a given aperture.

In addition to the usual stellar annual and diurnal aberration, there is an aberrational effect  $v/c$  due to the component  $v$  at right angles to the line of sight of the satellite velocity relative to the earth, which has a magnitude of a couple of seconds arc; see Reference 1. This angle must be doubled in computing the displacement of a searchlight with respect to a telescope, to allow for the outgoing as well as the return light.

TN-1155

## Theodolites

Rather elaborate photo-recording cinetheodolites have been developed for aircraft and missile tracking, such as the Askania and the Contraves (Reference 3). Although an accuracy of  $\pm 20''$  for a single frame is stated, theodolites do not seem capable of geodetic accuracy for satellite tracking because, in addition to sharing the timing difficulties of cameras, they require the full refraction correction of Equation 145, entailing computation of  $\mu_o$  from temperature and humidity observations, etc., by Equation 157.

## Cameras

For a film requiring an energy density  $E_x$ , a film and lens combination of resolution characterized by "spot" diameter  $a_x$ , in a camera of aperture  $a$  and focal length  $f$ , photographing an object with an angular rate of travel with respect to the camera of  $\omega$ , and exposure time  $\Delta t$ , the required flux  $S_R$  is

$$S_R = \frac{\pi a_x^2 + 4 a_x f \omega \Delta t}{\pi a^2 \Delta t} E_x . \quad (148)$$

The value of  $E_x$  is typically 0.004 lumens-seconds/meters<sup>2</sup> (or ASA 250) to give sufficient contrast above film fog, and  $a_x$  ranges from 18 to 30 microns. For a tracking camera, the second term in the numerator of Equation 148 becomes 0; for a fixed camera photographing a moving, continually illuminated object, the first term in the numerator becomes negligible.

The design of the Baker-Nunn telescope, a tracking camera with a Schmidt-type optical system, is described in detail by Henize (References 215 and 216). It is capable of tracking either a satellite or the stars (including oscillating between them), has an aperture of 500 mm, a focal length of 500 mm, and yields images of 20 to 30 microns diameter. The camera has a spherical focal surface and uses 56 mm film. The accuracy of

the camera-film-plate measurement system (using a Mann comparator) is  $\pm 1''$  to  $\pm 2''$  ( $\pm 2.5$  to  $\pm 5$  microns) for stellar images (Reference 217). The accuracy has not been tested for satellite images, since the cameras have never been used in simultaneous observations; however, a preliminary estimate is  $\pm 6''$  (Reference 218). The timing accuracy depends upon the simultaneity of a gas-discharge lamp illuminated photo of a slave clock of the crystal-controlled system and of the center point of the telescope photo frame defined by a sweep shutter, in addition to the factors described on page 71. Using HF time services, the times obtained are believed to be trustworthy to within 10 milliseconds, and some to within 2 milliseconds (Reference 219); there should be some improvement using VLF time signals.

The system of twelve Baker-Nunn telescopes operated by the Smithsonian Institution Astrophysical Observatory average 1200 successful observations per month (Reference 220). These observations are published in the series Research in Space Sciences, Special Reports, first in preliminary form and later in precise form.

Markowitz (Reference 221) has designed and constructed a camera system which simultaneously tracks the satellite and the stars by passing the satellite image through a rotating glass plate 13 mm thick. Aperture of the camera is 178 mm, and focal length 1015 mm; position measurement accuracy is  $\pm 5''$ , and timing accuracy  $\pm 0.002$ .

The advantage of the tracking cameras (References 215 and 221) is lost if the satellite image is a flash rather than continuous, since the full effect of any tracking irregularity would be felt. In such cases stationary observations would have to be made and the time measured either by a simultaneous radio signal or by photoelectric cell (Reference 198).

Several fixed camera systems for satellite observation have been developed: the ballistic cameras (References 178, 197, and 222), aperture 117 mm and focal length 304 mm; modified aerial reconnaissance cameras (Reference 205), aperture 203 mm, focal length 1015 mm; and an especially constructed camera (Reference 223), aperture 145 mm, focal length 910 mm. All of these cameras possess the advantages, relative to the Baker-Nunn telescope, of using glass plates rather than film, and of being mobile; they have the disadvantage of being fixed, having a small aperture, and requiring a much more intense source. For this reason, as well as to overcome shimmer and increase angular accuracy, a larger ballistic camera of aperture 300 mm, focal length 1200 mm is proposed (Reference 197). The timing accuracy of the ballistic cameras and modified aerial cameras is on the order of  $\pm 0.010$ , which is amply accurate for stellar orientation and for simultaneous observation of a flare or satellite flash. The camera of Hewitt (Reference 223) has an estimated timing accuracy of  $\pm 0.001$  by measuring the passage of the disc shutter with a photoelectric cell in coordination with the flash lamp illuminated photo of a clock.

The plate measurement accuracy of the ballistic cameras for flare images has been well confirmed as  $\pm 3$  microns standard deviation by simultaneous observations in redundant geometrical configurations (References 178, 197, and 224).

Several proposals have been made for simultaneous observations of rocket flashes against a stellar background (References 174, 176, 178, 197, 205, 225, and 226). Tests actually carried out include: (1) flares on a balloon at 15-20 km altitude observed by reflecting telescopes of 689 and 1,031 mm focal length at Helsinki and Turku (153 km apart) with a deduced rms error of direction of  $\pm 2''$  (Reference 175); and (2) flares at more than 700 km altitude observed by three ballistic cameras located on Bermuda and on the east coast of the United States from which an rms error of position of  $\pm 18$  m for Bermuda was deduced (Reference 224).

In summary, camera techniques can attain the  $\pm 10$  meters positional accuracy by non-simultaneous techniques, mentioned in Paragraph 4 of Section II, as well as obtaining more detailed gravity information, if timing errors are reduced to  $\pm 0.001$ : probably through use of a radio signal broadcast by the satellite simultaneous with a flash. An alternative might be a flash control by closely monitored clock on the satellite.

An optical technique of considerable possibilities both in sensitivity and accuracy is photoelectric tracking (Reference 227), in which there is timed the light from a satellite or star as it crosses a slit.

## Satellite Photogrammetry

As has occurred in the conventional application of the two techniques, it may be expected that eventually satellite photogrammetry will take over many of the tasks of satellite geodesy. So far, the subject has received very little discussion in print (References 228 and 229).

Two essentials of such a system are:

- (1) A camera of high geometric fidelity, and
- (2) Wide angle coverage to limit the number of stereoscopic models to bridge between existing geodetic control.

A combination of (1) and (2) will necessarily result in low resolution, thus requiring:

- (3) A means of accurately matching low resolution photography to geodetic control.

A camera of high geometric fidelity further implies:

- (4) Highly stable film, and

- (5) Recovery of film.

For strengthening the control of the photogrammetry, there is further needed:

- (6) Orientation by a stellar camera to within 5", coordinated to within about 0.01 with the ground camera, and
- (7) An accurately computed orbit, with ground tracking.

Consideration of velocity and illumination further indicates:

- (8) Image motion compensation.

A photogrammetric satellite will benefit greatly from the orbiting astronomical observatory (Reference 230) which has similar problems of stabilization, orientation, dimensional stability under temperature changes, etc., in more acute form.

### 3. RADIO TECHNIQUES

Any radio observation measurement depends upon the relation in phase between a received signal and a reference standard of the same, or nearly the same, frequency. Interferometry uses the difference in phase of signals from the same source received at the same instant at two different antennas on the ground:

$$\Delta_s \Phi = \frac{\omega}{c} (r_1 - r_2) \quad (149)$$

where  $\omega$  is the frequency (radians/sec) in terms of which the phase difference is measured and  $c$  is the velocity of light.

Doppler uses the difference in rate of change of phase of the received signal and a standard at the ground station:

$$\Delta \omega = \dot{\Delta \Phi} = \frac{\omega}{c} \dot{r} . \quad (150)$$

Range measurement uses the change in phase of a signal from the time it was transmitted from the ground station to a transponder or reflector to the time it is received back again:

$$\Delta_t \Phi = 2 \frac{\omega}{c} r . \quad (151)$$

The  $t$  index in Equation 151 denotes that it is a temporal phase difference, in distinction from the spatial phase difference  $\Delta_s \Phi$  of Equation 149.

Aberration affects Equations 149, 150, and 151 in that the satellite or rocket position and velocity change during the time interval of travel of the signal, and small corrections must be applied to these equations to make them refer to the instant the signal leaves the satellite or rocket.

Equations 149 through 151 imply constancy of  $c$ , which constancy occurs in a vacuum; allowance must be made for the effect of the medium through which the signal travels, these effects are discussed in the following paragraph.

## Environmental Effects on Propagation

The actual phase changes which take place upon propagation through the atmosphere are

$$\Delta_s \Phi = \frac{\omega}{c} \left[ \left( \int \mu ds \right)_1 - \left( \int \mu ds \right)_2 \right] \quad (152)$$

$$\Delta \omega = \frac{\omega}{c} \frac{d}{dt} \left( \int \mu ds \right) \quad (153)$$

$$\Delta_t \Phi = \frac{\omega}{c} \left[ \left( \int \mu ds \right)_{up} + \left( \int \mu ds \right)_{down} \right] \quad (154)$$

where  $\mu$  is the refractive index and the integrals are over the ray path.

The change in phase difference  $\delta \Delta \Phi$  of an interferometric system with a baseline of length  $\Delta x$  due to the rotation  $\delta \psi$  of the wave front emanating from the source as it arrives at the ground stations is

$$\delta \Delta \Phi = \frac{\omega}{c} \Delta x \sin \psi \delta \psi \quad (155)$$

where  $\psi$  is the angle between the baseline and the ray as it arrives at the baseline. The mathematical expression for  $\delta \psi$  is the negative of Equation 145. Radio interferometry has additional complications beyond optical observations in that the refractive index at the source and the horizontal gradients of the index may both be of appreciable effect. The "wedge component" due to the horizontal gradients has received the most detailed theoretical analysis in connection with radio astronomy (Reference 231). Application to satellite signals is discussed in References 232 and 233.

In carrying out the differentiation with respect to time of the Doppler equation (Equation 153), the change of the upper limit of integration due to motion of the source must be

considered. The result, applying Fermat's principle and assuming isotropy of  $\mu$  (Reference 234) is

$$\Delta\omega = \frac{\omega}{c} \left( \mu_s \mathbf{t}_s \cdot \dot{\mathbf{r}} + \int \frac{\partial\mu}{\partial t} ds \right) \quad (156)$$

where  $\mathbf{t}_s$  is the unit vector tangent to the ray at the source. Usually, the refraction effects in this first term in Equation 156 will be larger than those of the second term, in which the effects of irregularities are smoothed out by the integration.

For integration of the second term in Equation 156, or integration of the two integrals in the range equation (Equation 154) (these integrals have only higher order differences) there are the alternatives of using assumed values of  $\mu$  or  $\partial\mu/\partial t$  and numerically integrating by ray tracing methods, or of developing  $\int \mu ds$  or  $\int (\partial\mu/\partial t) ds$  analytically in negative powers of  $\omega$  (or  $f$ ), as is done by Guier and Weiffenbach (References 187 and 188), and Davisson (Reference 235). The effectiveness of either of these procedures depends upon the developments being largely in terms of one, or a few, parameters, the effect of which can thus be eliminated by using multiple frequencies. The feasibility of the procedures depends upon the physical nature of the refractive index  $\mu$ , which is split into two distinct parts.

(1) Tropospheric refraction is already familiar in geodesy through its effect on airborne electronic methods (Reference 236), expressed by a standard formula such as that adopted by the I.U.G.G. (Reference 237):

$$(\mu - 1) 10^6 = \frac{103.49}{T} (p - e) + \frac{86.26}{T} \left( 1 + \frac{5748}{T} \right) e \quad (157)$$

in which air pressure  $p$  and water vapor pressure  $e$  are in mm of mercury and temperature  $T$  in degrees Kelvin. Bean (Reference 238) discusses formulas for extrapolating  $\mu(h)$  given the ground level value  $\mu_0$  and obtains from eight year's of data over the United States separate rules for the segments 0 to 1 km and 1 to 9 km, which represent  $\mu$  within  $10^{-5}$ . At 9 km altitude  $(\mu - 1)$  averages  $105 \times 10^{-6}$  and varies over a range of only  $8 \times 10^{-6}$ . Above 9 km  $(\mu - 1)$  is representable within  $\pm 15$  percent by Equation 158:

$$\mu - 1 = 105 \times 10^{-6} \exp [-0.142 (h - 9)] , \quad h \geq 9 \text{ km.} \quad (158)$$

(2) Ionospheric refraction is dependent upon the electron density (Reference 160). Thus,

$$\mu = \left( 1 - \frac{4\pi N e^2}{\epsilon_0 m \omega^2} \right)^{\frac{1}{2}} = \left( 1 - \frac{3.18 \times 10^9 N}{\omega^2} \right)^{\frac{1}{2}} \quad (159)$$

where  $N$  is in electrons per cubic centimeter,  $e$  and  $m$  are, respectively, the charge and mass of an electron, and  $\epsilon_0$  is the dielectric constant. For frequency in cycles per second  $f = 2\pi\omega$ ,  $f \geq 10^8$  cps, and  $N$  in electrons per cubic meter Equation 159 becomes

$$\mu = 1 - \frac{40N}{f^2} = 1 - \frac{1.6 \times 10^3 N}{\omega^2} \quad (160)$$

The electron density  $N$  is a function of the intensity of ionizing radiation, the atmospheric density, and the atmospheric chemical composition — all three determine the production rate of electrons and the latter two determine the destruction rate through recombination. Assuming constant coefficients for the rates of these two processes, equilibrium between the processes, ionizing radiation to come from the sun, and atmospheric density to vary exponentially as in Equation 96, the Chapman model of electron density is obtained (Reference 160):

$$N = N_{\max} \cos^{-\frac{1}{2}\chi} \exp \frac{1}{2} [1 - z - e^{-z} \sec \chi] \quad (161)$$

where  $z = (h - h_0)/H$ ,  $h_0$  is the altitude at which  $N_{\max}$  occurs, and  $\chi$  is the solar angle. The angle  $\chi$  is inconvenient to compute, the ionizing and recombination coefficients are unsure, and the geomagnetic field influences the intensity of radiation, so a model (Equation 162) based on observations is usually applied:

$$N = N_{\max} (h_0, \phi, \lambda, t) \exp \frac{1}{2} [1 - z - e^{-z}] \quad (162)$$

The time  $t$  in Equation 162 is significant for the time of day, the time of year, and the phases of the 11-year and 27-day solar cycles. The factor  $N_{\max}$  is obtained by setting  $\mu = 0$  and using the observed  $f_{\max}$ , the highest frequency reflected by the ionosphere in Equation 162;  $h_0$  is obtained from the time delay of this signal. Based on these ionosonde observations, monthly predicted  $f_{\max}$  and  $h_0$  for  $(\phi, \lambda)$  and time of day and 11-year sunspot cycle are published in the Basic Radio Propagation Predictions of the National Bureau of Standards and in similar services of about twelve other countries.

The Chapman model (Equation 162) indicates that most of the electron content significant for satellites at geodetically useful altitudes will be around and above  $h_0$ . Electron content below  $h_0$  (240 to 440 km) has been well mapped by ionosonde; it can be expected that deviations from a simple model will be even greater above  $h_0$ , so further observations are desirable. With the advent of satellites and more powerful VHF and UHF radar a variety of experimental results have been obtained, by such techniques as rotation of polarization of satellite or lunar-reflected signals; differing Doppler shifts on two frequencies, after Equation 156; frequency shift of back-scattered UHF radar; direct sampling; etc. — most of them either limited in coverage or uncertain in interpretation. The principal properties of the F2  $h_0$  are described in standard texts (References 160 and 239); observations by new techniques above  $h_0$  are in many papers such as those included in reports of recent symposiums (References 240 and 241):

- (1) The world-wide and all-time average daily maximum for equatorial and temperate  $N_{\max}$  is  $2 \times 10^{12}$  electrons/meter<sup>3</sup> with  $h_o$  of 400 km.
- (2) With the 11-year sunspot cycle, there are variations of the annual average of the daily maximum  $N_{\max}$  from  $1$  to  $3 \times 10^{12}$  electrons/meter<sup>3</sup>.
- (3) There are irregular seasonal variations in  $N_{\max}$  mostly negatively correlated with the solar latitude.
- (4) The average daily variations in equatorial and temperate  $N_{\max}$  and  $h_o$  are from about  $2 \times 10^{12}$  electrons/meter<sup>3</sup> at 2 p.m. and 400 km at 12-2 p.m. to about  $2.5 \times 10^{11}$  electrons/meter<sup>3</sup> at 5 a.m. and 240 km at 1-5 a.m.; polar  $N_{\max}$  remain at about  $2 \times 10^{11}$  electrons/meter<sup>3</sup> at 400 km.
- (5) Magnetic storms can cause an order of magnitude drop in  $N_{\max}$  and a rise in  $h_o$ .
- (6) Seasonal variations in the total (temperate) electron content for early afternoon are on the order of  $3 \times 10^{17}$  electrons/meter<sup>2</sup> in summer and  $6 \times 10^{17}$  electrons/meter<sup>2</sup> in winter.
- (7) Day-to-day irregular variations in total electron content are on the order of 20 to 30 percent.
- (8) The regular daily variations of total electron content rise from a minimum just before dawn to a maximum about 3 times as great in the early afternoon.
- (9) The ratio of electron content above  $h_o$  to electron content below  $h_o$  varies from 1.5 to 5 in different experiments.
- (10) The electron densities observed up to around 1000 km require a scale height  $H$  on the order of 100 km to approximate the Chapman model (Equation 162).
- (11) Throughout the ionosphere, there can exist "clouds" differing in electron density by as much as an order of magnitude, as little as 1 km in vertical extent and rapidly moving.

For a satellite altitude of 1000 km and transmission frequency of  $10^8$  cps, items (1) and (10) indicate refractive effects of the order  $10^{-3}$  on interferometry and Doppler, while item (6) indicates a refractive effect of order  $10^{-3}$  on range observations. Items (5), (7), and (11) indicate that variations with respect to any model will be a major fraction of these total effects; hence, geodetic accuracy requires either multiple frequencies of more than  $10^8$  cps, or single frequencies of more than  $10^9$  cps. [Another possibility (Reference 235) is to obtain a refraction-corrected range on a single carrier frequency by combining pulse, affected by group delay, and continuous wave, affected by phase delay, techniques.]

The ionosphere also attenuates radio signals; this attenuation is proportionate to  $f^{-2}$ , and is negligible for the frequencies in excess of  $10^8$  cps required from refractive considerations.

## Interferometry

The Minitrack system (References 211, 242, 203, and 243) has three pairs of antennas spaced respectively 500, 64, and 12 feet apart on a north-south line, and two pairs of antennas spaced 500 and 64 feet apart on an east-west line, to give a fan-shaped reception pattern 100 degrees wide from north to south and 10 degrees wide from east to west. The signals from a satellite received on a pair of antennas are mixed with the output of a local oscillator and combined to form an audio frequency signal which is compared with a reference signal to measure phase difference with a precision of 0.001 cycle, equivalent at 108 mc/sec to geometrical angular precision of 4". The phase difference is recorded in both analogue and digital form, with the time to an accuracy of about 0.001. The system is calibrated by tracking, and photographing against the stellar background, an aircraft carrying a flashing light. This calibration not only obtains the orientation with respect to the inertial system, mentioned on page 71, but also obtains corrections for misalignments and imperfections in the antennas and other elements of the system. These corrections are expressed as polynomial coefficients in obtaining a smoothed solution for the direction cosines ( $\ell, m$ ) with respect to the two baselines at the integral second of time closest to the system meridian. The refraction correction is then applied to the direction cosines:

$$\ell_{\text{corr.}} = \ell_{\text{obs}} - \delta\ell = \ell_{\text{obs}} + \sin\psi\delta\psi \approx \ell_{\text{obs}}(1 + \mu_o - \mu_s) \quad (163)$$

where  $\mu_s$  is obtained from the propagation predictions (Equations 162 and 160) and  $\mu_o$  is obtained from Equation 157. Since an appreciable part of the ionospheric refractive effect depends on the electron density along one line — the satellite orbit — the smoothed solution acts to diminish the effects of irregular fluctuations in this quantity.

The instrumental accuracy of the Minitrack system at 108 megacycles per second with a 500-foot baseline is estimated to be  $\pm 20''$ , an appreciable part of which is slowly varying error in orientation, as evidenced by the changes therein from one calibration to the next (Reference 243). Transmitting satellites are observed an average of six times a day by the network of 13 stations, which is being converted to 136 megacycles per second frequency.

A simpler system, the Mark II Minitrack (Reference 244), has only one pair of antennas 1000 feet apart on each baseline and only a null-detection, rather than a phase comparison, for signals in this pattern. Calibration of the Mark II Minitrack by radio

stars has been attempted (Reference 245), but was not adequate. Mark II Minitrack stations have been operated on about six islands in the Pacific. Another interferometric system is Microlock (Reference 246).

## Doppler

The Transit system satellite (References 188, 202, and 247) transmits on four frequencies: 54 and 324 megacycles controlled by one crystal oscillator and 162 and 216 megacycles controlled by another; each oscillator is stable to better than  $10^{-9}$  in 15 minutes. Upon receipt of the signals at the ground station, a reference frequency is subtracted. The resulting audio signal is admitted once every two seconds into a preset counter where the duration ( $\leq 1^s$ ) of a specified number of cycles is measured by observing the number of 1-mc cycles that pass through and are registered on a digital counter. At the end of a count, the signal is registered on an output tape with the time. The same frequency standard, stable within  $10^{-9}$  in 15 minutes, provides the reference frequency, the pulses controlling the gate to the counter, the 1-mc counting cycles, and the clock providing the time; the frequency standard in turn is compared to the standard time services.

The two received frequencies ( $i = 1, 2$ ) are used to eliminate a parameter  $\alpha(t)$  from a pair of equations (compare with Equation 156):

$$\Delta f_i(t) = \frac{f_i}{c} |\dot{\mathbf{r}}_T| + \frac{\alpha(t)}{f_i} . \quad (166)$$

All the data points for an entire pass are then used in the solution for an orbit (or, alternatively, for station coordinates from a fixed orbit). In this solution, a correction to frequency standard in the satellite is included as a separate unknown for each pass. A better, but more elaborate, solution of the frequency standard problem would be to place a transponder in the satellite, so that the signal received from the satellite is controlled by the same frequency standard as the ground reference frequency.

Another Doppler system is Doploc (Reference 248).

## Ranging

Secor (Reference 249) is a modulated continuous wave system. The ground station emits a signal with a carrier frequency of 421.2 mc modulated by four frequencies:  $f_1$ ,  $f_1 - f_2$ ,  $f_1 - f_3$ , and  $f_1 - f_2 + f_4$  such that  $f_1$  is  $c/2^9$  meters (about 586 kc) and  $f_2$  is

$2^{-4} \times f_1$ ;  $f_3$  is  $2^{-8} \times f_1$ ; and  $f_4$  is  $2^{-11} \times f_1$ . The satellite transponder returns a signal with a carrier frequency of 448.8 mc and the same four modulations plus a signal of carrier 224.4 mc and the  $f_1$  modulation only. An unambiguous phase shift is obtained by measuring the phase shifts of all four modulation frequencies received from the satellite with respect to standard frequencies maintained in the ground receiver. The phase precision of 0.001 cycle is equivalent to  $10^{-3} c/2^9$  meters, or 0.5 meter range precision. The discrepancy between the phase shifts obtained on the 224.4 mc and 448.8 mc carriers is used to obtain a first order corrected range  $r$  (and incidentally an estimate of total electron content between ground and satellite) by assuming in Equation 154 that, using Equation 160,

$$\left( \int \mu ds \right)_{\text{up}} + \left( \int \mu ds \right)_{\text{down}} = 2 \left[ r + \Delta r_{\text{tr}} - \frac{40}{f^2} \left( \int N_{\text{ds}} \right)_{\text{down}} \right] \quad (167)$$

where the tropospheric effect  $\Delta r_{\text{tr}}$  is of the order of 3 meters by Equations 157 and 160.

Secor, like Minitrack and Transit, has provision for frequent readout of corrected results with time, and for the monitoring of frequency and absolute time by the time service VLF signals.

A geodetic Secor system of four ground stations will go into operation in 1961.

References 199 and 200 consider the use of a pulse, rather than a continuous wave, ranging system, and Reference 235 considers a combination of the two techniques. Pulse systems could apparently attain the same accuracy and maximum range for a given average power, but require heavier components to accommodate the much higher peak power requirements.

Ranging systems are not as sensitive as Doppler to frequency stability, but do depend much more on accurate knowledge of the velocity of light in vacuum, for which the presently accepted value is  $299,792.5 \pm 0.4$  km/sec (Reference 237).

There appears to be no inherent limitation on radio tracking systems. The second-order ionospheric effects we have neglected in this discussion are all slight; see References 200 and 235. So the questions affecting choice of a radio tracking system are cost and engineering difficulty. Radio systems have the advantages over optical of all-weather and daytime tracking, and require less power in the satellite than a flashing light of comparable range (for example, 0.2 watts standby and 27 watts operating for Secor with 6000 km maximum range).

A system now in development to obtain considerably increased accuracy in range, range-rate, and directional measurements from fixed installations is Mistran (References 197 and 250).

## SECTION IV

### LUNAR TECHNIQUES

#### 1. LUNAR TOPOGRAPHY EFFECTS

The principal common difficulty of all lunar techniques is the relationship of points on the moon's surface which are used in observations to the center of mass which appears in the equations of lunar motion. An error in the position of such a point is expressible as  $\epsilon(b_1, b_2)$  in Equations 119 through 121, and thus has a comparable effect on the corresponding coordinates deduced for the observer's position. Hence, it is desirable to map the features of lunar topography as accurately as possible, and, most important, to reduce to a minimum systematic error so that accuracy of deduced geodetic positions can be significantly improved by repeated observations using different topographic features.

The zone of interest comprises those topographic features which may appear on the limb at some position of libration: an area on each limb about  $18^\circ$  wide in selenographic longitude. The published compilations, the maps of Hayn (Reference 251) and the profiles of Weimer (Reference 252), are estimated to give errors on the order of  $0.2$  to  $0.3$ , equivalent to 400 to 500 meters position. The improved compilation of Watts (References 253 and 254), due for publication late in 1961, is estimated to give rms errors of about  $\pm 0.07$ . The improvement is due not only to a more elaborate measurement and control systems, but also to the closer interval of lunar profiles: 503 were used to cover the entire possible range of combined librations in latitude and longitude. See Reference 5, pp. 59-78.

#### 2. ECLIPSES

Eclipses were observed and studied extensively 1944-1954 for geodetic purposes by both photographic and photoelectric methods. Most attempts were spoiled by poor weather or equipment difficulties; the most successful was a connection in 1947 from Gold Coast to Brazil by Kukkamäki and Hirvonen (Reference 255), for which an uncertainty of  $\pm 94$  meters is estimated, including the error due to Hayn's charts. A comprehensive discussion of eclipse methods is given by Berroth and Hofmann (Reference 5, pp. 147-242).

### 3. OCCULTATIONS

Photoelectric observations of occultations, developed by O'Keefe, Henriksen, and others (References 104, 185, 256 and 257, and Reference 5, pp. 243-267), have been carried out extensively since 1950. A Cassegranian telescope of 480 cm focal length and 30 cm aperture is used. The occultation of a star by the moon is a very abrupt event; the principal problem in timing this event is the signal-to-noise ratio of the starlight to the light scattered from the nearby bright part of the moon. The solution employed is to use a field stop which limits the field of view to 10" for light entering the photocell, as well as a series of baffles in the telescope tube. The small field in turn necessitates accurate mirrors and an ingenious guiding system. The photocell is an RCA IP21 photomultiplier, which has a sensitivity of  $10^{-14}$  lumens at 25°C. Occultations of stars as small as 9th magnitude are observed with 0.01 timing accuracy.

The effect of error in lunar topography is minimized by the controlled, or equal-limb-line, method (mentioned in Paragraph 3 of Section II) in which the occultation is observed from two points for which the starlight is cut off by the same lunar feature. This method is effective because the variations in the lunar profile described in Paragraph 1 of this section are rather smooth, that is, there is a high correlation in the departures from sphericity of the lunar surface. In calculating the location of points on the same line, refraction must be taken into account.

The accuracy of the occultation technique indicated by the internal consistency of redundant observations is of the order of  $\pm 200$  meters in relative position (Reference 257). An adjusted solution is being carried out of a network of more than 48 observed occultation pairs in the Pacific (Reference 185).

### 4. LUNAR CAMERA

The lunar camera of Markowitz (Reference 181 and Reference 5, pp. 282-293), in operation since 1952, has been installed at twenty observatories. It may be attached to refracting telescopes of 20 cm or more aperture and 2 to 6 meters focal length. The moon's image is intercepted by a 1.8 mm thick plane parallel plate filter of transmission factor 0.001. The rate of tilt of the plate holds the moon fixed relative to the stars. The epoch of the observation is defined by parallelism of the filter plate and a fixed plate. Exposure time is 10 to 20 seconds. Timing error is eliminated by reversing the camera.

In measuring the photo plate, about 10 stars and 30 points on the lunar limbs are used. The probable error of a night's observation is about  $\pm 0''.15$  in each coordinate; since 100 nights a year is a typical program, systematic errors are much more significant. These errors are in the telescopes and in the plate measuring engines. The former are calibrated

by comparing observations of the same stellar field; the latter are estimated to have about 0.1 micron systematic error. Markowitz estimates about  $\pm 0''.02$  error for a year's observations (Reference 180).

## 5. RADAR RANGING

Since 1950, a continuously increasing program of radar studies of the moon has been carried out by several installations. Those by Yaplee and associates (References 106, 107, and 108) have emphasized accuracy of range determination, using 10 cm and 21 cm wave lengths on the 50-foot reflector of the Naval Research Laboratory over many months. Precision of determination of the time of receipt of the reflected pulse is  $\pm 2 \times 10^{-6}$  seconds, and the internal uncertainty of a night's range determination is  $\pm 0.3$  km. However, the nature of the reflection from the moon, including the extent of the reflecting area, is still uncertain. Furthermore, there is a monthly periodic variation in the residual of the measured lunar distance with respect to that from orbital theory of about 4.0 km amplitude, believed due to irregularities in the shape of the moon. The most recently published result, allowing  $\pm 1$  km for the moon's radius, is  $384402 \pm 1.2$  km for the earth-moon distance (Reference 108).



## SECTION V

### COMBINATION OF CELESTIAL AND TERRESTRIAL GEODESY

#### 1. COORDINATE FORMS AND UNITS

The relationships between the various coordinate forms (References 1 and 39):

$$\left. \begin{array}{rclcl}
 \text{Geodetic} & & \text{Rectan-} & & \text{Spherical} & & \text{Ellipsoidal} \\
 & & \text{gular} & & & & \\
 (\nu + h) \cos \phi_g \cos \lambda & = & x & = & r \cos \phi \cos \lambda & = & \sqrt{\rho^2 + c^2} \sqrt{1 - \sigma^2} \cos \lambda \\
 (\nu + h) \cos \phi_g \sin \lambda & = & y & = & r \cos \phi \sin \lambda & = & \sqrt{\rho^2 + c^2} \sqrt{1 - \sigma^2} \sin \lambda \\
 [(1 - e^2)\nu + h] \sin \phi_g & = & z & = & r \sin \phi & = & \rho \sigma
 \end{array} \right\} \quad (168)$$

where the radius of curvature in the prime vertical  $\nu = a_e (1 - e^2 \sin^2 \phi_g)^{-\frac{1}{2}}$ ;  $e$  is the eccentricity and  $a_e$  the equatorial radius. If the astronomically convenient choice  $c = a_e J_2^{\frac{1}{2}}$  is made for the shape parameter of the ellipsoidal coordinates (page 22 of this report and References 38 and 39), then the relationship to the geodetic coordinates is complicated by the fact that geodetic coordinates are referred not to a gravitational equipotential, but to a gravity equipotential; that is, the rotational potential of the earth must be taken into account. The most convenient intermediaries become the parameters of the gravitational field,  $\mu = kM$  and the  $J_{2n}$ . Lambert (References 258, 259), Cook (Reference 260), and Cohen (Reference 261) have developed the necessary formulas for the external potential of a rotating ellipsoid; the leading terms are:

$$\left. \begin{array}{l}
 kM = a_e^2 g_e \left[ 1 + \frac{3}{2} m - f - \frac{15}{14} mf + O(f^3) \right] \\
 J_2 = \frac{2}{3} f \left( 1 - \frac{1}{2} f \right) - \frac{1}{3} m \left( 1 - \frac{3}{2} m - \frac{2}{7} f \right) + O(f^3) \\
 J_4 = -\frac{4}{35} f (7f - 5m) + O(f^3) \\
 J_6 = O(f^3)
 \end{array} \right\} \quad (169)$$

where  $g_e$  is the acceleration of gravity at the equator;  $m$  is the ratio of centrifugal force at the equator to  $g_e$ ; that is,  $(\dot{\theta})^2 a_e / g_e$ , and the flattening  $f = 1 - \sqrt{1 - e^2}$ .

Several additional formulas pertaining to a rotating ellipsoid and its external field are given in References 258, 261, 260 (in which the definition of  $m$  differs from that used here) and Reference 262, which gives the external field in the form of the components of acceleration, not of the potential.

For departures from the rotating ellipsoidal model defined by Equation 169 expressed in terms of gravitational acceleration  $\Delta g$  by  $(A_{nm}, B_{nm})$  or geoid height by  $(C_{nm}, D_{nm})$ :

$$\begin{bmatrix} J_{nm} \\ K_{nm} \end{bmatrix} = \frac{-a_e^2}{kM(n-1)} \begin{bmatrix} A_{nm} \\ B_{nm} \end{bmatrix} + O(f^3) = \frac{-a_e g_e}{kM} \begin{bmatrix} C_{nm} \\ D_{nm} \end{bmatrix} + O(f^3). \quad (170)$$

It is convenient to express the gravitational field in terms of normalized harmonics, because then coefficients of the same degree  $n$  can be directly compared, and also happen to be  $O(1)$  for  $(\bar{A}_{nm}, \bar{B}_{nm})$  in milligals ( $\text{cm} \times 10^{-3}/\text{sec}^2$ ) for  $n < 25$  (Reference 111):

$$\begin{bmatrix} \bar{A}_{nm} \\ \bar{B}_{nm} \end{bmatrix} = \left[ \frac{(n+m)!}{(n-m)! (2n+1) \kappa_m} \right]^{\frac{1}{2}} \begin{bmatrix} A_{nm} \\ B_{nm} \end{bmatrix} \quad (171)$$

where  $\kappa_0 = 1$  and  $\kappa_m = 2$  for  $m \neq 0$ .

Refinements of definition in comparing celestial and terrestrial determinations of the gravitational field have been discussed by Cook (Reference 263).

## 2. COMPARISON OF OBSERVATIONAL RESULTS

A comparison of the gravitational  $(J_{nm}, K_{nm})$  deduced from satellite motions with those obtained from terrestrial gravimetry is complicated by the different methods employed by investigators of the latter to solve the statistical problem of determining harmonic coefficients pertaining to the whole earth from observations covering only a minor fraction thereof. The problem exists because the long wave variations expressed by the low degree harmonics constitute a very minor part of the total gravity anomaly  $\Delta g$  measured by a gravity meter at the earth's surface: the 39 terms of degrees  $n = 2$  through 5 are estimated to account for less than 8 percent of the total anomalous variance  $\sigma^2(\Delta g)$  (Reference 111). Further, the distribution of observations is affected by the topography, which is correlated (to an extent in dispute) with the gravity anomalies. So there is both a high noise level and a bias with which to contend. All methods of treatment concur in correcting gravity anomalies for correlation with topography to estimate the mean anomalies for limited areas; they also concur in that the function to be treated is not  $g$ , the observed quantity, but  $\Delta g$ , the discrepancy of observation from an ellipsoidal model. The treatment beyond the formation of mean anomalies for limited areas can be characterized by two extremes:

- (1) Determine the gravitational coefficients ( $A_{nm}, B_{nm}$ ) by least squares fit to the estimated anomalies for areas for which they are available, and disregard areas without observations.
- (2) Extrapolate gravity anomaly estimates from areas with observations to areas without to the point where the anomaly estimate can practically be assumed zero or a function of the topography (by either statistical correlation or assumed isostatic compensation; Reference 264 investigates combining these methods). The harmonic coefficients ( $A_{nm}, B_{nm}$ ) then become merely the transform of the spatial representation, computed by numerical integration.

Of the principal investigations, Jeffreys (Reference 110), Heiskanen and Uotila (Reference 265) and Zhongolovich for degrees two and three (Reference 266) incline toward method (1); while Kaula (Reference 111), Uotila (quoted in Reference 267) and Zhongolovich for degrees four through eight (Reference 266) incline toward method (2). Of the two methods, (1) yields the larger coefficients, and generally has the greatest amplitudes in the areas with the fewest observations. As contended by Reference 111, with incomplete information the most probable estimates of small departures from an equilibrium model should have a lesser amplitude than the true departures. However, the estimates by method (2), whether statistical or isostatic, should be of even lesser amplitude than the most probable estimates, because the step-by-step extrapolation procedure implicitly assumes that the probabilistic relationships for gravity anomalies a distance  $s$  apart can be expressed in the form  $\exp(-P_{ij}s)$ . There is no physical reason why gravity anomaly correlation should be expressible by such a form, and, in fact, the magnitude of the low degree harmonics inferred from satellite orbits and from autocovariance analysis indicates that such an extrapolation rule, if fitted to data for short distances on the order of  $1^\circ$ , should give appreciable underestimates for distances greater than  $10^\circ$ . Even greater underestimates are obtained using topography alone.

The comparison of celestial and terrestrial estimates is set forth in Table 4, including estimated orders of magnitude based on autocovariance analysis of terrestrial gravimetry (Reference 111), and coefficients based on the assumption of perfect isostatic compensation at a depth of 30 km.

For comparison of celestial and terrestrial determinations of  $kM$ , there is needed a terrestrial estimate of scale. Here there is less doubt as to the data to be considered, these being one determination published based on much more data than any other, that of Mrs. Fischer (Reference 268) using astrogeodetic heights covering 19 percent of the earth (in  $10^\circ \times 10^\circ$  square units):  $a_e = 6378166$  meters. Assuming  $\sigma(a_e) = \pm 21$  meters and using a  $g_e$  of  $978.0307 \pm 0.000027 \times 10^{14} \text{ m}^3/\text{sec}^2$ ,  $kM = 3.986036 \pm 0.000027 \times 10^{14} \text{ m}^3/\text{sec}^2$  is obtained, which does not agree with the celestially derived value on page 40 using Rabe's  $\mu_M/\mu_E$ , but does with that using Delano's value.

Table 4  
Comparison of Celestial and Terrestrial Estimates  
of Gravitational Coefficients

Source	$g_e^{\dagger}$ cm/sec <sup>2</sup>	$J_2 \times 10^6$	$J_3 \times 10^6$	$J_4 \times 10^6$	$J_5 \times 10^6$	$J_{22} \times 10^6$	$K_{22} \times 10^6$
Celestial (see pages 39, 41)		1082.3 $\pm 0.2$	-2.3 $\pm 0.1$	-1.8 $\pm 0.2$	-0.3 $\pm 0.2$	-0.5	+2.0
Jeffreys (Reference 110)	978.038	1093.2 $\pm 5.0$				-4.2 $\pm 1.5$	
Heiskanen and Uotila (Reference 265)	978.037	1090.6				-3.4	+0.7
Zhongolovich (Reference 266)	978.044	1095.0 $\pm 4.3$	-4.3	-3.0	-0.7	-5.7	+1.6
Kaula (Reference 111)	978.031	1087.0	-0.2 $\pm 1.3$	-3.0 $\pm 0.9$	+1.7 $\pm 0.6$	-0.5 $\pm 0.7$	+0.4 $\pm 0.7$
Uotila (quoted in Reference 267)			-0.7	-2.2	+0.7		
Magnitude expected from autocovariance			$\pm 3.$	$\pm 2.$	$\pm 1.$	$\pm 1.$	$\pm 1.$
Topography and perfect isostasy			+0.20	-0.33	+0.69	+0.17	+0.02

<sup>†</sup>Including -0.013 cm/sec<sup>2</sup> absolute correction to Potsdam System.

The astro-geodetic geoid data have not been combined with gravimetry to make a complete determination of the geoid based solely on terrestrial data, but a combination has been made by Kaula (Reference 269) of all the astro-geodetic data in Reference 268, the gravimetry in Reference 111 plus Reference 266, and the secular and long-period satellite motions of satellites 1957  $\beta$  (Reference 94) and 1958  $\beta_2$  (Reference 87), to determine ellipsoid parameters, datum shifts, and the 76 possible gravitational coefficients up to  $n_m = 88$ . A generalization of least squares taking into account correlation was used, with the variances and covariances of the gravimetric and astro-geodetic data estimated from the autocovariance analysis in Reference 111 and the variances of the satellite motions taken from References 94 and 87. The resulting quadratic sum  $y^T W^{-1} y$  was 44 percent higher than expected on the assumption of normally distributed errors, but this result is not too disappointing considering the approximations involved in  $W$ . The principal results, after increasing standard deviations in accord with the obtained  $y^T W^{-1} y$ : an equatorial radius of  $6378163 \pm 21$  meters; a flattening of  $1/298.24 \pm 0.01$ ; an equatorial gravity of  $978030.7 \pm 1.2$  milligals (incorporating -12.9 milligals correction to the Potsdam system for absolute  $g$ ); datum shifts (with three-dimensional standard deviation) for the Americas system ( $\pm 35$  m), Europe-Africa-Siberia-India system ( $\pm 38$  m), and Japan-

Korea-Manchuria system ( $\pm 68$  m); 76 coefficients in the spherical harmonic expression of the gravity field up to  $nm = 88$  with a mean standard error of about  $\pm 0.7$  milligals for the 68 coefficients with  $m \neq 0$ ; world-wide geoid heights with standard error ranging from  $\pm 10$  m to  $\pm 22$  m.



## SECTION VI

### GEOPHYSICAL IMPLICATIONS

As can be seen by comparing the first and last lines in Table 4, the gravitational coefficients obtained from satellite motions are appreciably larger than expected on the assumption that isostasy prevails for larger scale features, thus supporting the inferences from terrestrial data of Jeffreys (Reference 110) rather than those of Heiskanen and Vening-Meinesz (Reference 270). The more accurate value of  $J_2$  obtained from satellites enables the extension of the last line of Table 4 to include the  $J_2$  column, because, as O'Keefe (References 107 and 271), and Henriksen (Reference 272) have pointed out, an accurate value of the polar moment of inertia is now obtainable. Thus

$$\frac{J_2}{H} = \frac{\left( \frac{C-A}{M a_e^2} \right)}{\left( \frac{C-A}{C} \right)} = \frac{C}{M a_e^2} \quad (172)$$

where  $C$  and  $A$  are the moments of inertia about polar and equatorial axes, respectively. We have from the theory of a rotating fluid (Reference 110, p. 151):

$$\frac{C}{M a_e^2} = \frac{2}{3} \left\{ 1 - \frac{2}{5} \left[ \frac{5m}{2f} \left( 1 - \frac{3}{2} m \right) - 1 \right]^{\frac{1}{2}} \right\} + O(f^2). \quad (173)$$

The value  $1/305.3$  is obtained for  $H$  from  $\mu_M/\mu_E = 1/81.375$  (Reference 102) and the rate of precession of the earth's axis (Reference 110, p. 152); using it with  $J_2 = 1.0823 \times 10^{-3}$  and  $m = 1/288.4$  yields  $f = 1/300.3$ . If second order terms are included,  $f$  becomes  $1/299.8$  (Reference 271), from which, by Equation 169, we get a "hydrostatic"  $J_2$  of  $1.0711 \times 10^{-3}$  and a  $J_4$  of  $-2.95 \times 10^{-6}$ , which is appropriately subtracted from the observational estimates of  $J_4$  in Table 4 before comparing them with the isostatic figure in the last row.

The difference  $\Delta J_2$  between the observed  $J_2$  of  $1.0823 \times 10^{-3}$  and the hydrostatic  $J_2$  of  $1.0711 \times 10^{-3}$  is equivalent to a lag of 10 million years in adjustment of the figure to the decelerating rotation at the present rate of  $5 \times 10^{-22} \text{ sec}^{-2}$ , estimated by Munk and MacDonald (Reference 273). However, Baussus (Reference 264) suggests  $\Delta J_2$  can be

explained by considering thermal, as well as mechanical, equilibrium of a fluid under latitudinal variation of temperature.

The earth's response to rotation can also be expressed in terms of the Love numbers:  $k$ , the ratio of the mass-shift potential  $U_{2G}$  to the rotational  $U_{2R}$ ; and  $h$ , the ratio of the actual surface rise to the rise of a zero density fluid in response to  $U_{2R}$  (Reference 119, pp. 24-28 and Reference 274). Thus,

$$k = \frac{U_{2G}}{U_{2R}} = \frac{3J_2\mu}{a_e^3(\dot{\theta})^2} \approx \frac{2f}{m} - 1; \quad h = \frac{\frac{2a_e f P_2}{3}}{\frac{U_{2R}}{g_o}} \approx \frac{2g_e f}{a_e(\dot{\theta})^2} = \frac{2f}{m}. \quad (174)$$

The ratio  $k/h \approx (1 - m/2f) = 0.48$  obtained from Equation 174 is about the same value as the  $k/h$  obtained from various theoretical models of an elastic earth (Reference 274); this agreement does not seem to signify much more than that the same parts of the earth are participating in both responses.

Most discussions (References 271, 273, and 275) of possible sources of the large  $\Delta J_2$  and  $J_3$  found from satellite motions conclude that it is impossible to explain them by variations associated with the crust; (the same conclusion applies to the  $J_{22}$ ,  $K_{22}$  given in Table 4: normalized,  $\bar{J}_{22}$  is  $-0.8 \times 10^{-6}$ ;  $\bar{K}_{22}$  is  $+3.1 \times 10^{-6}$ ; and  $\Delta \bar{J}_2$  is  $+5.0 \times 10^{-6}$ ). The necessary density anomalies must be in the mantle. Thermal history considerations and the Gutenberg low-velocity layer in the 100 km just below the crust further suggest that the density anomalies are rather deep in the mantle. The fair degree of correlation of the long wave features of the gravity field with the geomagnetic field and core depths from seismology, noted by Vogel (Reference 276), even suggests a source in or near the core. However, the density anomalies which would be needed in the core to explain the observed gravity field are several orders of magnitude greater than those needed for the convection to maintain the geomagnetic dynamo (Reference 277). Furthermore, if the density anomalies are deep, then in the corresponding gravity anomalies there should be a rapid decline in amplitude, or degree variance, with increasing degree  $n$  (equivalent to decreasing wave length). For example, if we assume a distribution of density anomalies in the form of equal degree variances  $\sigma_n^2(\Delta\rho)$  on a surface at depth 1000 km, then the sum  $\sum_n \sigma_n^2(\Delta g)$  for  $n = 3, 4, 5, 6$  would be about six times as great as for  $n = 9, 10, 11, 12$ ; at 500 km, the ratio would be slightly more than 2.0. In the estimates of these sums from autocovariance of gravimetry (Reference 111), the ratio is about 1.7, the difference of which from the ratio for 500 km depth could be well explained by crustal variations.

Density anomalies are most closely tied to the inelastic properties, which act to reduce the anomalies. Use of the viscosity of  $10^{22}$  poises, deduced from postglacial uplift, in the theories of Vening-Meinesz (Reference 270) for plastic readjustment of the crust

(Reference 271) and for convective flow in the mantle (Reference 278) leads to unreasonably high rates of response; the material of the mantle must have a considerably greater stiffness for the observed  $\Delta J_2$ ,  $J_3$ , etc., to exist. The simplest conclusion is that the density anomalies have existed in their present form ever since the mantle was formed. However, this conclusion is difficult to reconcile with laboratory observations of the yielding properties of rock (Reference 279), or with the paleomagnetic and paleoclimatic evidence of polar wandering (Reference 119, pp. 250-285 and Reference 273). Munk and MacDonald (Reference 273) suggest that evidence of adjustment to polar movement would be that the gravity anomaly coefficients ( $A_{nm}$ ,  $B_{nm}$ ) are systematically smaller for  $m$  odd than for  $m$  even; this is not shown by the 72 (normalized) coefficients of degrees 3 through 8 in Reference 269, for which the rms magnitudes  $\sigma(\bar{A}_{nm}, \bar{B}_{nm})$  are  $\pm 0.81$  mgal for  $m$  even,  $\pm 0.98$  mgal for  $m$  odd.

The gravitational variations obtained from satellite motions are significant indicators of some present and past properties of the earth's interior, particularly in that they necessitate certain minimums in the shearing stresses in the mantle. However, the most they can contribute at present is to confirm Jeffreys' estimate that these shearing stresses are at least  $1.5 \times 10^8$  dynes (Reference 110, p. 210). Further contribution to the understanding of the interior and its evolution depend upon the solution of what can be summarized as two problems (Reference 280): (1) the rheological equations of state expressing the mechanical properties of rocks for temperatures, pressures, and durations in excess of those attainable in the laboratory; and (2) a mathematical continuous field theory adequate to express the energy and matter relationships in the interior on a geological time scale, distinguishing the significant from the insignificant and the probable from the improbable.



## ACKNOWLEDGMENTS

I am indebted to Dr. Boris Garfinkel, Dr. Charles J. Cohen, Mr. Duane C. Brown, Mr. Robert W. Bryant, Dr. Yoshihide Kozai, Dr. Robert R. Newton, Mr. H. Lee Kyle, Dr. W. Priester, Mr. O. K. Moe, Dr. A. H. Cook, Mr. O. W. Williams, Dr. I. I. Shapiro, Dr. Kurt Arnold, Mr. H. F. Michielsen, Mr. W. E. Strange, Mr. B. H. Chovitz, and Mr. D. G. King-Hele for corrections and comments on the manuscript.



## REFERENCES

1. Veis, G., "Geodetic Uses of Artificial Satellites," Smithsonian Inst. Astrophys. Obs., Contrib. to Astrophys. 3(9):95-161, 1960
2. Whitten, C. A., and Drummond, K. H., eds., "Contemporary Geodesy," Proc. Conf. Contemp. Geodesy, Harvard College Observatory, 1958, Amer. Geophys. Un., Geophys. Monograph 4, 1959
3. Thomas, P. D., "Use of Near Earth Satellite Orbits for Geodetic Information," U. S. Coast and Geodetic Survey, Tech. Bull. No. 11, 1960
4. Woollard, G. P., "Geodesy," Science in Space 3:4-13, Washington, D. C.: U.S. Nat. Acad. Sci., 1960
5. Berroth, A., and Hofmann, W., "Kosmische Geodäsie," Karlsruhe: Verlag G. Braun, 1960
6. Goldstein, H., "Classical Mechanics," Cambridge, Massachusetts: Addison-Wesley Press, 1950
7. Corben, H. C., and Stehle, P., "Classical Mechanics," 2nd ed., New York: John Wiley and Sons, 1960
8. Synge, J. L., "Classical Dynamics," Handbuch der Physik 3/1:1-225, Berlin: Springer Verlag, 1960
9. Plummer, H. C. K., "An Introductory Treatise on Dynamical Astronomy," New York: Dover, 1960 (originally published in 1918)
10. Smart, W. M., "Celestial Mechanics," London: Longmans, Green and Co., 1953
11. Moulton, F. R., "An Introduction to Celestial Mechanics," New York: Macmillan Co., 1935 (originally published in 1914)
12. Herget, P., "The Computation of Orbits," Cincinnati, Ohio (privately published), 1948
13. Bowden, G. E., and Flis, J., eds., "Notes of the Summer Institute in Dynamical Astronomy at Yale University," Yale Univ. Obs., New Haven, Connecticut, July 1959
14. Baker, R. M. L., Jr., and Makemson, M. W., "An Introduction to Astrodynamics," New York: Academic Press, 1960
15. Brouwer, D., and Clemence, G. M., "Methods of Celestial Mechanics," New York: Academic Press, 1961

16. Krause, H. G. L., "Die säkularen und periodischen Störungen der Bahn eines künstlichen Satelliten," Proc. 7th Int. Astronaut. Cong., Rome, Italy: 523-585, 1956
17. von Zeipel, H., "Recherches sur le mouvement des petites planètes," Arkiv för Matematik, Astronomi och Fysik 11(1):1-58, 1916
18. Garfinkel, B., "Variation of Elements," Notes Summer Institute on Dyn. Astr., Yale Univ., New Haven, Connecticut, 263-291, 1960
19. Brown, E. W., "An Introductory Treatise on the Lunar Theory," New York: Dover, 1960 (originally published in 1896)
20. Kovalevsky, J., "Influence des termes du second ordre sur la théorie du mouvement d'un satellite artificiel," Space Res., Proc. 1st Int. Space Sci. Sym., Amsterdam: North Holland Publ. Co., pp. 458-465, 1960
21. Veis, G., and Moore, C. H., "Smithsonian Astrophysical Observatory Differential Orbit Improvement Program," Seminar Proc.: Tracking Programs and Orbit Determination, Jet Propulsion Lab., Calif. Inst. Tech., 1960:165-189, 1960
22. Blackman, R. B., and Tukey, J. W., "The Measurement of Power Spectra, from the Point of View of Communications Engineering," New York: Dover, 1959
23. Kozai, Y., "The Motion of a Close Earth Satellite," Astronom. J. 64(9):367-377, November 1959
24. Scarborough, J. B., "Numerical Mathematical Analysis," 4th ed., Baltimore, Maryland: Johns Hopkins Press, 1958
25. Willers, F. A., "Practical Analysis, Graphical and Numerical Methods," New York: Dover, 1948 (originally published in 1928)
26. Vienop, E., and Brady, J. L., "The Themis Code: An Astronomical Numerical Integration Program for the IBM-704," Univ. Calif. Rad. Lab. Rept. 5242, 1958
27. Smith, V. S., Bruijnes, H. R., and Sherman, N. W., "The Satellite Code: A Numerical Satellite Integration Program for the IBM-704," Univ. Calif. Rad. Lab., Rept. 5462, 1959
28. Brouwer, D., "On the Accumulation of Errors in Numerical Integration," Astronom. J. 46(16):149-153, October 1937
29. Musen, P., "Special Perturbations of the Vectorial Elements," Astronom. J. 59(7): 262-267, August 1954
30. Thomas, L. H., "Numerical Integration of Ordinary Differential Equations at an Interval Which May Be Compared With Some Periods in the Defining Functions," Astronom. J. 63(10):459-460, November 1958
31. Eckert, W. J., "Improvement by Numerical Methods of Brown's Expressions for the Coordinates of the Moon," Astronom. J. 63(10):415-418, November 1958

32. Porter, J. G., "A Comparative Study of Perturbation Methods," *Astronom. J.* 63(10): 405-406, November 1958
33. Baker, R. M. L., Jr., et al., "Efficient Precision Orbit Computation Techniques," *Amer. Rocket Soc. J.* 30(8):740-747, August 1960
34. Pines, S., Payne, M., and Wolf, H., "Comparison of Special Perturbation Methods in Celestial Mechanics," Republic Aviation Corp., Farmingdale, N. Y., Aeronaut. Res. Lab., Wright Patterson AFB, Ohio. ARL Tech. Rept. 60-281, August 1960
35. Garfinkel, B., "The Orbit of a Satellite of an Oblate Planet," *Astronom. J.* 64(9):353-367, November 1959
36. Krause, H. G. L., "Die Säkularstörungen einer Aussenstationsbahn," *Probleme aus der Astronautischen Grundlagenforschung*, Proc. 3rd Int. Astronaut. Cong., 1952: 162-173, Stuttgart: Gesellschaft für Weltraumforschung, 1952
37. Spitzer, L., Jr., "Perturbations of a Satellite Orbit," *J. Brit. Interplanetary Soc.* 9: 131-136, May 1950
38. Vinti, J. P., "New Method of Solution for Unretarded Satellite Orbits," *J. Res. Nat. Bur. Stds.* 62B(2):105-116, October-December 1959
39. Izsak, I. G., "A Theory of Satellite Motion About an Oblate Planet: I. A Second-Order Solution of Vinti's Dynamical Problem," *Smithsonian Inst. Astrophys. Obs., Res. Space Sci., Spec. Rept. No. 52*, November 21, 1960
40. Brouwer, D., "Solution of the Problem of Artificial Satellite Theory Without Drag," *Astronom. J.* 64(9):378-397, November 1959
41. Kaula, W. M., "Analysis of Gravitational and Geometric Aspects of Geodetic Utilization of Satellites," *Geophys. J.* 5(2):104-133, July 1961
42. Cook, A. H., "Report on the Determination of the Earth's Gravitational Potential from Observations of Artificial Satellites," presented at the 12th Gen. Assy. of Int. Un. Geodesy and Geophysics, Helsinki, August 1960
43. Hergenroth, G., "Die Bestimmung der Erdgestalt mit Hilfe künstlicher Satelliten," *Zeitsch. für Vermessungswesen*, 85:342-350, 363-371, October 1960
44. Garfinkel, B., "On the Motion of a Satellite of an Oblate Planet," *Astronom. J.* 63(3): 88-96, March 1958
45. Sterne, T. E., "The Gravitational Orbit of a Satellite of an Oblate Planet," *Astronom. J.* 63(1):28-40, January 1958
46. Vinti, J. P., "Theory of an Accurate Intermediary Orbit for Satellite Astronomy," *U. S. Nat. Bur. Standards*, NBS Rept. No. 7154, May 22, 1961
47. Vinti, J. P., "Theory of the Orbit of an Artificial Satellite with Use of Spheroidal Coordinates," *Astronom. J.* 65(6):353-354, August 1960

48. Brouwer, D., "The Motion of a Particle With Negligible Mass Under the Gravitational Attraction of a Spheroid," *Astronom. J.* 51(8):223-231, February 1946
49. Brouwer, D., "Outlines of General Theories of the Hill-Brown and Delaunay Types for Orbits of Artificial Satellites," *Astronom. J.* 63(10):433-438, November 1958
50. Musen, P., "Application of Hansen's Theory to the Motion of an Artificial Satellite in the Gravitational Field of the Earth," *J. Geophys. Res.* 64(12):2271-2279, December 1959
51. Musen, P., "A Modified Hansen's Theory as Applied to the Motion of Artificial Satellites," NASA Tech. Note D-492, November 1960
52. Musen, P., "On the Motion of a Satellite in an Asymmetrical Gravitational Field," *J. Geophys. Res.* 65(9):2783-2792, September 1960
53. Bryant, R. W., "Interim Definitive Orbits Determined at the NASA Computing Center," *Seminar Proc.: Tracking Programs and Orbit Determination, Jet Propulsion Lab., Calif. Inst. Tech.*, pp. 108-113, 1960
54. Bryant, R. W., "NASA Computing Center Predictions," *Seminar Proc.: Tracking Programs and Orbit Determination, Jet Propulsion Lab., Calif. Inst. Tech.*, pp. 114-118, 1960
55. Siry, J. W., "The Vanguard Orbit Determination Program," *Annals Int. Geophys. Yr.* 12(1):91-104, New York: Pergamon Press, 1960
56. Musen, P., "The Theory of Artificial Satellites in Terms of Orbital True Longitude," *J. Geophys. Res.* 66(2):403-409, February 1961
57. King-Hele, D. G., "The Effect of the Earth's Oblateness on the Orbit of a Near Satellite," *Proc. Roy. Soc. London* 247A(1248):49-72, September 9, 1958
58. Brenner, J. L., and Latta, G. E., "The Theory of Satellite Orbits, Based on a New Coordinate System," *Proc. Roy. Soc. London* 258A(1295):470-485, November 8, 1960
59. Zhongolovich, I. D., "Nekotorye formuly, otnosiashchiesia k dvizheniiu material'noi tochki v pole tiagoteniia urovennogo ellipsoida vrashcheniia," ("Formulae Relating to the Motion of a Particle in the Gravitational Field of a Level Ellipsoid of Revolution"), *Biulleten' Instituta Teoreticheskoi Astronomii* 7(7):521-536, 1960
60. Merson, R. H., "The Motion of a Satellite in an Axi-symmetric Gravitational Field," *Geophys. J.* 4:17-52, 1961
61. Barrar, R. B., "Some Remarks on the Motion of a Satellite of an Oblate Planet," *Astronom. J.* 66(1):11-14, February 1961
62. Struble, R. A., "The Geometry of the Orbits of Artificial Satellites," *Archives for Rational Mechanics and Analysis* 7(2):87-104, February 28, 1961
63. Petty, C. M., and Breakwell, J. V., "Satellite Orbits about a Planet with Rotational Symmetry," *J. of the Franklin Inst.* 270(4):259-282, October 1960

64. Michielsen, H. F., "Orbital Theory for Artificial Satellites," Lockheed Aircraft Corp. Miss. and Space Div. Rept. 326080, Palo Alto, California, 1960
65. Brouwer, D., and Hori, G. I., "Theoretical Evaluation of Atmospheric Drag Effects in the Motion of an Artificial Satellite," *Astronom. J.* 66(5):193-225, June 1961
66. Bailie, A., and Bryant, R., "Osculating Elements Derived from the Modified Hansen Theory for the Motion of an Artificial Satellite," *Astronom. J.* 65(8):451-453, October 1960; also NASA Tech. Note D-568, January 1961
67. Message, P. J., "On Mr. King-Hele's Theory of the Effect of the Earth's Oblateness on the Orbit of a Close Satellite," *Monthly Notices Roy. Astron. Soc.* 121(1):1-4, 1960
68. Hori, G., "The Motion of an Artificial Satellite in the Vicinity of the Critical Inclination," *Astronom. J.* 65(5):291-300, June 1960
69. Garfinkel, B., "On the Motion of a Satellite in the Vicinity of the Critical Inclination," *Astronom. J.* 65(10):624-627, December 1960
70. Hagihara, Y., "Libration of an Earth Satellite with Critical Inclination," *Smithsonian Contrib. Astrophys.* 5(5):39-51, 1961
71. Kozai, Y., "Motion of a Particle with Critical Inclination in the Gravitational Field of a Spheroid," *Smithsonian Contrib. to Astrophys.* 5(5):53-58, 1961
72. Izsak, I. G., "On Satellite Orbits with Very Small Eccentricities," *Astronom. J.* 66(3):129-131, April 1961
73. Kozai, Y., "Note on the Motion of a Close Earth Satellite with a Small Eccentricity," *Astronom. J.* 66(3):132-134, April 1961
74. Newton, R. R., "Variables That Are Determinate for Any Orbit," *Amer. Rocket Soc. J.* 31(3):364-366, March 1961
75. Kozai, Y., "Effect of Precession and Nutation on the Orbital Elements of a Close Earth Satellite," *Astronom. J.* 65(10):621-623, December 1960
76. Kozai, Y., "On the Effects of the Sun and the Moon Upon the Motion of a Close Earth Satellite," *Smithsonian Inst. Astrophys. Obs., Res. Space Sci., Spec. Rept. No. 22*:7-10, March 20, 1959
77. Musen, P., Bailie, A., and Upton, E., "Development of the Lunar and Solar Perturbations in the Motion of an Artificial Satellite," NASA Tech. Note D-494, January 1961
78. Musen, P., "Contributions to the Theory of Satellite Orbits," *Space Research, Proc. 1st Internat. Space Sci. Sym., Amsterdam: North Holland Publ. Co., pp. 434-447, 1960*
79. Hansen, P. A., "Fundamenta nova investigationis orbitae verae quam luna perlustrat," *Gotha: K. Glaeser, 1838*
80. Hansen, P. A., "Darlegung der theoretischen Berechnungen der in den Mondtafeln angewandten Störungen," *Abhandlungen der sächsischen Gesellschaft der Wissenschaften* 6(3):91-498, 1862; 7(1):1-399, 1864

81. Delaunay, M., "Theorie du mouvement de la Lune," *Memoirs Acad. des Sciences*, Paris 28:1-883, 1860; 29:1-931, 1867
82. Hill, G. W., "On the Part of the Motion of the Lunar Perigee Which is a Function of the Mean Motions of the Sun and the Moon," *Acta Mathematica* 8(1):1-36, (2):129-147, (3):245-260, 1886; also *Collected Mathematical Works of George William Hill* 1:243-276, Washington, D. C.: Carnegie Institution of Washington, 1905
83. Hill, G. W., "Researches in the Lunar Theory," *Amer. J. Math.* 1(1):5-26, 1878; also *Collected Mathematical Works of George William Hill* 1:284-335, Washington, D. C.: Carnegie Institution of Washington, 1905
84. Tisserand, F. F., "Traité de mécanique céleste, tome III: Exposé de l'ensemble des théories relatives au mouvement de la Lune," Paris: Gauthier-Villars et Fils, 1894
85. Brown, E. W., "Theory of the Motion of the Moon; Containing a New Calculation of the Expressions for the Coordinates of the Moon in Terms of the Time," *Memoirs Roy. Astronom. Soc.* 53:39-116, 163-202, 1896-1899; 54:1-64, 1899-1901; 57:51-145, 1905-1908; 59:1-104, 1908-1910
86. Eckert, W. J., Jones, R., and Clark, H. K., "Construction of the Lunar Ephemeris," *Improved Lunar Ephemeris 1952-1959*:283-363, Washington, D. C.: U. S. Govt. Printing Office, 1954
87. O'Keefe, J. A., Eckels, A., and Squires, K. R., "The Gravitational Field of the Earth," *Astronom. J.* 64(7):245-253, September 1959
88. Sundman, K. F., "The Motions of the Moon and the Sun at the Solar Eclipse of 1945 July 9," *L'activité de la Commission Géodésique Baltique pendant les années 1944-1947*:63-94, Helsinki, 1948
89. Hirvonen, R. A., "The Motions of the Moon and Sun at the Solar Eclipse of 1947 May 20," *Veröff. Finn. Geod. Inst.* 40:1-33, May 1951
90. King-Hele, D. G., and Merson, R. H., "New Value for the Earth's Flattening Derived from Satellite Orbits," *Nature* 183 (4665):881-882, March 28, 1959
91. Groves, G. V., "Motion of a Satellite in the Earth's Gravitational Field," *Proc. Roy. Soc. London* 254A (1276):48-65, January 19, 1960
92. Kozai, Y., "The Earth's Gravitational Potential Derived from the Motion of Satellite 1958 Beta Two," *Smithsonian Inst. Astrophys. Obs., Res. Space Sci., Spec. Rept. No.* 22:1-6, March 20, 1959
93. Helmert, F. R., "Die mathematischen und physikalischen Theorien der höheren Geodesie. II. Die physikalischen Theorien," Leipzig: B. G. Teubner, 1884
94. King-Hele, D. G., "The Earth's Gravitational Potential, Deduced from the Orbits of Artificial Satellites," *Geophys. J.* 4:3-16, 1961

95. Kozai, Y., "The Gravitational Field of the Earth Derived from Motions of Three Satellites," *Astronom. J.* 66(1):8-10, February 1961
96. Michielsen, H. F., "The Odd Harmonics of the Earth's Gravitational Field," *Proc. 7th Annual Meeting Amer. Astronaut. Soc.*, in publication
97. Makemson, M. W., et al., "Analysis and Standardization of Astrodynamic Constants," *J. Astronaut. Sci.*, 8:1-13, Jan.-March 1961
98. Cohen, C. J., and Anderle, R. J., "Verification of Earth's 'Pear Shape' Gravitational Harmonic," *Science* 132(3430):807-808, September 23, 1960
99. Brenner, J. L., Fulton, R., and Sherman, N., "Symmetry of the Earth's Figure," *Amer. Rocket Soc. J.* 30(3):278-279, March 1960
100. Newton, R. R., "Potential Geodetic Applications of the Transit Satellite," Presented at the 42nd Annual Meeting Amer. Geophys. Un., Washington, 1961
101. Jeffreys, H., "On the Lunar Equation," *Monthly Notices of the Roy. Astronom. Soc.* 102(4):194-204, 1942
102. Rabe, E., "Derivation of Fundamental Astronomical Constants from the Observations of Eros During 1926-1945," *Astronom. J.* 55(4):112-126, May 1950
103. Delano, E., "The Lunar Equation from Observations of Eros 1930-1931," *Astronom. J.* 55(5):129-133, August 1950
104. O'Keefe, J. A., and Anderson, P. J., "The Earth's Equatorial Radius and the Distance of the Moon," *Astronom. J.* 57(4):108-121, August 1952; also *Bull. Geod.* 29: 219-248, 1952
105. Fischer, I., "The Geometric Parallax of the Moon," Presented at the 42nd Annual Meeting Amer. Geophys. Un., Washington, 1961
106. Yaplee, B. S., et al., "Radar Echoes from the Moon at a Wavelength of 10 CM," *Proc. IRE* 46(1):293-297, January 1958
107. O'Keefe, J. A., et al., "Ellipsoid Parameters from Satellite Data," *Contemporary Geodesy. Proceedings of a Conference on Contemporary Geodesy, Harvard College Observatory, 1958, Amer. Geophys. Un., Geophys. Monograph 4:45-51, 1959*
108. Bruton, R. H., Craig, K. J., and Yaplee, B. S., "The Radius of the Earth and the Parallax of the Moon from Radar Range Measurements on the Moon," *Astronom. J.* 64(8):325, October 1959
109. O'Keefe, J. A., and Batchlor, C. D., "Perturbations of a Close Satellite by the Equatorial Ellipticity of the Earth," *Astronom. J.* 62(6):183-185, August 1957
110. Jeffreys, H., "The Earth; Its Origin, History and Physical Constitution," 4th ed., Cambridge, England: University Press, 1959

111. Kaula, W. M., "Statistical and Harmonic Analysis of Gravity," J. Geophys. Res. 64(12):2401-2421, December 1959
112. Izsak, I. G., "A Determination of the Ellipticity of the Earth's Equator from the Motion of Two Satellites," Smithsonian Inst. Astrophys. Obs., Res. in Space Sci., Spec. Rept. No. 56:11-24, January 30, 1961; also Astronom. J. 66(5):226-229, June 1961
113. Kozai, Y., "Tesseral Harmonics of the Potential of the Earth as Derived from Satellite Motions," Smithsonian Inst. Astrophys. Obs., Res. in Space Sci., Sci., Spec. Rept. No. 72, August 9, 1961; also Astronom. J., 66(7):355-358, Sept. 1961
114. Kaula, W. M., "Estimation of Longitudinal Variations in the Earth's Gravitational Field from Minitrack Observations," J. Astronaut. Sci., 8:83-88, Autumn, 1961
115. Kaula, W. M., "Analysis of Satellite Observations for Longitudinal Variations of the Gravitational Field," Proc. 2nd Int. Space Sci. Sym., Amsterdam: North Holland Publ. Co., in publication
116. Bartlett, M. S., "An Introduction to Stochastic Processes," Cambridge, England: University Press, 1955
117. Ramakrishnan, A., "Probability and Stochastic Processes," Handbuch der Physik 3/2:524-651, Berlin: Springer Verlag, 1959
118. Cook, A. H., "Resonant Orbits of Artificial Satellites and Longitude Terms in the Earth's External Gravitational Potential," Geophys. J. 4:53-72, 1961
119. Munk, W. H., and MacDonald, G. J. F., "The Rotation of the Earth: a Geophysical Discussion," Cambridge: University Press, 1960
120. Melchior, P. J., "Earth Tides," Advances in Geophys. 4:391-443, New York: Academic Press, 1958
121. Doodson, A. T., "Oceanic Tides," Advances in Geophys. 5:117-152, New York: Academic Press, 1958
122. Bergmann, P. G., "Introduction to the Theory of Relativity," New York: Prentice-Hall, 1942
123. Clemence, G. M., "Controlled Experiments in Celestial Mechanics," Astronom. J. 65(5):272-273, June 1960
124. Dicke, R. H., "The Nature of Gravitation," Sci. in Space 2:1-21, Washington, D. C.: U. S. Nat. Acad. Sci., 1960
125. Ginzburg, W. L., "Experimentelle Prüfung der allgemeinen Relativitätstheorie," Fortschritte der Physik 5(1):16-50, 1957
126. Nariai, H., and Ueno, Y., "On the Tests of Gravitational Theories in Terms of an Artificial Satellite," Prog. Theoret. Phys. 20(5):703-714, November 1958

127. Epstein, P. S., "On the Resistance Experienced by Spheres in their Motion Through Gases," *Phys. Rev.*, 2nd series, 23(6):710-733, June 1924
128. Jastrow, R., and Pearse, C. A., "Atmospheric Drag on the Satellite," *J. Geophys. Res.* 62(3):413-423, September 1957
129. Sterne, T. E., "An Atmospheric Model and Some Remarks on the Inference of Density from the Orbit of a Close Earth Satellite," *Astronom. J.* 63(3):81-87, March 1958
130. Cook, G. B., King-Hele, D. G., and Walker, D. M. C., "The Contraction of Satellite Orbits under the Influence of Air Drag. I. With Spherically Symmetric Atmosphere," *Proc. Roy. Soc. London* 257A (1289):224-229, October 6, 1960
131. King-Hele, D. G., "Method for Determining the Change in Satellite Orbits Due to Air Drag," *Space Research, Proc. 1st Int. Space Sci. Sym:* 8-23, Amsterdam: North Holland Publ. Co., 1960
132. Sterne, T., "Effect of the Rotation of a Planetary Atmosphere Upon the Orbit of a Close Satellite," *Amer. Rocket Soc. J.* 29(10):777-782, October 1959
133. Izsak, I. G., "Periodic Drag Perturbations of Artificial Satellites," *Astronom. J.* 65(6):355-357, August 1960
134. Jacchia, L. G., "The Effect of a Variable Scale Height on Determinations of Atmospheric Density from Satellite Accelerations," *Smithsonian Inst. Astrophys. Obs., Res. in Space Sci., Spec. Rept. No. 46:*1-4, July 11, 1960
135. Groves, G. V., "Determination of Upper-Atmosphere Air Density and Scale Height from Satellite Observations," *Proc. Roy. Soc. London* 252A (1268):16-34, August 25, 1959
136. Cook, G. E., and Plimmer, R. N. A., "The Effect of Atmospheric Rotation on the Orbital Plane of a Near Earth Satellite," *Proc. Roy. Soc. London* 258A (1295):516-528, November 8, 1960
137. Parkyn, D. G., "Satellite Orbits in an Oblate Atmosphere," *J. Geophys. Res.* 65(1): 9-17, January 1960
138. Beard, D. B., and Johnson, F. S., "Charge and Magnetic Field Interaction with Satellites," *J. Geophys. Res.* 65(1):1-7, January 1960
139. Chopra, K. P., "Interactions of Rapidly Moving Bodies in Terrestrial Atmosphere," *Revs. Modern Phys.* 33(2):153-189, April 1961
140. Joos, G., and Freeman, I. M., "Theoretical Physics," 3rd ed., London: Blackie and Son Ltd., 1958
141. Byers, H. R., "The Atmosphere up to 30 Kilometers," *The Earth as a Planet*, (G. Kuiper, ed.), 299-370, Chicago, University of Chicago Press, 1954

175. Väisälä, Y., and Oterma, L., "Anwendung der astronomische triangulations methode," Veröff. Finn. Geod. Inst., 55, 1960
176. Kukkamäki, T. J., "Stellar Triangulation," Bulletin Géodésique 1959(54):53-60, December 1, 1959
177. Brown, D. C., "A Solution of the General Problem of Multiple Station Analytical Stereotriangulation," RCA Data Reduc. Tech. Rept. 43, 1958
178. Brown, D. C., "Photogrammetric Flare Triangulation," RCA Data Reduc. Tech. Rept. 46, 1958
179. Brown, D. C., "A Treatment of Analytical Photogrammetry with Emphasis on Ballistic Camera Applications," RCA Data Reduc. Tech. Rept. 39, 1957
180. Markowitz, W., "Geocentric Co-ordinates from Lunar and Stellar Observations," Bulletin Géodésique 1958(49):41-49, September 1, 1958
181. Markowitz, W., "Photographic Determination of the Moon's Position, and Applications to the Measure of Time, Rotation of the Earth, and Geodesy," Astronom. J. 59(2):69-73, March 1954
182. Potter, Kh. I., "On the Use of Observations of the Moon for Geodetic Purposes," Acad. Sci. USSR Astron. J., 35:618-622, also Soviet Astronomy AJ 2(4):573-577, July-August 1958
183. Bonsdorff, I., "Die Astronomischegeodätischen Arbeiten während der Sonnenfinsternis den 9 Juli 1945," Baltische Geod. Kom. Tätigkeit, 1942-43, Helsinki, 5:12-16, 1944
184. Lambert, W. D., "Geodetic Applications of Eclipses and Occultations," Bulletin Géodésique 1949(13):274-292, September 1, 1949
185. Henriksen, S. W., "Mathematical Theory of Occultation Survey," presented at the XII Gen. Assy. Int. Un. Geodesy and Geophysics, Helsinki, 1960; also Army Map Service Tech. Rept., in publication
186. Schmid, H., "An Analytical Treatment of the Problem of Triangulation by Stereophotogrammetry," Photogrammetria 13(2):67-77, (3):91-116, 1956-1957
187. Guier, W. H. and Weiffenbach, G. C., "Theoretical Analysis of Doppler Radio Signals from Earth Satellites," Johns Hopkins Univ. Applied Physics Lab., Bumblebee Ser. Rept. 276, 1958
188. Guier, W. H., and Weiffenbach, G. C., "A Satellite Doppler Navigation System," Proc. IRE 48(4):507-516, April 1960
189. Guier, W. H., "The Tracking of Satellites by Doppler Methods," Space Research, Proc. 1st Int. Space Sci. Sym. 481-491, Amsterdam: North Holland Publ. Co., 1960

190. Izsak, I. G., "Orbit Determination from Simultaneous Doppler-Shift Measurements," Smithsonian Inst. Astrophys. Obs., Res. in Space Sci., Spec. Rept. No. 38, January 15, 1960
191. Koskela, P., Nicola, L., and Walters, L. G., "The Stationkeeping Implications of an Artificial Satellite," Aeroneutronics Div., Ford Motor Co., Aeroneutronic Publ. No. U-806, 1960
192. Kahn, W. D., "Determination of Corrections to Mark II Minitrack Station Coordinates from Artificial Satellite Observations," J. Geophys. Res. 65(3):845-849, March 1960
193. Groves, G. V. and Davies, M. C., "Methods of Analyzing Observations on Satellites," Proceedings 10th Intl. Astronaut. Cong., London 1959 2:933-946, Wien: Springer Verlag, 1960
194. Brown, D. C., "A Matrix Treatment of the General Problem of Least Squares Considering Correlated Observations," Ballistic Res. Labs. Rept. 937, 1955
195. Kaula, W. M., and Fischer, I., "U. S. Army World Geodetic System 1959 (Part 1: Methods)," Army Map Service Tech. Rept. 27, November 1959
196. Cohen, C. J., and Kemper, W. A., "Errors of Prediction of a Satellite Orbit Due to Noise in Doppler Observations," U. S. Nav. Weap. Lab. Rept. 1723, 1961
197. Brown, D. C., "Results in Geodetic Photogrammetry II," RCA Data Proc. Tech. Rept. 65, 1960
198. Whitney, C. A., and Veis, G., "A Flashing Satellite for Geodetic Studies," Smithsonian Inst. Astrophys. Obs., Res. in Space Sci., Spec. Rept. No. 19:9-19, December 6, 1958
199. Murray, B. C., "The Artificial Earth Satellite — A New Geodetic Tool," Amer. Rocket Soc. J., 31(7):924-931, July 1961
200. Lees, A. B., et al., "The Geodetic Use of Artificial Earth Satellites," Systems Lab. Corp., AFCRC-TR-59-276, 2 Parts, August 15, 1959
201. Newton, R. R., "Geodetic Measurements by Analysis of the Doppler Frequency Received from a Satellite," Space Research, Proc. 1st Int. Space Sci. Sym.: 532-539, Amsterdam: North Holland Publ. Co., 1960
202. Kershner, R. B., "The Transit Program," Astronautics 5(6):30-31, 104-105, June 1960
203. Posner, J., ed., "Considerations Affecting Satellite and Space Probe Research with Emphasis on the 'Scout' as a Launch Vehicle," NASA Tech. Rept. R-97, 1961
204. Newell, H. E., Jr., ed., "Sounding Rockets," New York: McGraw-Hill, 1959
205. Williams, O. W., "The Impact of Rocket Flash Triangulation upon World Geodesy," Annals of the Acad. Sci. Fennicae A III, in publication

206. Davis, R. J., "Timing Satellite Observations," Smithsonian Inst. Astrophys. Obs., Spec. Rept. No. 14:26-31, July 15, 1958
207. Strand, K. A., and Franz, O. G., eds., "The Second Astrometric Conference, A Conference Sponsored by the National Science Foundation and the University of Cincinnati, Ohio, May 17-21, 1959," *Astronom. J.* 65(4):167-170, May 1960
208. van de Hulst, H. C., "Scattering in the Atmospheres of the Earth and the Planets," *The Atmospheres of the Earth and Planets*, (G. P. Kuiper, ed.), (3):49-111, Chicago: University Press, 1949
209. Zirker, J. B., Whipple, F. L., and Davis, R. J., "Time Available for the Optical Observation of an Earth Satellite," *Scientific Uses of Earth Satellites*, Ann Arbor, Michigan: University of Michigan Press, pp. 23-28, 1956
210. Hoffmann, W. F., Krotkov, R., and Dicke, R. H., "Precision Optical Tracking of Artificial Satellites," *IRE Trans. on Military Electronics MIL-4(1)*:28-31, January 1960
211. Wilson, R. H., Jr., "Optical and Electronic Tracking," *Contemporary Geodesy*, Proc. of a Conf. on Contemporary Geodesy, Harvard Obs., 1958, Amer. Geophys. Un., *Geophys. Monograph* 4:67-78, 1959
212. Brettler, B. J., et al., "Geodetic Flashing Light System Study," Edgerton, Germeshausen and Grier, Rept. B-1966, 1959
213. Brown, D. C., "Optical Refraction With Emphasis on Corrections for Points Outside the Atmosphere," *Amer. Rocket Soc. J.* 31(4):549-550, April 1961
214. Nettleblad, F., "Studies of Astronomical Scintillation," *Lund Obs. Publ.* II 130, 1953
215. Henize, K. G., "The Baker-Nunn Satellite Tracking Camera," *Sky and Telescope* 16(3):108-111, January 1957
216. Henize, K. G., "Tracking Artificial Satellites and Space Vehicles," *Advances in Space Science* 2:117-142, New York: Academic Press, 1960
217. Lassovszky, K., "The Catalogue of Precise Satellite Positions," Smithsonian Inst. Astrophys. Obs., Res. in Space Sci., Spec. Rept. No. 41:1-10, May 24, 1960
218. Hynek, J. A., "On the Accuracy of Satellite Tracking," *Publ. Inst. Geod. Photogr., Cart., Ohio State Univ.*, 7:59-64, 1957
219. Weston, E., "Preliminary Time Reduction for the Determination of Precise Satellite Positions," Smithsonian Inst. Astrophys. Obs., Res. in Space Sci., Spec. Rept. No. 41:11-13, May 24, 1960
220. Veis, G., and Whipple, F. L., "Experience in Precision Optical Tracking of Satellites for Geodesy," *Proc. 2nd Int. Space Sci. Sym.*, Amsterdam: North Holland Publ. Co., in publication

221. Markowitz, W., "The Dual-Rate Satellite Camera," J. Geophys. Res. 64(8):1115 (abstract), August 1959
222. Schmid, H., "Some Problems Connected with the Execution of Photogrammetric Mult-Station Triangulations," Proc. Sym. Geodesy in Space Age, Columbus, Ohio, 56-65, 1961
223. Hewitt, J., "A Camera for Recording Satellite Positions with High Accuracy," Space Res., Proc. 1st Int. Space Sci. Sym., Amsterdam: North Holland Publ. Co., pp. 425-433, 1960
224. Brown, D. C., "Results in Geodetic Photogrammetry. I. The Precise Determination of the Location of Bermuda from Photogrammetric Observations of Flares Ejected from Juno II," RCA Data Processing Tech. Rept. No. 54, 1959
225. Berroth, A., "Die Bedeutung der geodätischen Astronomie für die Überbrückung der Ozeane," Geofisica pura e applicata 18:45-54, 1950
226. Atkinson, R. d'E., "Surveying by Astrometry of Rocket Flashes," Annals Int. Geophys. Yr. 12(1):201-206, New York: Pergamon Press, 1960
227. Bowen, R. P., "Development of a Photoelectric Satellite Tracker," Proc. 2nd Int. Space Sci. Sym., Amsterdam: North Holland Publ. Co., in publication
228. Rosenberg, P., "Earth Satellite Photogrammetry," Photogrammetric Engineering 24(3):353-360, June 1958
229. Katz, A. H., "Observation Satellites: Problems and Prospects," Astronautics 5(8): 30-31, 59, 60, 62, 64, August 1960
230. Spitzer, L., Jr., "Space Telescopes and Components," Astronom. J. 65(5):242-263, June 1960
231. Komesaroff, M. M., "Ionospheric Refraction in Radio Astronomy, I. Theory," Australian J. of Physics 13(2):153-167, June 1960
232. Carru, H., Gendrin, R., and Reyssat, M., "La réfraction ionosphérique pour des fréquences de 20, 40, 108 MHz et son application à l'effet doppler des satellites," Space Res., Proc. 1st Space Sci. Sym., Amsterdam: North Holland Publ. Co., pp. 286-303, 1960
233. Siry, J. W., "Study of the Upper Ionosphere by Means of Minitrack and Optical Observations of Satellites," Manual on Rockets and Satellites; Annals Int. Geophys. Yr. 6:431-438, New York: Pergamon Press, 1958
234. Kelso, J. M., "Doppler Shifts and Faraday Rotation of Radio Signals in a Time-Varying, Inhomogeneous Ionosphere. Part I. Single Signal Case," J. Geophys. Res. 65(12):3909-3914, December 1960

235. Davisson, R. J., "Precision of Compensated Tracking Systems," Hermes Electronic Co., Cambridge, Mass., Rept. No. HEI M-810, AFCRC-TR-59-356, November 5, 1959
236. Aslakson, C. I., and Fickeissen, O. O., "The Effect of Meteorological Conditions on the Measurement of Long Distances by Electronics," Trans. Amer. Geophys. Un. 31(6):816-826, December 1950
237. International Union of Geodesy and Geophysics, "Resolution No. 1, 12th Gen. Assy., Int. Un. Geodesy and Geophys., Helsinki," Bulletin Géodésique 1960(58):413, December 1, 1960
238. Bean, B. R., "Atmospheric Bending of Radio Waves," Electromagnetic Wave Propagation: Proc. of a Conf. Sponsored by the Postal and Telecommunications Group of the Brussels Universal Exhibition, 1958:163-181, New York: Academic Press, 1960
239. McNish, A. G., et al., U. S. Nat. Bur. Standards, "Ionospheric Radio Propagation," NBS Circular 462, June 25, 1948
240. Hines, C. O., "Symposium on the Exosphere and Upper F Region, Summary of the Proceedings," J. Geophys. Res. 65(9):2563-2569, September 1960
241. Kallmann Bijl, H., ed., "Space Research, Proceedings of the First International Space Science Symposium," Amsterdam: North Holland Publ. Co., 1960
242. Mengel, J. T., "Tracking the Earth Satellite, and Data Transmission, by Radio," Proc. IRE 44(6):755-760, June 1956
243. Berbert, J. H., "Effect of Tracking Accuracy Requirements on Design of Minitrack Satellite Tracking Systems," IRE Trans. on Instrumentation I-9(2):84-88, September 1960
244. Easton, R. L., "The Minitrack Mark II Radio-Tracking System," Manual on Rockets and Satellites; Annals Int. Geophys. Yr. 6:384-410, New York: Pergamon Press, 1958
245. Kahn, W. D., "Calibration of Minitrack Mark II," Astronom. J. 62(10):396-399, December 1957
246. Richter, H. L., Jr., "The Microlock Radio-Tracking System," Manual on Rockets and Satellites; Annals Int. Geophys. Yr. 6:410-417, New York: Pergamon Press, 1958
247. Weiffenbach, G. C., "Measurement of the Doppler Shift of Radio Transmissions From Satellites," Proc. IRE 48(4):750-754, April 1960
248. deBey, L. G., "Tracking in Space by DOPLOC," IRE Trans. on Military Electronics MIL-4(2-3):332-335, April-July 1960
249. Henriksen, S. W., "SECOR — An Instrument for Measuring Very Long Distances," J. Geophys. Res. 65(8):2497 (abstract), August 1960

250. Mullen, E. B., and Woods C. R., "Precision Radio Tracking of Space Vehicles," Proc. 2nd Int. Space Sci. Sym., Amsterdam: North Holland Publ. Co., in publication
251. Hayn, F., "Selenographische Koordinaten," Abhandlungen der Mathematischen physikalischen Klasse, Königliche sächsische Gesellschaft der Wissenschaften 27(9):863-921, 1902; 29(1):1-142, 1904; 30(1):1-104, 1907; 33(1):1-113, 1914
252. Weimer, T., "Atlas de profils lunaires," Paris: Observatoire, 1952
253. Watts, C. B., and Adams, A. N., "Photographic and Photoelectric Technique for Mapping the Marginal Zone of the Moon," Astronom. J. 55(3):81-82, April 1950
254. Scott, D. K., "Measuring of the Profile of the Moon's Visible Limb," Publ. Inst. Geod., Photogr., Cart., Ohio State Univ., 7:50-53, 1957
255. Kukkamäki, T. J., "Results Obtained by the Finnish Solar Eclipse Expeditions, 1947," Trans. Amer. Geophys. Un. 35(1):99-102, February 1954
256. O'Keefe, J. A., and Mears, D. D., "The 800-Inch Telescope," J. Royal Astronom. Soc. Canada 48(1):3-15, January-February 1954
257. Henriksen, S. W., et al., "Surveying by Occultations," Astronom. J. 63(7):291-295, July 1958; also Amer. Geophys. Un. Trans., 38:651-656, 1957
258. Lambert, W. D., "The Gravity Field for an Ellipsoid of Revolution as a Level Surface (III)," Annals Acad. Sci. Fennicae A. III, 57; also, Publ. Inst. Geod., Photogr., and Cart., 14
259. Lambert, W. D., "Note on the Paper of A. H. Cook, 'The External Gravity Field of a Rotating Spheroid to the Order of  $e^3$ ,'" Geophys. J. 3(3):360-366, September 1960
260. Cook, A. H., "The External Gravity Field of a Rotating Spheroid to the Order of  $e^3$ ," Geophys. J. 2(3):199-214, September 1959
261. Cohen, C. J., "A Mathematical Model of the Gravity Field Surrounding the Earth," U. S. Navy Prov. Grd. Rept. 1514, 1957
262. Hirvonen, R. A., "New Theory of Gravimetric Geodesy," Pub. Isos. Inst. Int. Assoc. Geod., 32; also Annals of Acad. Sci. Fennical A. III, 56, 1960
263. Cook, A. H., "The Comparison of the Earth's Gravitational Potential Derived from Satellite Observations with Gravity Observations on the Surface," Geophys. J. 5:29-33, 1961
264. Baussus, H. G., "A Unified Isostatic and Statistical Theory of Gravity Anomalies and its Significance," presented at the XII Gen. Assy. Int. Un. Geodesy and Geophys., Helsinki, 1960
265. Heiskanen, W. A., and Uotila, U. A., "Some Recent Studies on Gravity Formulas," Contributions to Geophysics in Honor of Beno Gutenberg (H. Benioff, ed.), London: Pergamon Press, 1958

266. Zhongolovich, I., "Vneshnee gravitatsionnoe pole zemli i fundamental 'nye postoiannye, sviazannye s nim" (The External Gravity Field of the Earth and the Fundamental Constants Connected with It), *Akademiia nauk SSSR, Institut Teoreticheskoi Astronomii, Trudy*: 1952(3):3-125, 1952
267. Heiskanen, W. A., "The Latest Achievements of Physical Geodesy," *J. Geophys. Res.* 65(9):2827-2836, September 1960
268. Fischer, I., "The Present Extent of the Astrogeodetic Geoid and the Geodetic World Datum Derived from It," *J. Geophys. Res.*, 65:2067-2076
269. Kaula, W. M., "A Geoid and World Geodetic System Based on a Combination of Gravimetric, Astrogeodetic and Satellite Data," *J. Geophys. Res.* 66(6):1799-1811, June 1961
270. Heiskanen, W. A., and Vening-Meinesz, F. A., "The Earth and Its Gravity Field," New York: McGraw-Hill, 1958
271. O'Keefe, J. A., "Zonal Harmonics of the Earth's Gravitational Field and the Basic Hypothesis of Geodesy," *J. Geophys. Res.* 64(12):2389-2399, December 1959
272. Henriksen, S. W., "The Hydrostatic Flattening of the Earth," *Annals Int. Geophys. Yr.* 12(1):197-198, New York: Pergamon Press, 1960
273. Munk, W. H., and MacDonald, G. J. F., "Continentality and the Gravitational Field of the Earth," *J. Geophys. Res.* 65(7):2169-2172, July 1960
274. Slichter, L. B., "Earth Tides," *McGraw-Hill Encyclopedia of Science and Technology* 4:346-351. New York: McGraw-Hill, 1960
275. Arnold, K., "Die Präzessionsbewegung der Erde und der Bahn der künstlichen Erdsatelliten, die Abplattung der Erde und die Dichteverteilung im Erdinnern," *Gerlands Beiträge zur Geophysik* 69(4):191-199, 1960
276. Vogel, A., "Über Unregelmässigkeiten der äusseren Begrenzung des Erdkerns auf Grund von am Erdkern reflektierten Erdbebenwellen," *Gerlands Beiträge zur Geophysik* 69(3):159-174, 1960
277. Elsasser, W. M., "Hydromagnetic Dynamo Theory," *Rev. Modern Phys.* 28(2):135-163, April 1956
278. Licht, A. L., "Convection Currents in the Earth's Mantle," *J. Geophys. Res.* 65(1):349-353, January 1960
279. Griggs, D., and Handin, J., eds., "Symposium on Rock Deformation," New York: Geological Society of America, 1960
280. Kaula, W. M., "The Interaction between Geodesy and the Space Sciences," *Proc. Sym. Geodesy in Space Age*, Columbus, Ohio, pp. 168-173, 1961